This is to certify that the

thesis entitled

AN EMISSION SPECTROCHEMICAL DETECTOR
FOR CHROMATOGRAPHY

presented by

Robert Knight Lantz

has been accepted towards fulfillment
of the requirements for

Ph.D. degree in Chemistry

Major professor
Stanley R. Crouch

Date 11/18/77

O-7639

AN EMISSION SPECTROCHEMICAL DETECTOR FOR CHROMATOGRAPHY

By

Robert Knight Lantz

A DISSERTATION

Submitted to

Michigan State University

in partial fulfillment of the requirements

for the degree of

DOCTOR OF PHILOSOPHY

Department of Chemistry

1977

ABSTRACT

AN EMISSION SPECTROCHEMICAL DETECTOR
FOR CHROMATOGRAPHY

By

Robert Knight Lantz

A spark emission spectrochemical detector (SED) has been developed and evaluated for gas and liquid chromatography. A low energy, high power, miniature coaxial spark discharge is used to atomize and excite analytes to produce characteristic atomic emissions. Time-resolved photometric measurement of the light emitted from the spark allows the isolation, in time, of the desired emission signals from the background continuum.

Continuous, element-specific analysis of chromatographic effluents is demonstrated for carbon, hydrogen, oxygen, boron, nitrogen, sulfur, silicon, and phosphorus and for most metals. Only the alkali metals, iron, and the halogens had detection limits worse than 1 μg. Amenable elements are detected to the nanogram and picogram levels, and detector response is linear over 10^3 to 10^8 fold concentration changes for all elements studied.

The multi-element capability of the SED is used to

determine empirical formulae and to help resolve effluent components which otherwise would not be separated chromatographically. In particular, barbituates and other nitrogenous drugs are separated and identified in GC effluent both by their retention times and by their empirical formulae. Other nitrogenous compounds in serum, such as caffeine and theobromine, are easily differentiated from drugs with similar retention times but different empirical formulae, such as amobarbital and secobarbital. Similarly, the sulfur-containing amino acids in urine are specifically detected and quantitated with the SED following separation by HPLC.

Compound classes are also derivatized with heteroatom labels to aid their resolution from other compounds with initially similar retention times and empirical formulae. The selective formation of amino acid silyl ethers in a simple urine extract allows their differentiation from a large number of similar compounds which do not form silyl derivatives to the same extent. Similarly, the formation of n-butyl boronate esters of sugar alcohols from a biological matrix allows their identification even in the presence of other polyols and aminols.

In addition to being a very sensitive, element-specific detector for GC and HPLC, the SED is easily made at small cost ($300 plus filters or monochromator) and is facilely adaptable to most commercially available

chromatographs. The dead-volume is only 50 µl for the GC version. Band-spreading is not apparent when used with GC or HPLC, though the HPLC version does use a small nebulizer-desolvation system.

To my parents and

my brother

ACKNOWLEDGMENTS

The author wants to thank Professor Stanley Crouch for his scientific guidance. Thanks also go to Professor Andrew Timnick for acting as a diligent second reader and a good hunting/smelting companion.

He would also like to thank Messrs. Martin Rabb, Len Eisele, Chuck Hacker and Ron Haas of the Chemistry Department machine and electronic shops for their invaluable help.

Similarly, it is quite appropriate to thank the spark group members, Gary Seng and Sandy Koeplin and the enzyme group members, Dan Kasprzak and Martin Joseph, on whose jaw I broke my knee (only 9999 philistines left?), who have continued my work with great enthusiasm.

Patricia Salik - more than anyone else.

TABLE OF CONTENTS

LIST OF TABLES

Table Page

LIST OF FIGURES

CHAPTER I

INTRODUCTION

I will find a way,
or I will make one.

Hannibal

The major need in real-world chromatography is not increased universal sensitivity, but is the ability to ignore extraneous material eluting from the chromatographic column. Selective detection has improved the availability and practicality of gas and liquid chromatographic analysis in clinical and environmental laboratories. It was the author's intent to develop a sensitive, element-specific detector for such practical purposes.

The ideal chromatographic detector should have the following virtues:

1. Sensitivity;
2. Selectivity for element, compound, or functional class;
3. Proportionality;
4. Reliability; and
5. Low cost.

The increasing popularity of the nitrogen-selective alkalai flame ionization detector for drug analyses is due to its relative blindness to extraneous compounds, not to any inherently greater absolute sensitivity. Similarly, the flame photometric and electrolytic conductivity detectors are important in residue analysis because of

their better selectivity than the more sensitive electron capture detector. In both instances, the true need is for greater effective sensitivity, which is most easily produced by the decreased production of background signal.

A lack of proportional response is another serious fault of nearly all chromatographic detectors. Even for detectors with a large linear dynamic range, as the flame ionization detector, functional group and molecular structural effects cause equal masses of different compounds, even of the same empirical formulae, to give different detector responses. The only universal way to circumvent the proportionality problem is to reduce all analyte compounds to atoms, and then to excite those atoms. This is the solution which has been applied in the following work.

Two final problems in new detector design are reliability and low cost of the final product. Remote, unattended monitoring, as on the Mariner Mars probes or at EPA monitoring sites, is possible only with maintenance-free, reliable detectors such as the photoionization detector (Mariner) and the thermal conductivity detector (previous NASA flights). Low cost is also a necessary design objective, as even the very best detector is quite useless if potential users cannot afford it. The computerized GC/mass spectrometer is often touted as

the ideal system for emergency toxicologic analysis, as it can identify and quantitate unknown analytes. Unfortunately, few GC/MS instruments are actually available for STAT use. In metropolitan Detroit hospitals, there is only one such instrument, and it is not always available to the clinician.

All of the above criteria were considered in the choice of detection method and during the design of the instrument. The resulting nanosecond spark emission detector is element specific, quite sensitive, free of functionality and structural effects, linear in response, quite reliable, and may be built at rather low cost ($200 plus monochromator).

CHAPTER II

THE HISTORY OF GAS CHROMATOGRAPHIC DETECTORS

It is possible to classify chromatographic detectors in several different ways. The most common are: universal or selective response, mass concentration sensitivity, and reaction (active) or passive mechanism. In the following discussion, all three logical approaches are used to help explain the development and usefulness of the many available chromatographic detectors. Modifications to primarily GLC detectors for use with liquid chromatographs are discussed in Chapter III with the LC detectors. David (28), Adlard (2), Sternberg (81), Novak (82), and Sevcik (73), have reviewed detectors and quantitation in chromatography, and Ettre and McFadden (72) have discussed ancillary techniques.

Detectors respond to the analyte mass flow rate, to the analyte concentration, or to some combination of both. The flame ionization (FID) and thermal conductivity (TC) detectors are, respectively, mass flow rate and concentration sensitive.

For a "concentration detector", a simplified analysis of its response gives: $R = mC$ where R = Response

m = Proportionality constant

C = Concentration of the analyte in the detector at time t, where C is a step-function.

If the integrated area A of a peak is

$$A = \int_{t_1}^{t_2} R dt \qquad (1)$$

then

$$A = \int_{t_1}^{t_2} m\,C dt = m \int_{t_1}^{t_2} C dt = m\,C\Delta t \qquad (2)$$

If C = M/V and V = Ft, where M = Mass and V = Volume of the detection cell; F = carrier gas flow rate, and t = time of time of flow,

then,

$$A = m \frac{M}{V} \frac{V}{F} = m \frac{M}{F} \qquad (3)$$

Equation 3 shows that, for a true concentration-dependent detector, the integrated response is proportional to mass, but is also inversely dependent on carrier flow rate. Two problems are immediately apparent: fluctuations in carrier gas flow rate will degrade detector reproducibility, and the optimum carrier flow rate for detectability may not be the best for the separation.

If detector response were dependent on mass flow rate, and response R were expressed as

$$R = m \left(\frac{dM}{dt}\right),$$

then, by analogy,

$$A = \int_{t_1}^{t_2} R\,dt = \int_{t_1}^{t_2} m \left(\frac{dM}{dt}\right) dt = m\,M \qquad (4)$$

Therefore, the integrated response ("peak area") of a mass flow rate responsive detector is independent of carrier gas flow rate. The response of a thermal conductivity detector (TCD) to analyte concentration is due to the cooling of heated elements by carrier and effluent gases. Therefore, its response is proportional to the integrated heat capacity of the gases passed through it during some Δt, and making the TCD concentration-sensitive. The FID response is proportional to the total number of analyte atoms passing through it in some increment of time Δt. Thus, it is quite blind to carrier gas atoms or molecules, and is mass flow rate responsive. All of the detectors discussed in the following chapter are considered on this basis, though few detectors respond in a single, uniform manner.

A. Universal Detectors

The universal gas chromatography detectors range from the truly catholic catharometer (TCD) and helium ionization detectors to the carbon sensitive flame ionization detector. Because the TCD and FID are so very well known, they are discussed only as bases for understanding the less-common detectors.

1. Thermal Conductivity Detector (Catharometer)

Daynes (1) described the use of the first universal gas detector in 1933, long before the advent of gas chromatography. His analyses of gas mixtures used the thermal conductivities of the analyte gases as indicators of their purity. Relatively little about the thermal conductivity (TC) detector has changed since then other than decreased cell dead-volume (2), increased detector ruggedness (3), and occasional use of semiconductors (thermistors) (4) instead of heated wires in a Wheatstone bridge arrangement.

The essential TC detector consists of one or more heated elements placed in a massive thermostated block through which the column effluent travels. The heated elements, metallic or semiconductor, lose energy by thermal conduction to the gas, by convection, by radiation, and by losses at the electrical contact points. Radiative losses are

proportional to the difference of the fourth powers of the Kelvin temperatures of the block and filaments (Stefan-Boltzmann), and are negligible for common conditions, as are losses through the metal electrical contacts. Thermal losses from forced convection may be minimized by the use of "diffusion-fed" filaments, which are not in the direct path of the carrier gas. However, dead volume is increased by such methods.

Use of a carrier with a large thermal conductivity (λ) (Table 1)

Table 1. Thermal Conductivities of Gases. (Reference 5, page 93)

	$\lambda \times 10^5$ @ 0°C	M. Wt.
Hydrogen	41.6	2
Helium	34.8	4
Methane	7.2	16
Nitrogen	5.8	28
Pentane	3.1	72
Hexane	3.0	86

will increase detector sensitivity, and will cause energy loss by gaseous thermal conductivity to predominate. Large carrier gas thermal conductivities also minimize

the effects of convection.

The TC detector sensitivity (5) is given by

$$S = K\, I^2 R \left(\frac{\lambda_c - \lambda_s}{\lambda_c}\right) (T_f - T_b)\, |m| \qquad (5)$$

where

S = Sensitivity;
K = Cell constant dependent on geometry of cell
I = Current in resistive element
λ_c = Thermal conductivity of carrier
λ_s = Thermal conductivity of sample
T_f = Filament temperature
T_b = Block temperature
m = Temperature coefficient of resistance

Therefore, increasing element current and temperature coefficient will improve sensitivity, as will increasing λ_c. The sign of the temperature coefficient of resistance (m) is not important.

The factor $(\lambda_c - \lambda_s)$ also describes a serious problem in the use of the TCD. If all analytes were to possess identical molar or gram thermal conductivities, each peak area would be directly proportional to the mass of the analyte compound. As λ_s is quite variable, "raw-area normalization" of peak areas is not usable for quantitation without correction factors. All commercially

available GC detectors, except for the microcoulometric and the cross-section detectors, now require the use of analogous "carbon numbers". Similarly, the TCD is not responsive to any compounds whose λ is close to that of the carrier gas. Keulemans (6) found that, using area normalization, tabulated heat capacity (at constant pressure)/mass ratios generally were too high for low molecular weight compounds in an homologus series. Dal Nogare and Juvet (7) also found that the use of nitrogen rather than helium or hydrogen increased functional group effects.

The TCD sensitivity is also increased by improved cell geometry (K) and increased filament temperature (T_f). The smallest dead volume cell now available (2) has a 2.6 ul dead volume (Taylor Servomex, Ltd., England). It consists of two tiny chambers formed by slots cut in a pair of mica discs sandwiched between halves of the heater block and contains 7.5 μm diameter platinum wires. Unfortunately, filament temperature is somewhat limited by filament fragility.

Replacement of the heated wires by small thermistors is also very useful for lower temperature applications, and in low dead volume cells. Such metal oxides cannot be used with hydrogen as a carrier gas or at temperatures above 250°C.

2. Gas Density Balance

The gas density balance (GDB), invented by Martin and James (8), was an early competitor of the TCD, but was not widely used until Nerheim (9) resolved construction problems. The GDB (now made by Gow-Mac Instruments Co.) is quite similar to the conventional TCD in that the resistances of two sensors (thermistors or Pt wires) in a Wheatstone bridge depend upon the integrated heat capacities of the gases flowing around them. The singular difference is that the sample never contacts the sensors. This totally alleviates the problem of filament corrosion, but at the expense of a larger cell dead volume and an increased dependence on carrier gas flow fluctuations. The sensitivity depends on differences between the density of reference gas and the analyte gas. Helium and hydrogen cannot be used as they have very little resistance to analyte diffusion, and allow corrosive analytes to contact the filaments.

Detection limits are roughly equal to those for the TCD, but the GDB will give response directly in weight percent (5, page 116) for known compounds without need for detector calibration. If peak areas (A) are multiplied by the reduced molecular weight (K) of the sample [$K = \frac{M_s}{M_s - M_c}$], then mass [$s = K\ A\ X$], where X is a constant peculiar to an instrument design, and M_s and M_c are the molecular weights of sample and carrier gas, respectively.

A third, and nearly unique, use for the GDB is the determination of the molecular weights of effluents. Phillips and Timms (10), and others (11,12), developed the concept, and an instrument which uses two identical columns, two GDBs, and two different carrier gases simultaneously (e.g., N_2 and SiF_6), is now commercially available. Molecular weights up to approximately 400 can be determined with an accuracy of 1% with a one-point instrument calibration (14).

3. Reaction Coulometer

The reaction coulometer (15,17) ideally requires no calibration at all, and is the only commercially available absolute detector (16,13). As each component elutes from the column, it is burned in oxygen over a platinum catalyst. The oxygen consumed is replaced coulometrically.

Although the sensitivity (2) is nearly equal to that of the FID, the reaction coulometer is somewhat troublesome to use, has a slow response time, has a limited upper range (dependent on the electrode limiting current) and is subject to large functional group errors. It does not, however, show deviations within most homologus series of compounds without heteroatoms. Littlewood and Wiseman (18) and Lovelock (78) have also used the electrochemical generation of hydrogen to detect reducible effluent compounds, and the most important uses of the

microcoulometric detector (MCD) are not as a universal, but as a selective detector. Those applications are discussed under "selective-electrochemical" detectors.

4. Sorption Detector

The sorption (piezoelectric) detector also was developed as a universal detector and later modified for improved selectivity. It was initially developed by Bevan and Thorburn (19) as an integral mass detector in which organic effluents were adsorbed to a charcoal pad on a microbalance. The response was directly proportioned to mass, but the integral nature of the system made its routine use impractical. Replacement of the charcoal adsorbant and balance by a liquid-coated piezoelectric crystal (20) allowed desorption, improved sensitivity, and made the detector differential in response. The piezoelectric (PZ) system also made the response vary greatly between compounds. The linearity was adequate over a mass range of 10^4 or greater from the detection limit (10^{-9} grams), and the response time was approximately 50 msec. The discrimination has been enhanced by the use of selective coatings on the piezocrystal (21, 22). Guilbault (22) claimed that a solid coating of acetyl-cholinesterase provided specificity for anticholinergic pesticides. The large, irreversible affinity of several organophosphates for the enzyme also caused the

permanent blockage of the enzyme active-sites with concommitant disappearance of sensitivity and selectivity.

Regardless of the coating material selectivity, the detector response is dependent on the crystal frequency shift (f) induced by the added analyte mass. Equation (6) shows that the frequency shift depends on several parameters.

$$f = f_o \frac{M}{M_o} \qquad (6)$$

where f_o = natural oscillation frequency of the crystal;

M = sorbed analyte mass;

M_o = mass of crystal coating

Equation (7) expresses the response R in somewhat different form (21):

$$R = K \left(\frac{M V_r}{V + MV_r}\right) \qquad (7)$$

where R = response

K = proportionality constant

V_r = specific retention volume (ml/gram)

V = detector dead volume

The PZ detector response time is shorter than that of the TCD, and the sensitivity is in the nanogram range.

However, the sensitivity is variable and depends on the particular compound being analyzed. The PZ detector is now available commercially (Laboratory Data Control, Riviera Beach, FL).

An analogous sorption detector (23) has been developed by Guglya and Dergumov. A TiO_2 film exposed to column effluent was found to change its resistance as the square root of analyte concentration. The detector was somewhat selective for species with electron donating capability (ketones, alcohols, and amines), but was insensitive to nitrogen and the permanent gases. Detection limits were approximately 1 ppm in carrier, but varied with analyte structure. Winefordner and Glenn (38) suggested that selectivity was also possible with semiconductor detectors, and Scott (202) developed a theoretical treatment of a sorption detector variant in which the heat of sorption was measured (203).

5. Frequency Modulation Detectors

Two other universal detectors which employ frequency modulation by the sample are the dielectric constant detector (24) and the ultrasonic detector of Lawley (25) and Noble (26).

In the dielectric constant detector (DCD), the effluent passes between the parallel plates of a capacitor. A change in dielectric constant of the effluent gas

causes a change in the capacitance of the cell which is part of an oscillator circuit. The capacitance C depends upon the dielectric constant K, plate separation d, and plate area s, as shown in Equation (8).

$$C = 0.0885 \frac{K\ s}{d} \qquad (8)$$

The dielectric constant K is temperature and frequency dependent as well as variable with analyte species. Although the DCD is relatively insensitive, and is not commercially made, it is analogous to many more successful detectors.

The ultrasonic detector also depends on effluent density changes for performance. As the density of a medium varies, the velocity of sound through that medium also varies. If the difference in sound velocity through the column effluent and through the pure carrier gas is expressed as a phase shift, ϕ, then the response will be proportional to K, the reduced sample molecular weight, $K=\frac{M_s-M_c}{M_s}$, the sample mass, the square root of the temperature, and other factors (27,28). M_s and M_c are the sample and carrier gas molecular weights, respectively.

The sensitivity was found (27) to be in the nanogram range for hydrogen in helium, and its linear dynamic range to be 10^4. However, its usefulness is somewhat hampered by the "roll-over" with each 360° phase shift. This feature may be viewed as an auto-attenuation feature

(26), but may also cause great difficulties in practice. The ultrasonic detector shows little selectivity, but does require the use of response factors (27).

6. Ionization Detectors

a. The Flame Ionization Detector

The most important of all universal detectors is the flame ionization detector (FID). Not only is the FID the detector to which all other detectors must be compared, it is the progenitor of a family of selective detectors. The FID features excellent sensitivity (10^{-11} grams) and linearity (10^{6}), which is often subject to structural and heteroatom effects (see Table 2).

The FID has changed relatively little since 1958, when the concept was suggested by Ryce and Bryce (29) and Harley and Pretorius (30) and developed by McWilliams and Dewar (31). The dominant patent was awarded to McWilliams (36). Our present understanding of the mechanism of the FID response has improved due to the renewed interest in ionization phenomena in flames used for other purposes. Bocek and Janek (32) have exhaustively reviewed flame ionization phenomena, and Blades (33), Dressler (34) and David (28, pp. 42-74) have discussed practical concerns in detail.

Although the FID is a mass-flow sensitive detector,

Table 2. FID Relative Response Factors.

1-butanol	1	1-bromoprop-2-ene	4000
1-chlorobutane	1	trans-dichloroethylene	370
2-chlorobutane	2	cis-dichloroethylene	90
1,2 dichlorobutane	110	chloroform	6×10^4
1,4 dichlorobutane	15	carbon tetrachloride	4×10^5
1-bromobutane	280	2,3-butane dione	5×10^4
1-iodobutane	9×10^4	acetone	0.5

many chromatographic and detector parameters, such as carrier and fuel flow rates, must be optimized to obtain maximum response and good linearity and precision. Electron emission, incomplete sample burning ("blow-by"), multiple ion formation and ion-pulse overlap often cause non-ideal response. Use of the FID requires either structurally comparable internal standards or "response factors". Direct, steady-state calibration has been used successfully (37), but is not of great practicality or necessity.

The response of the FID results from the rapid burning of air, hydrogen, and sample with a resultant chemi-ionization of one in 10^5 sample molecules (35). Ions produced in the flame migrate in an electric field to collector electrodes, and the current is measured. The possibility that thermal ionization might be responsible for the ionization is greatly diminished by the following observations:

1) The majority of the ionization does not occur at the zone of maximum temperature;
2) certain very hot flames (CS_2/O_2 or H_2S/O_2) give very low ionization and small FID response; and
3) relatively cool flames give large ionization response (32).

b. The Photoionization Detector

Photoionization probably occurs to a very small extent in the FID, but may be made a very efficient means of ion production. Lovelock's 1961 (35) review of ionization detectors discussed the problems inherent in the photoionization detector (PID). The PIDs then available used glow or microwave discharges, at sub-atmospheric pressure (43,44,45,46), and were generally complex, unstable, and admirably sensitive. Poulson (46) monitored both ionization and photoemission in an early PID which will be discussed further with the selective emission detectors.

The microwave discharge (45) PID produced greater ionization and sensitivity than did earlier PID, but did not circumvent the problems of vacuum operation and alteration of the plasma by the sample. Higher intensity, self-contained hydrogen and deuterium discharge lamps made it possible for Sevcik and Krysl (47) and Ostojic and Sternberg (48) to use a PID with the sample outside of the light source and at ambient pressure. Driscoll and Spaziani (49,50) have reported a commercially available PID (51) with several different photon sources.

Photoionization, as used chromatographically, depends on the absorption of 10.2 eV photons (Lyman H_α line) emitted from a deuterium discharge lamp or other source. Two processes are possible, dependent on carrier gas type:

1. He or other permanent gas carrier:

$$M + h\nu \rightarrow M^+ + e^- \qquad (9)$$

2. N_2 or other absorbing gas:

$$N_2 + h\nu \rightarrow N_2^*$$
$$N_2^* + M \rightarrow N_2 + M^+ + e^- \qquad (10)$$

Analytical results with helium and nitrogen are comparable, indicative of the efficiency of the second mechanism. Helium and other species with ionization potentials greater than 10.2 eV produce no measurable ion current. Therefore, the PID is blind to small aliphatic hydrocarbons (n = 4 or less), carbon dioxide, nitrogen oxygen, ethylene and similar small molecules with high ionization potentials. The sensitivity of the PID is somewhat greater than that of the FID. Photoionization efficiency is greater in the PID (47,49) than is chemionization efficiency in the FID (43). Ion-quenching by O_2^- also does not decrease PID sensitivity as it does FID sensitivity. The PID also exhibits very low rms noise levels ($\sim 2 \times 10^{-14}$ A), comparable to the commercial FID. The linear dynamic range (LDR) for detectable compounds is from the detection limit ($\sim 2 \times 10^{-12}$ grams) to 30 ug. The only commercially available detector is limited to operation at 250°C. Sensitivity to flow rate variation is minimal (49).

c. Other Ionization Detectors

Two other analogs of the FID and the electron-capture detector (ECD) are the helium or argon ionization (HI) detector, and the cross-section (XC) detector. The basis of the cross-section detector, as described by Pompeo, Otvos, and Stevenson (39,40) of Shell Development Company, is the formation of ion pairs by β-particles emitted from strontium-90 or tritium or by α-particles from radium. The current produced in an electric field then is proportional to the analyte concentration, its ionization cross section (Q), and the radiation intensity. Tritium possesses a long (7-1/2 year) half-life and ionization cross-sections are easily available in the reference literature. Thus, the XCD is truly one of the most predictable detectors available. The molecular ionization cross-section is merely the sum of the atomic cross-sections for the constituent atoms and is independent of chemical factors. Therefore, the XCD is completely universal in response, with a sensitivity of ∿1 ng and a useful range from the detection limit to nearly 100% analyte in effluent. Its failings have been excessive dead volume and the formation of helium metastables, which causes non-linear response. However, design improvements made by several groups (41,42), and the use of H_2 or 3% methane in helium as carrier gases have alleviated both problems with the XCD.

The helium ionization detector (HID) has also been somewhat neglected as a universal detector because it is too sensitive for use with nearly all common stationary phases. As a result, its use is limited to separations using Porapak, Carboseive, molecular seives, and other solid and quasi-solid stationary phases.

Construction of the HID is very similar to that of the XCD, except that the collector/polarizer electrode plates are much closer (∿1 mm), and the resultant field gradient (∿4000 V/cm) is much larger. Some of the helium (or argon) carrier atoms are excited to the 19.8 eV metastable (11.6 eV for argon) level, and then are able to ionize compounds with lower ionization potentials. All organics, and nearly all other species, cause an increased ion current. Detection limits are equal to those for the electron capture detector, 10^{-14} grams, but correction factors are much more reliably calculated (83,84). The mechanism has interesting similarity to that of the nanosecond spark detector and the latest Hewlett-Packard version of the thermionic detector (discussed below). Bros and Lasa (76) discussed proposed mechanisms for the HID response, as did Lovelock (77). Hartman and Dimick (78) and others (79) investigated the operational parameters of the HID.

The helium ionization detector is the quintessential universal detector. In its extreme sensitivity and universality lies its failure and the failures of all

sensitive, universal detectors.

B. Selective Detectors

"Selective detectors" discriminate between compounds and functional groups better than do the "universal detectors" only by degree. Just as no universal detector is actually catholic in response, very few selective detectors are truly specific for compound, element or functional group. Furthermore, selectivity and sensitivity are often inversely related. Selective detectors are generally thought of as being sensitive for particular elements or compounds, but their blindness toward solvent and column bleed is an equal or greater benefit.

1. Alkalai Flame Ionization Detector (Thermionic Detector)

Ionization detectors have been made more selective by several modifications of the basic FID and helium ionization or cross-section detectors. The "thermionic detector" (TID), more aptly termed "alkalai FID" (AFID) evolved from studies of thermoelectric emission (52) at elevated temperatures. Cermer (53,56) developed the first AFID for gas chromatography based on the physical studies of Rice (54) and the leak-detector made by White and Hickey (55).

The mechanism of the AFID is not well understood,

but Bocek and Janik's work (32) on FID phenomena has been used extensively in attempts to understand AFID processes. Brazhnikov (51) has reviewed the enormous mass of data concerning the AFID, and has concluded that the true nature of the problem is perplexing. What is certain is that all AFID's function by the production of an increased ion current due to the presence of halogen (58,59), phosphorus (60), sulfur (62), heavy metals (63), or nitrogen (61,64) in a detector body containing a heated alkali salt. Although the first studies on the AFID (66), were aimed at increased halogen sensitivity, the preeminence of the electron capture detector has shifted applications efforts toward phosphorus and nitrogen detection. Early AFID workers placed an alkalai metal salt pellet around the flame of a commercial FID. However, results depended on the artfulness of the chromatographer, and detectors made in this manner were neither stable nor long-lived. By monitoring ionization at several points (67) along the flame axis, it is possible to have good (10^3 fold) selectivity for phosphorus over nitrogen. Minimal selectivity is found in the opposite situation. Selectivity for P or N over carbon is nearly five orders of magnitude. Perkin-Elmer Corp. workers (68) and Scolnik (69) at Varian Associates have significantly improved the AFID's response and stability by electrically heating a salt ring concentric about the

flame. Hewlett-Packard (70) will soon introduce an AFID which uses a hydrogen glow discharge rather than a flame. That development gives credence to the Brazhnikov argument (57) that photoionization from the salt surface might be important. It also appears that halogens cause an increased ion current (58) by increased volatilization of the salt. Conversely, nitrogen and phosphorus do not increase salt volatility, but do increase alkalai metal ionization (65).

Good selectivity (10^4) for N or P over halogens can be maintained for commercial systems, and the AFID response is linear from the detection limit (10^{-11}g N, 10^{-13}g P) to 10^{-7}g N or P. The response is also extremely sensitive to carrier and fuel flow rates, with 0.01 ml/min H_2 flow rate variation easily detectable and troublesome.

Although the AFID is used for nitrogen and phosphorus detection more frequently than for halogen analysis, it can be modified (58) to detect fluorine compounds by on-line catalytic exchange of chlorine in heated $CaCl_2$ crystals for fluorine. Nowak and Malmstadt (71) modified the AFID concept by simultaneously monitoring the sodium emission and the ion current produced. Slightly increased sensitivity over the usual AFID was found for their "sensitized flame detector", but no commercial development has occurred. Other "sensitized flames" have used light emission and ion current from copper foil in the flame to detect halogens (74,75).

2. Electron Capture Detector

The electron capture detector (ECD) was developed by Lovelock and Lipsky (80) from the helium ionization detector (HID) after their observation of negative responses by the HID to several classes of compounds. In the HID, beta particle-generated helium or argon metastables (76) produced Penning ionization of analyte compounds, which resulted in an increased cell current with increasing analyte concentration. The ECD response is a function of the decreased current produced as analyte molecules capture electrons produced by the beta emission. As a result, early approaches used the assumption of a Beer's Law relationship, $I = I_o e^{-kcx}$, where I_o and I are the currents measured with no analyte and with analyte of concentration, c, with molar electron absorptivity, k, in a cell with proportionality constant, x. As with conventional spectrophotometry, the logarithmic relationship made the linear dynamic range (LDR) of the ECD small (two orders of magnitude or less). It is this lack of linearity which has been most troublesome to ECD users. With such a small LDR, different portions of a chromatographic peak may have different molar responses.

Purnell (85) derived an expression for maximum peak concentration in terms of the adjusted retention volume, V_r^o, the number of theoretical plates N, and the mass injected m:

$$C = \frac{N^{1/2}m}{(2\pi)^{1/2}} (V_r^o) \qquad (11)$$

this equation predicts that the ECD response should vary with peak width, as was demonstrated experimentally by Mendoza (86).

Calculational modifications have been made to give a larger useful LDR by means of a log divider network (95), and by several mathematical rearrangements of the original Beer's Law type equation. Lovelock (88) proposed that $kc = (\frac{I_o - I}{I})$ should be used rather than $kc = (\frac{I - I_o}{I_o})$. The LDR was appreciably improved, but at capture efficiencies of 0.8 or more, precision and linearity collapsed. Error propagation of $kc = (\frac{(I_o - I)}{I})$ is expressed as $\frac{\sigma_c}{kc} = [I = (\frac{I_o}{I})^2]^{1/2} \frac{\sigma_I}{(I_o - I)}$. As $I_o - I$ is maximized, the bracketed term dominates and, for $(I_o/I) = 1$, 9, and 99, the bracketed term reaches $\sqrt{2}$, ~ 9 and ~ 99. Therefore, although the linear range is approximately 10^4, non-linearity occurs at low concentration. Other calculational methods give the opposite effect (89).

Non-linearity and imprecision in the ECD are not solely calculational. The original ECD design (80) utilized a small dc potential (5-15 volts) between concentric electrodes optimized for each compound. The small potential allowed space charges to form at the anode and cathode due to the different mobilities of electrons and positive ions. Response varied randomly with space charge formation. An asymmetric detector cell

with carrier flow from anode to cathode (90) partially alleviated the problem. At the high accelerating voltages needed to realize the full value of the asymmetric design, the electrons were collected at the anode before they could react with analyte, and sensitivity decreased sharply.

A pulsed cell voltage was used by Lovelock (91) to provide an intense (50 volt), short duration (0.5 μsec), low duty cycle (1:200) pulse. Sensitivity and linearity of the pulsed ECD are improved if a mixture of 5-10% methane in argon is used for the carrier gas. The large methane cross-section causes the high energy primary electrons to reach thermal equilibrium, which results in a more nearly constant concentration of uniform-energy electrons. Analyte molecules are not able to modulate the average electron energy, and the resultant response, as the electrons already are of low energy. The greater electron drift velocity (6.0 cm/μsec in CH_4/Ar vs. 0.5 cm/μsec in N_2) also allows the free electrons to travel between the source foil and the anode during the pulse. Wentworth, Chen, and Lovelock (92) analyzed pulsed EC detection and correlated known electron affinities, half-wave potentials and ECD responses for many types of compounds.

Although the pulsed ECD has a larger dynamic range than the constant voltage ECD, its poor sensitivity (93), its need for a special carrier gas, and its greater

complexity (94), limit its common use, and commercial pulsed ECD's are generally offered with dc capability.

The major problem in achieving sensitivity and linearity with dc or pulsed ECD's is that the current measured varies with the analyte concentration in a non-linear manner. Constant current EC detection (94) (CCECD) has overcome that problem by use of a pulse train whose frequency varies with analyte concentration such that the total current monitored is constant. The CCECD signal is a function of the number of pulses applied per unit time. Maggs et al. (87) proved that the frequency difference (f_o-f) is directly proportional to the sample concentration within the cell, and that there is an inherently linear relationship between integrated pulses and sample mass. Of course, reality is somewhat different, but the variable frequency ECD is certainly superior to all other ECDs (97), although a small improvement is still evident with CH_4/Ar over nitrogen carrier.

The bias pulse used in the CCECD is long enough to collect all of the electrons at the anode, but short enough not to collect the slower positive and negative molecular ions. Thus, the number of free electrons in the detector cell becomes essentially zero after the pulse. While the bias voltage is off, the electron concentration, N_e, changes due to constant electron production and electron attachment at a rate proportional

to N_e and to the number of molecules present, N_m. That is: $\frac{d\,N_e}{dt} = k_o - K\,N_m\,N_e$, for one electron-capturing species. At $t = 0$, $N_e = 0$, therefore, $N_e = \frac{k_o}{k\,N_m} \cdot (1-e^{-kNt})$. For short pulses, at frequency f, which collect a charge Q, each pulse will collect $Q = \frac{k_o q}{k\,N_m}\,(1 - e^{\frac{-k\,N}{f}})$. The charge of one electron is q, and the average current, I, is

$$I = \frac{k_o q}{k}\,\frac{f}{N_m}\,[1 - e^{(\frac{-kN}{f})}] \qquad (12)$$

Therefore, for a constant current, I, the frequency will vary directly with N_m. The upper concentration limit should depend on the initiation of pulse overlap, and low frequency/low concentration limits result from the need for the pulse period to be short compared to other electron loss mechanisms. This allows the intended electron capture process to dominate. However, the large electron affinity of many compounds may actually cause complete depletion of free electrons. This effect has been used for coulometric GC analysis with an electron capture detector (107).

All of the ECD designs are affected by the choice of radiation source. Alpha-particles produce so many electrons per particle ($\sim 10^5$) that pulse noise is excessive, and gamma-rays are too inefficient as electron-producers. A low energy beta-particle will generally produce a more

useful number of electrons (2-10 per beta-particle). Technetium-99 and Strontium-90 produce excessively strong beta-particles which make the detector act like an argon ionization detector, rather than as an electron capture detector. Although ionization always increases in the presence of analyte, an electron concentration decrease results from a greater tendency by analyte to capture electrons than to produce them. If the ionizing particles are too energetic, ionization will dominate. Therefore, the choice of source nuclide generally is made between tritium (18 keV) and nickel-63 (60 keV). Both have adequate half-lives (7-1/2 and 85 years, respectively) and moderate energy beta-particles. The low specific activity of Ni-63 is more than compensated for by its longer half-life, greater high-temperature stability, and higher energy beta-particle. The slightly higher-energy beta-particle allows operation with a dirtier ECD cell and longer intervals between cell cleaning. The high-temperature stability of the nickel foil or nickel plate allows high cell-temperature operation, which further decreases liquid phase contamination. A high cell-temperature also aids in maintaining a constant cell temperature, which is important because of the temperature dependence of the electron-capture phenomenon (98,105). Use of the EC radioactive source also entails the semi-annual AEC (ERDA) "wipe test" to detect radioactive

contamination (99). Kahn and Goldberg (100) investigated the radiation hazards of two commercially available tritium-based ECDs, and found them to evolve 10^6 times the allowable (99) tritium level. They recommended venting the ECD into a hood. Improved tritium sources are available (101,102), but none is as trouble-free as is the usual nickel source.

When the ECD is working at its best, it is the most sensitive GC detector. However, its response to new compounds is quite unpredictable, as shown in Table 2. Calibration of the ECD is essential because of the enormous variation in electron affinity of apparently similar compounds (103). Electron affinity generally increases in the order F < Cl < Br < I, and response to additional halogen or other electron-attaching groups is disproportionately great. This is illustrated by the relative responses (104) of trifluoroacetyl testosterone (0.012) and of chlorodifluoroacetyl testosterone (1.67), and a sensitivity difference of 10^3 for 1,2-dichlorobutane and 1,2-dibromobutane (89). Pellizzari (106) has discussed extensively the relationship between structure and response for EC detectors, but prediction of an ECD response factor is difficult at best.

The electron capture detector is sensitive and now fairly reliable, but possesses many negative qualities in routine use. It is not compound-, group-, or element-

specific, although it is highly selective for compounds with strong electron affinity and is the ultimate in ionization detectors.

3. Electrochemical Detectors

Electrochemical analysis is intrinsically desirable by virtue of its selective and, often, absolute nature. The first electrochemical chromatographic detector was developed by Coulson and Cavanaugh (108) for the determination of chlorinated organic compounds. Their argentometric detector, was not nearly as sensitive as was Lovelock's concurrent ECD, but was far more selective for halogens.

Ideally, but not practically, coulometric detection requires no standardization. The GC effluent, mixed with oxygen or hydrogen enters a catalytic reactor, which causes the compounds to be oxidized or reduced. The simple acid or base anhydrides are then continuously dissolved in flowing water, which enters a coulometric cell in which titrant is generated. The most commonly used titrants are coulometrically generated OH^- and H^+. Coulson (108) also used a voltage- and current-variable, four-electrode dc system to maintain a constant concentration of silver ion used to titrate chloride or other amenable ions produced in the reaction cell. Later workers (109-111) have used much the same system with various titrants except for many variations in catalysts, selective scrubbers, and cell size.

Martin (113) determined nitrogen by its hydrogenation, and Littlewood and Wiseman (112) identified and measured alkenes by their dehydrogenation (and resultant increase in cell hydrogen concentration) to alkynes. Both measured hydrogen gas concentration potentiometrically. Sulfur may be measured by oxidation to SO_2 or by reduction to H_2S (114,116). However, iodometric or bromometric titration will not detect SO_3 formed catalytically, and chlorine and nitrogen containing compounds (110) will interfere by the formation of small amounts of Cl_2 and NO_x. The reductive mode is subject to nitrogen interference in the coulometric titration. Mercaptans have been titrated with silver ions without combustion (115). Carbon monoxide was oxidized selectively at a platinum electrode (124,215,216).

Selectivities of the coulometric detector for nitrogen and halogens over other elements (117) are generally at least 1000-fold, but other elements are often less selectively detected. Cell dead volumes are large (1 ml is common), sensitivities (110,117) are only 4 ng for chlorine and nitrogen, and linear dynamic ranges are generally less than three orders of magnitude. Response times are often long (0.5 sec), and peak shapes, which affect quantitation, are distorted. The detector is often troublesome to use in routine operation, but its user-variable selectivity compensates for its faults.

Calibration is necessary because the gas-liquid contactor is not totally efficient.

Lovelock (118,122) has developed the most interesting modification of an existing detector the author has yet found. He proposed that, in a miniature (1 cm x 2 cm) chromatograph, chemically machined into a ceramic support, a hydrogenation cell could produce hydrogen carrier gas which would, after traversing the column, reenter the coulometric cell and be measured potentiometrically. The potential is developed across a palladium-silver membrane on one side of which is the carrier/effluent and on the other a molten (220°C) KOH/LiOH half-cell (133).

Electrochemical detection of the same catalytically-produced compounds is also possible by measuring their solution conductance. The electrolytic conductivity detector is quite selective for nitrogen and chlorine (109,119), and sensitivity and selectivity have been improved further by use of non-aqueous solvents in place of water and by use of an AC conductance monitor (120). The conductivity detector signal requires no amplification or other signal processing and is relatively free of carrier flow deviation effects.

The two major electrochemical detectors had nearly comparable capabilities until Hall (120) redesigned the detection cell, separator solvent system, and electronics (123). Detection limits, according to the

manufacturer, Tracor Instrument Co, were reduced to 0.01 ng for N, X and S, and linear dynamic range was increased to nearly 10^5. There is no firm reason that coulometric detection could not also be improved by many of the same means. Both detectors are commercially available (Tracor Instrument Co. and Dohrmann/Envirotech) and are commonly used in conjunction with an ECD to confirm the identity peaks from pesticide residue samples (121).

Sulfur, chlorine and fluorine have been measured in effluent reaction products with ion-selective electrodes (152,154), and chlorine/fluorine ratios have been determined by the use of two selective electrodes in series (155). The response was predictably non-linear, and sensitivity, selectivity, and dead-volume were not adequate. However, the concept is valuable and improved performance should be expected in the future.

4. Spectrochemical Detectors

Element-specific detection can be provided easily only by atomic spectroscopic techniques. Because of this, many attempts have been made to develop atomic emission or atomic absorption GC detectors.

The flame photometric detector (FPD), initiated by Van der Smissen (129) and developed by Brody and Chaney (127) and Braman (128), uses molecular emission from a

cool, hydrogen-rich flame. Though metals (131,132) and many non-metals can be detected by the FPD, its major use is for sulfur and phosphorus-containing analytes. The molecular emission band heads of S_2 and PO occur at 394 nm and 526 nm, respectively, for the flame conditions cited. The band emission of C_2^+ may also be used for carbon analysis (128), but with poor sensitivity. Boron compounds have also been measured by the FPD. Commercially available FPDs are used to detect sulfur and phosphorus and act as a FID simultaneously. This is necessary because sulfur, phosphorus, and carbon mutually interfere in the FPD (130). Interferences vary with analyte concentration and phosphorus emission interferes more with sulfur than conversely. The band emission of CN and C_2^+ interfere at the 0.01% carbon in gas level for both sulfur and phosphorus (147), and several sulfur-free compounds appear to quench S_2 emission (148). Structural effects are also common (149), as would be expected for any such low energy system. Sulfur sensitivity and specificity have been improved (150) by conversion of effluent sulfur to H_2S (150) and by use of subtractive scrubbers (151).

Sulfur emission (S_2) is dependent on the square of the sulfur concentration; therefore, a semi-log intensity/concentration plot must be made graphically or electronically to "linearize" the detector response. Emission is temperature- and flow-sensitive (134,135), and

linear dynamic ranges are 10^2 (sulfur, log-log) and 10^3 (phosphorus), limited by self-absorption (149). Sensitivities for sulfur and phosphorus are 3×10^{-8}g and 10^{-10}g, respectively.

The use of the FPD with metal chelates and halides (158) is particularly attractive because of the corrosion resistance of the detector itself. Sensitivities for the metal chelates approximate those for the FID. The FPD is quite reliable and convenient in routine use, even if not truely element specific. However, the FPD does require venting of the solvent plug to prevent flame-out.

The FPD selectivity for halogens has been altered by the addition of indium or copper mesh (136,137) in the flame to produce Cu-X or In-X emission at 360 nm. Control of the indium pellet temperature is necessary for maximum sensitivity (153) and reduced interference from phosphorus and sulfur. The detector is sensitive (10^{-9}g chlorine), has a linear dynamic range of 10^5, and is selective for chlorine by 10^4 over carbon and phosphorus. However, it responds strongly to sulfur. No structural/functional group effects were found by several authors, but it is rather unlikely that this detector is free of such problems due to the relatively moderate-temperature environment of the hydrogen-rich flame. The halogens (Cl, Br, I) mutually interfere, and it is not possible

to identify individual halogen emissions. The detector is blind to fluorine, but an analogous fluorine-selective detector was made by Gutsche and Herrmann (138). Calcium vapor added to the flame gave CaF band emission at 530 nm with a detection limit of 50 ng. Temperature-programming could be used, since the detector was neither carbon- nor temperature-sensitive.

A sodium-sensitized flame (AFID) was also modified (139,140) to enable chlorine detection by monitoring sodium atomic emission (589 nm). The sensitivity (10^{-9}g halogen) was comparable to that of the other FPDs, but linearity was only 10^2. Temperature programming caused a large, negative drift in the baseline signal.

Atomic emission or absorption, rather than molecular emission, was the obvious next improvement to photometric detectors. Morrow et al. (141) used the 2516 Å Si emission line from an oxyacetylene flame or atomic absorption of the same line in a nitrous oxide-acetylene laminar flame. Both modes gave 300-800 ng Si sensitivity, but linearity was poor (10^2), probably because the flame used was unable to break, or eliminate formation of Si-O bonds. Atomic absorption (AA) has also been used to determine lead alkyls (142) and mercury by non-flame atomization (143,144).

Metal chelates have been used in GC (157,159) by many workers to effect concentration of metals from

dilute aqueous solutions and to free metals from complex matricies which may interfere with conventional atomic spectroscopic methods. Maximum sensitivity is generally obtained if halogenated chelates are used with an ECD, but decomposition products of the chelates then also give spurious signals, which reduce sensitivity and selectivity. Wolf (156) has introduced GC effluent metal chelates directly into a commercial atomic absorption spectrophotometer, with a resultant detection limit for chromium from a biological matrix (NBS SRM 1751 orchard leaves) of 1.0 ng. The solvent front gave a small signal due to light scattering, and it was necessary to heat the entire AAS mixing chamber to prevent condensation of the hexafluoroacetylacetonates.

Atomic absorption techniques are somewhat limited in linear dynamic range and in the number of elements which may be assayed simultaneously, and atomic emission or atomic fluorescence would seem to be more promising, as multi-channel detectors become increasingly useful and practical. Winefordner, Vickers and Overfield (145,146) have used signal-to-noise ratio concepts to derive an expression for calculation of the detection limits for flame emission gas chromatography. A significant problem alluded to in their discussion of flame emission detectors is that of incomplete atomization. All of the reaction detectors previously discussed in this chapter

have suffered from structural/functional group effects because they were insufficiently energetic to atomize totally the effluent compounds. The optimum spectrochemical GC detector should alleviate this problem completely.

Glow discharges have been used to atomize and excite GC effluents (160,161), but have not overcome matrix and molecular emission problems. Poulson (160) measured molecular and atomic emissions from a Tesla glow discharge as well as its conductance. Detection limits were comparable to those of the FID, and it was possible to identify several molecular emission spectra. Similar plasmas are so gentle toward organic compounds that isotopic-labeling of sensitive biologicals has been accomplished by passage of the vapors, mixed with D_2O or T_2O, through the glow. Such plasmas, in argon, also emit primarily red arc-like lines, rather than the blue spark-like lines of a more energetic excitation system. The inability of such detectors to provide purely atomic emission is, therefore, understandable.

McCormack, Tong, and Cooke (162) first used a 2450 MHz electrodeless discharge (EDL) to produce atomic and molecular emission from GC effluent. This work followed McCormack's similar use of the plasma above a hydrogen-oxygen flame as an excitation source for gas chromatographic detection (163). Though greater atomic emission

was attained with the EDL, the emission intensities of CN, C_2^+, C-X, and OH bands were used analytically, and the expected logarithmic behavior was found. Molecular emission also greatly limited selectivity for hetero-organics, particularly chlorinated hydrocarbons. When atomic emission could be induced, as 2062 Å line for iodine, selectivity for iodine atoms over carbon was 10^4. Structural effects were observed, and atomic carbon emission (2478 Å) was miniscule. Phosphorus emission occurred at the 2534, 2535.7, 2543.3, and 2554.9 Å atomic lines, and PO molecular emission bands at 3240 Å and 3271 Å were superimposed on the CN bands. Band emission from PS appeared in the 4600-4900 Å range. Many other unassignable emission lines were found. Microwave power level changes unpredictably affected the emission intensities from analytes with similar bonds. Sensitivity for carbon, iodine, and chlorine was improved by Dagnall and coworkers (164) by use of higher microwave power and a different cavity design. The band emission of Cl_2 at 256 nm was measured, rather than the 278.8 nm C-Cl band used by McCormack, and selectivity was markedly improved. At lower microwave power, the 182 nm atomic sulfur line was quite strong. All sensitivities (C, S, P, Cl, I) were in the 10^{-7} to 10^{-9} g range, but selectivities for sulfur and phosphorus over carbon were only 460 and 150, respectively, due to carbon band emission.

Microwave plasma GC work has been extended to include herbicide (165), pesticide (166), and metal chelate analysis (168). The use of a low pressure helium plasma (167,169) improves sensitivities, but retention times are significantly shortened and oxygen and nitrogen generally must be used as scavengers for removal of tar deposits on the cavity walls. West (170) compared 30 MHz (RF) and 2450 MHz (microwave) plasmas as GC detectors, and Denton (171) discussed the spatial distribution of atomic and molecular species in the induction coupled plasma.

The microwave and radio frequency plasmas are superior to the glow discharge detectors, but they are limited in sensitivity by the opposing effects of atomization efficiency and background emission. Power supplies for all continuous, highly energetic plasmas are large and expensive. RF plasmas are generally less expensive than microwave plasmas, are operable at atmospheric pressure with almost any carrier, and are more easily maintained. The microwave plasma GC detectors require much less shielding, are more easily thermostated, and are commercially available (172), albeit at $25K per system. Both types of plasma are easily extinguished by the solvent plug, are physically altered by the presence of analyte, often give incomplete atomization, show functional group effects, and are often troublesome in routine use.

Bramen and Dynako (173) conducted gas chromatograph effluent into a conventional dc arc, with resultant detection limits equivalent to those obtained with the RF and microwave plasmas. Emission signals were obtained from a mixture of atomic and molecular species, as would be expected for such a low-power system.

A more energetic plasma than that in a dc system is easily found in the conventional spark. During the period of current conduction, electron concentrations and temperatures are much higher than in the conventional, continuous plasma, and molecular species should be completely eliminated. Dagnall and coworkers (174) used a conventional ac spark into which organic compounds were carried by a nitrogen or argon stream. Atomic iodine emission was observed at 2062 Å, but other species observed were diatomic (CN, NH, N_2, CH, C_2^+) and were quite similar to those from a continuous plasma. Argon produced larger continuum and analyte emission, and organic vapors in the electrode gap lowered gap resistance. Emission was monitored continuously, and continuum emission seriously limited the detector's usefulness.

Time-resolved emission spectrometric measurements with a high-frequency, very short duration miniature spark gave quite different results (175,176). Atomic analyte emission was measured apart in time from the majority of the continuum and molecular emission, and most atoms with

strong emission lines in the visible and near ultraviolet were excited. Easily ionized species, such as the alkalai metals, and elements with a large number of possible transitions (e.g., iron) gave poor emission signals, but all non-metals, except fluorine, had adequate detection limits. No interelement or temperature effects were found. Linear dynamic ranges for all usable elements were large (10^4 or greater), and element specificity was effectively complete. This detector is the subject of the work described here in later chapters.

5. Unclassified Detectors

An enormous number of GC detectors have been developed which are uncommon or quite specialized. The foremost of such detector is, of course, the mass spectrometer. GC/MS has been used extensively in nearly every conceivable application. The expense of a GC/MS is enormous, and the form and quantity of data necessitate computer acquisition. Furthermore, sensitivity is not always superior to that obtained with conventional ECD gas chromatography (177). The use of quadrupole MS and microprocessor-based systems should decrease costs, although it will not improve sensitivity. The use of GC/MS in clinical chemistry (178) and general analysis (179) have been reviewed recently. Therefore, the technique

will not be discussed further here.

Plasma chromatography (PC), which is similar to chemical ionization mass spectrometry in many ways, affords the determination of molecular and recombinant-ion mobilities in atmospheric pressure nitrogen carrier (180). From mass-mobility-charge relationships, it is possible to identify ions and, hopefully, their parent molecules. Several workers tried to correlate CIMS and PC spectra (181,182), and Revercomb and Mason (183) definitively treated plasma chromatography (PC) in general.

Cram and Chesler (184) first coupled PC and GC without the use of a molecular separator. By rapid (20 nsec) scanning of ion mobility spectra, they were able to identify and quantitate several "Freons" separated by GC. More recent work by Keller and Metro (185,186) indicates that GC/PC spectra are concentration dependent and that PC is not qualitatively useful due to poor resolution. Success with GC/PC has been predicated on the analysis of very simple compounds.

Martin and Smart (203) first used infra-red spectrophotometry to detect organic compounds following their conversion to carbon dioxide over a copper oxide catalyst, but sensitivity was low (100 ppm). The advent of rapid-scan infra-red spectrometers has made possible commercially-available "routine" on-line GC/IR systems (187). Effluent condensation ("cold-trapping") followed by off-line IR

is more sensitive, less expensive, and has higher resolution than does on-line IR (188), but the difference between them is decreasing rapidly. It is now possible to use a six second scan from 4000 to 670 cm^{-1} with resolution of 5-10 cm^{-1} and obtain vapor spectra (189). Rapid scan ultra-violet spectrophotometry and molecular fluorescence have also been used for GC detection (190,191) for the analysis of polynuclear aromatics and are commercially available. Selectivity and sensitivity were widely variable and of use in specialized situations.

Of even greater specificity, and more narrow utility, are the biological detectors. These are generally physiologically responsive body parts from pheromone - target insects. Shell Development scientists (192), among others, have used insect flight muscle to detect sex-attractants in the extremely complex mixtures resulting from female roach disintegration. Other workers (193) have used frog olfactory nerves similarly, but the most widely used biological detector has been the human nose (194). Flavors, fragrances, vaginal odors (195), and industrial wastes have been identified at nanogram and subnanogram levels with excellent qualitative accuracy (196).

No chromatographic detector is perfectly suited to all determinations. Therefore, multiple detectors and peak resolution by differential detector response (197,

198) and pattern recognition (199) are increasingly used to solve chromatographic and detection problems. Each of the detectors described has a place, somewhere, even if only in conjunction with another detector (73).

CHAPTER III

THE HISTORY OF LIQUID CHROMATOGRAPHIC DETECTORS

High pressure liquid chromatographic (HPLC) detectors are either modified GC detectors or inherently solution-based systems. Because of the very small carrier flows used, a major design consideration for either system type is the minimization of detector dead-volume. Selectivity for elements or functional groups is also important because of the difficult separations from complex samples attempted with HPLC. High sensitivity is desirable, but it should be coupled with selectivity and freedom from solvent interference. LC detectors have been reviewed (213-216) by Veening and others.

A. Modified Gas Chromatographic Detectors

Solvent removal is the major obstacle to the use of the common GC detectors with HPLC. Such systems also commonly destroy the sample, and, therefore, are useless for many LC applications. The conventional "moving wire" transport functions by the wetting of the surface of a wire with column effluent, followed by sample desolvation and pyrolysis. The pyrolysis products are then swept into a conventional GC detector, generally a FID, argon ionization detector or ECD. Sensitivity has been improved by nickel-catalyzed reduction, of carbon dioxide

produced in pyrolysis prior to FID or AID quantitation (205). A FID/wire transport combination has a detection limit of 100 ng lipid (210). Dead volume varies with the detector design (224), and only one such transport is commercially available (206). Moving wire and membrane interfaces have been described for LC/MS (207,208), but improvements are still needed. Many modifications have been made, and include the use of coated wires (209), steel springs (210), and a coated metal gauze disc (211,212).

Electron capture detection (216,218) and alkalai flame ionization (217) have been used successfully for hetero-atom detection, although the large dead volume produced tailing of peaks. The selectivity of ECD/LC has been improved by on-line formation of fluoroderivatives (251). The photoionization (PID) detector (225) and the gas density balance (226) have also been used following desolvation of the effluent.

LC effluents have also been aspirated directly into a conventional atomic absorption (AA) apparatus (219). AA has been used to detect chelating agents which removed copper from a copper-loaded ion-exchange column (220). Flame emission has been used to detect phosphorus and sulfur (FPD) molecular emission (221) and metals (222). Non-flame AA has been used to detect mercurials (223).

Improved atmospheric pressure ionization techniques have made on-line mass spectrometry (238) and plasma

chromatography more practical. As with the other GC detectors used for LC, the properties inherent in the device as a GC detector accrue to it as an LC detector, albeit with the disadvantage of increased system dead volume. Detection limits are comparable to those obtained with the GC versions.

Solution detection of LC analyte is inherently advantageous because of the lower overall dead-volume without a dsolvation system. However, element-specific detection is not then possible, and the analyst must be satisfied with less-sensitive, less-specific methods.

B. Optical Detectors

1. Spectrophotometric Detectors

Molecular absorption spectrophotometry is the major LC detection method (237). Instrumentation is available with a maximum sensitivity of 10^{-4} absorbance units (A) full scale. Compound sensitivity, of course, depends on the absorptitvity of the compound at usable wavelengths. Double-beam systems are commonly used to compensate for fluctuation in the solvent and to conceal the effects of unwanted absorbing compounds in post-column reaction techniques (239).

Derivatization reagents are now available for a large variety of functional groups such that a single wavelength

(254 nm) detector may be used for most work. Many of the derivatives are made before the separation and, therefore, affect the method of separation. All of the tagging compounds listed are available from Regis Chemical Co., Morton Grove, IL, and other sources.

Variable wavelength detection is necessary for the detection of saccharides and other compounds which do not absorb at those wavelengths (254, 368, 405 nm) at which low-pressuremercury lamps emit strongly. Pre-existing, obsolete, instrumentation, such as the Beckman DU (241), often is modified to avoid the high ($4-8,000) cost of commercially available variable wavelength LC detectors. Bylina et al. (242) used a mechanical rapid-scanning monochromator and Dessy (243) and McDowell and Pardue (244) have used diode array detectors with polychromators for LC.

An alternative to variable wavelength detection is the post-column, continuous formation of absorbing species. The use of 2,4-dinitrophenyl hydrazones has improved sensitivity for ketosteroids (245) to 1 ng. Fatty acids were benzylated (247) and carbohydrates reacted with sulfuric acid (248) to enhance UV absorption detectability. An infra-red laser also has been used to detect organic compounds by their C-H stretching vibrations (228). Hrinda (249) has developed a general flow-through reactor for on-line conversions of effluent.

2. Fluorescence Detectors

Fluorescence detection is commonly used because of both the increased sensitivity and selectivity, and the decreased dead-volume required for most fluorescence cell designs. Unfortunately, fluorescence detector cells generally are encumbered by multiple reflections, refraction, fluorescent solvent impurities, and fluorescence from adsorbed materials in the cell itself. Martin (250) has developed a novel fluorescence flow cell intended to alleviate several of these problems. Column eluent forms uniform size drops which fall through an exciting light beam. A reflective sphere surrounding the falling drops acts as an optical integrator. Using the cerate oxidation fluorescence method of Katz (251), a detection limit of 1 nanomole is obtainable with susceptable compounds. The fluorescence of Ce(III) has been widely used to detect compounds which reduce the non-fluorescent Ce(IV) ion. If the Ce(IV) reduction potential is modified in solution, selectivity may also be changed (252). Fluorescamine is commonly used to detect primary amines by fluorescence and secondary amines by absorption spectrophotometry.

3. Refractometric Detectors

Refractometric detectors (236) employ the eluent density changes which occur as analyte molecules enter the detector. Refractive index changes are measured commonly by the Fesnel and Christiansen effects.

The Fesnel-type (253), also known as "reflection-type", functions by the impinging of two collimated light beams passing through a prism on two glass-liquid interfaces formed by sample and reference solvents. Light which is not internally reflected at the glass-liquid interfaces is reflected to a dual photometric detector. Previous refractometers used for LC detection were of the beam-deflection (254,256) type in which the position of the refracted light indicated refractive index and solution density. More recent reflection-type detectors (256) monitor the intensity of the light reflected at the interface. Except for an exaggerated response to flow-cell bubbles, this form appears to be superior to older deflection and reflection approaches, and is now available commercially (252).

The Christiansen effect refractometer functions by the increasing transparency to monochromatic light of a fine powder in a liquid as the liquid's refractive index approaches that of the solid. In practice, monochromatic light passes through a pair of cells filled with solid particles whose refractive index is equal to

that of the solvent. Eluted compounds change the refractive index of the solution, and decrease the transmittance of the sample cell. Stability, sensitivity, and dead volume are at least equivalent to other RI detectors. Because neither moving parts nor finely polished optical components are needed, the Christiansen effect detector (258) is significantly less expensive than are other RI detectors. Each solid may be used over a range of 0.02 RI units, and must be changed when the solvent is changed. Solvent programming is more difficult with the Christiansen effect RI detector than with other RI detectors, but no RI detector is exceedingly useful with solvent programming.

All RI detectors also suffer from temperature-induced drift. As the temperature varies, the solvent density and refractive index also change. Many attempts have been made to thermostat RI cells adequately, but the sensitivity limit seems to be approximately 10^{-7} RI units. Detection limits vary enormously with compound and species. A somewhat analogous detector, which uses optical rotary dispersion, has been developed by Thomas and Tappin (240). Dielectric constant detectors, discussed under electrochemical detectors, are closely related to RI detectors.

Spectrophotometric detectors of any sort suffer from the problem of attempting to pass light through a pair

of small cylinders without undue production of reflective and refractive artifacts. None of the spectrophotometric detectors is truly universal and all must be calibrated for each compound analyzed. Often the carrier solvent can hinder solution detection just as much as does desolvation for the converted gas chromatographic detectors. Ideally, the HPLC detector should be blind to solvent and absolute in response.

C. Electrochemical Detection

Absolute response is very nearly possible only from electrochemical detectors. Polarographic detection, with a dropping mercury electrode, of low pressure LC effluents was first used in 1952 by Kemula and others (260,262) for the analysis of metal ions, pesticides, nitro compounds, and other reducible species. Koen (261) redesigned the detector cell for smaller dead-volume and shorter drop time. The dropping mercury electrode allowed only reductive mode analysis, but detection limits for parathion and methyl-parathion were in the low nanogram range. Detection limits were greatly affected by the chromatographic conditions and the relatively large dead-volume of the cell.

Kissinger's group (259) has developed a thin-layer chamber with a carbon paste electrode whose active volume

is approximately 0.7 µl. This is an order of magnitude smaller than that of the best commercial UV detector. The dead-volume between the column outlet and detector electrode is 8 µl. A potentiostat is used to maintain the applied potential, and amperometry is used to measure species concentration.

Because of the use of the carbon paste electrode, which must be quite pure, the detector functions best in the oxidative analysis of amines and similar species. Detection limits are in the low picogram range for suitable compounds, and discrimination is generally possible, though not complete. The analysis of biogenic amine has been the primary subject of Kissinger's work, but the detector should also be excellent for aminoglycoside antibiotics and similar compounds which are difficult to detect by optical methods. This detector is now available commercially (263) at a very modest cost, but many analyses of new compounds may require the use of cyclic voltammetry to determine the electrochemical properties of the desired species and best detector and solvent combination. Electrochemical detectors for HPLC recently have been reviewed by Kissinger (264) with emphasis on his group's work, and by Buchta and Papa (265).

CHAPTER IV

A SPARK EMISSION DETECTOR FOR GAS CHROMATOGRAPHY

The purpose of this work has been the development of a practical atomic emission detector for gas chromatography. Other element-selective detectors suffer variously from non-linearity, functional group and "carbon number" effects, inter-element interference, extreme complexity, and high cost. To justify the efforts of development, the new detector must avoid all such failings, and should be effectively, a "poor-man's mass spectrometer".

A. Construction of the Nanosecond Spark Source for Chromatographic Detection

The coaxial spark used by Zynger and Crouch (267) for fluorescence life-time measurements was chosen for this work as the basis for the spark emission detector (SED). Coaxial capacitor design produces a low-inductance, controllable-capacitance spark of high power and very short duration ($t_{on} \tilde{=} 50$ nsec). Zynger's work (266) demonstrated the feasibility of isolating the initial spark emission from the longer afterglow by time-resolved spectroscopy. In the present work, the miniature spark has been used to atomize and excite analytes, while minimizing the effects of background emission common to

conventional spark sources. This is possible only by the use of time-resolved spectroscopy. The small total energy and high power of the spark also allow both low cost construction and minimal matrix effects. Earlier work (267) on the nanosecond spark source was directed primarily toward construction of a light source for measuring fluorescence life-times and secondarily toward the development of an atomic emission source. Significant changes in system electronic and geometric design were necessary to adapt the spark discharge system for use as a chromatographic detector. In particular, the data acquisition, spark detection, and sample handling methods were totally reworked prior to any practical use of the NSS for chromatographic detection.

1. Mechanical and Optical Design of the Nanosecond Spark Detector

Preliminary studies of the miniature spark discharge under a variety of operating conditions demonstrated the need for a greater understanding of the physical and chemical processes within the spark. However, prior to the advancement of more elegant work on the spark, it was necessary to develop a convenient, workable system to study. The Nanosecond Spark Source (NSS) functioned well when used with particulate analytes, but large changes in spark environment and character appeared with the use

of gaseous analytes. It was apparent that the uniform distribution of a gaseous substance in the spark gap altered the environment to a far greater extent than did an equal mass of 10-100 μm diameter particulate matter. The solvent plug especially was found to produce a degraded spark performance with simultaneous C_2^+ emission. Molecular species persisted in the spark if impurities were present in concentrations greater than 1-5% in the column effluent gas. The cause of this source of interference was not immediately obvious.

Figure 1 illustrates the important components of the nanosecond spark source. Analyte species enter the spark chamber as either a gas or as small (10 μm) desolvated particles, depending on whether they were from a solution or gaseous source. Analyte molecules are atomized and excited by the spark. Light emitted from the spark gap triggers the digital control of the analog circuits which measure the emission for the spark. Analog data from the photomultiplier tube then is displayed on a chart recorder or storage oscilloscope or is acquired and processed by an on-line mini-computer. Element-specific atomic emission is isolated from the Bremstrahlang and radiation recombination induced continuum emission by time resolution of the signals.

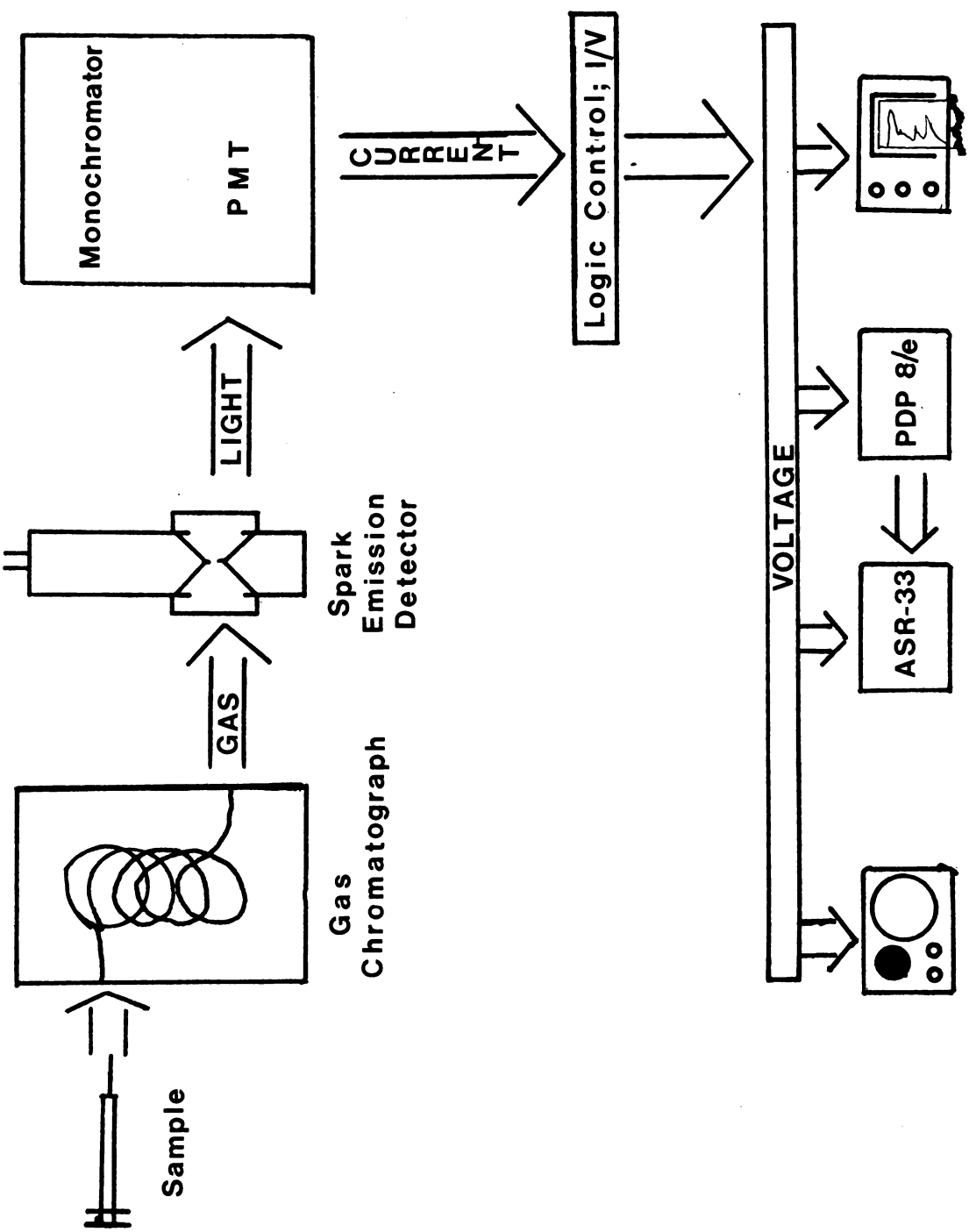

Figure 1. Block Diagram of the Miniature Spark Source.

a. Elimination of the Solvent Overload Effect

In an early attempt to alleviate the overloading of the spark by the solvent plug, a shunt valve controlled by two thermistors was used. The thermistors were upstream from the spark detector and electronically within the feedback loops of two uA741 operational amplifiers. As the solvent peak passed, the thermal conductivity of the carrier gas decreased markedly, which produced changes in the temperature and resistance of the thermistors. The signal from each OA was the input to a transistor switch which controlled a low-voltage, dc solenoid to actuate a sliding valve ahead of the spark. During the passage of the solvent plug, effluent was shunted away from the discharge through the sliding valve. After the solvent peak passed, the thermal conductivity of the carrier gas increased. The solenoid then was actuated to move the sliding valve to the position so that carrier gas was again directed through the spark gap. The added dead-volume required for the thermistor and transfer tube was the major reason for ending this approach. Instead, spark chamber design improvements were made which eliminated the need for a solvent escape valve.

The final design for the detector spark which incorporates the useful features of its several predecessors is shown in Figure 2. Although previous designs had placed the spark outside of the gas chromatographic oven,

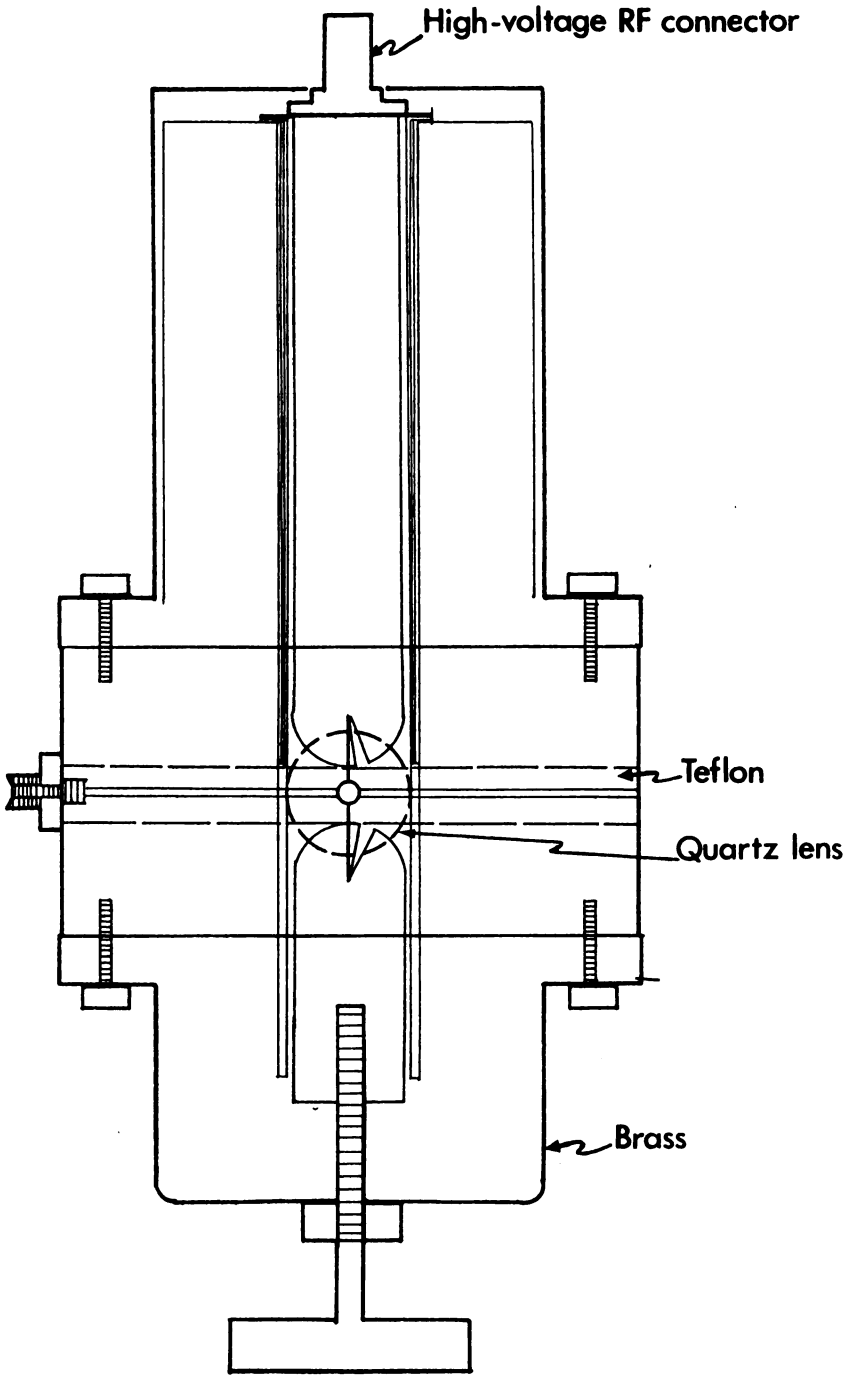

Figure 2. The Nanosecond Spark Source.

the final model could be placed within the laboratory-built oven, outside of a commercially available chromatograph, or connected to a desolvation apparatus for liquid chromatography.

b. Dielectric Material for the Coaxial Capacitor

It was also necessary to find an appropriate dielectric material for the coaxial capacitor. High Molecular Weight (HMW) polyethylene, used by Zynger (266), melted at temperatures far below those commonly used in gas chromatography. "Machinable ceramics" were either difficult to machine or too porous to prevent spark passage through the dielectric. Vitrification was uniformly unsuccessful. An improved ceramic may well be the best dielectric. Extensive experimentation with Teflon, in its various forms, conclusively demonstrated the high impurity content of even the best grade TFE. The cold-forming process used for the production of Teflon bar stock further contributed to the porosity of the finished insulators. A high average dielectric strength was meaningless as an indicator of insulation effectiveness since occasional pin-holes, 0.005" - 0.010" deep, were observed. The dielectric finally chosen was a TFE/silicone combination. After final preparation, the same dielectric was used until completion of the author's work, approximately 1500 operational hours, at temperatures ranging from

ambient to 275°C. Higher temperatures would likely decompose the Teflon.

c. Spark Chamber Design

The spark housing was constructed of a seamless copper tube and the electrodes and main body were machined of aluminum and brass, as indicated. The tube through which sample and carrier gases passed contained only stainless steel Swagelok fittings and Teflon, both machined to minimize dead-volume. The exit tube of the spark chamber was fitted with a 30 cm Teflon extension to carry away toxic effluents and to decrease diffusion of air into the spark gap. Diffusion of air into the spark chamber was further reduced by a second slow carrier gas flow between the outer capacitor plate and outer spark housing, providing a slight positive pressure toward the interior of the spark gap itself. This minimized sample carry-over and possible spark travel across the capacitor end due to the lower breakdown voltage of mixtures of sample effluent, carrier gas, and air otherwise in the spark housing.

Capacitance was varied by use of different diameter interchangeable aluminum capacitor cores with different thickness dielectric mantles. To obtain the lowest possible dead-volume and the greatest simplicity of construction, the spark chamber was placed within the chromatograph oven. No commercially available oven possessed

the required geometry, so one was built in the Chemistry Department shops. It contained a heater wire and autotransformer, a squirrel cage fan, carrier gas valves (Nupro, Crawford Fitting Co., Cleveland, Ohio) and low dead-volume stainless steel fittings (Swagelok). Those fittings which were not commercially available and the injection port itself were machined by the author. Only ballistic temperature programming and isothermal operation were used. The spark housing was held in a fixed mount attached to an oven wall, and a hole was cut to allow photoelectric detection of spark emission and the placement of light sensors for the digital timing circuitry. A 1" diameter, 1" focal length quartz lens was placed 1.1" from the spark axis to project a real, slightly magnified spark image on the monochromator entrance slit.

d. Carrier Gas Purification

Due to the great sensitivity of the NSS and the relative impurity of argon (3) and helium carrier gases, it was necessary to construct a carrier gas purification apparatus. Though helium could be freed of some impurities by passage through a sand-filled tube in a liquid nitrogen trap, argon was not so amenable to such simple treatment since it freezes at just above the nitrogen boiling point.

A series of 3/4" diameter tubes connected by Swagelok

fitting was made, and the contents of each tube were isolated from those of the other tubes by porous glass frits. Successive chambers contained activated carbon, for removal of hydrocarbons, 5A molecular sieve (Linde) for removal of water and small hydrocarbons, and Ascarite for absorption of carbon dioxide. Previous experiments with Ascarite absorbent had shown CO_2 to be the major source of carbon in the argon carrier, though it was not the sole source. Oxygen, detrimental both to chromatographic columns and to oxygen analysis, was removed in two stages. In the first, BASF catalyst removed much of the oxygen while in the second, a commercial preparation (Alltech, Inc., "Oxysorb"), which appeared to be similar to BASF catalyst, reduced oxygen to much lower concentrations than did the common BASF catalyst.

BASF and "Oxysorb" could both be regenerated by passing dry hydrogen through them while heating to 140°C in a muffle furnace. This was most important during experiments with helium, whose oxygen content was generally 100-1000 times that of the average argon sample. Oxygen analyses using helium carrier were difficult without additional pretreatment due to the very rapid exhaustion of oxygen scrubbers. A liquid nitrogen trap generally sufficed during helium carrier gas experiments, although it was not totally efficient. It was also inconvenient to use, as the gas line often plugged with water, carbon dioxide, and liquid oxygen. Gas purification system effects will

be discussed in detail in the appropriate section of each element.

Because of the extreme sensitivity of the NSS, a vacuum syringe cleaner had to be developed. Progressively more faint chromatograms, up to thirty in number, could be produced by repeated injections from a once-used "empty" syringe, even with syringes which contained sample only in the needle (Hamilton 7401). A heated syringe cleaner was constructed of Swagelok fittings and copper tubes and was connected to a water aspirator for evacuation. A similar device is now available from the Hamilton Co., Reno, Nevada. Only with the syringe cleaner was it possible to obtain successive chromatograms without "ghost peaks".

2. Electronic Design of the Nanosecond Spark Detector

a. Power Supplies

Pulsed and dc power supplies both were used for the NSS, and each type had advantages with respect to the other. A Xenon Corp. Model 437A Nanopulser was used to pulse the NSS at repetition rates to 1 kHz. Results were adequate, but it was found that an equally efficient power supply could be made of an automobile ignition coil (Robert Bosch, Gmbh), 6.3 V filament transformer, diode bridge, capacitors, and SCR or Triac.

A direct current power supply was constructed from a Spellman Corp. (Brooklyn, New York) high voltage autotransformer, model UM24P-1500-D, 0-24KV @ 50 μA maximum. Current limiting and voltage output monitoring capability were possible via a voltage divider consisting of ten 50 Ω high-voltage (15 KV max.) resistors and requisite high-voltage insulators and stand-offs. Low voltage to the transformer was provided either by a 12 volt lantern battery or a Heath Corp., Low Voltage Power Supply. A transformer of higher current capability was available and would have greatly increased the spark repetition rate, but was not used for reasons of safety and the likelihood of arc formation. At no time did the pulsed or the dc supply pose any serious danger to the operator.

b. Spark Sensor Circuits

Digital logic controllers, as shown in Figures 4 and 5 were triggered by one of several light sensing methods (Figure 3). The sensor used depended upon the sensitivity required for use with an individual carrier gas and spark housing configuration. Studies of spark character early in time (0.3-1.0 μsec after spark initiation) required a photosensor with rise-time, t_r, of ∿100 nsec. Although the Motorola MRD 500 Photodiode (Figure 2a) possessed adequate sensitivity to the continuum emission of argon, predominately blue and UV, it was necessary

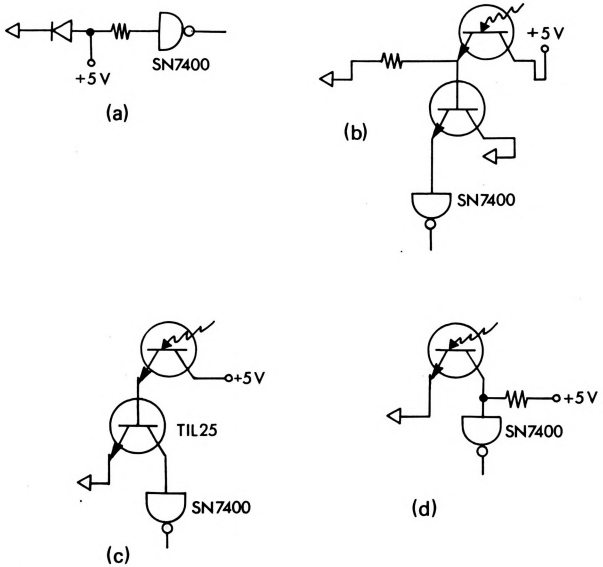

Figure 3. Spark Sensor Circuits.

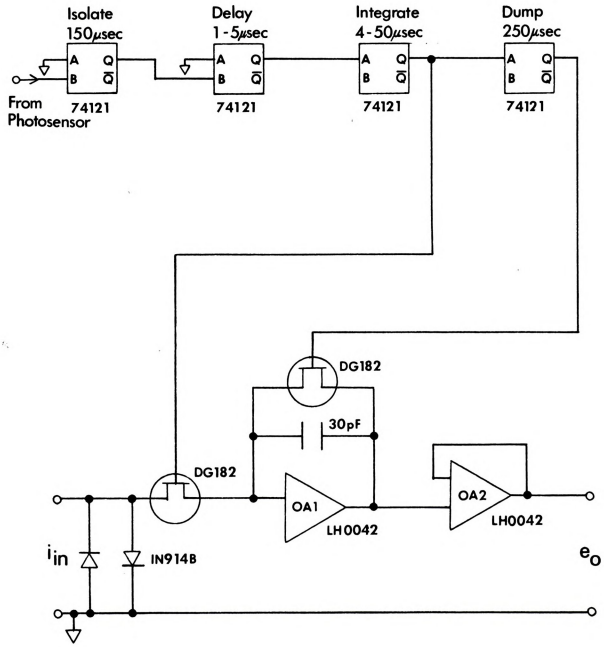

Figure 4. Gated Integrator Circuit for Signal Acquisition.

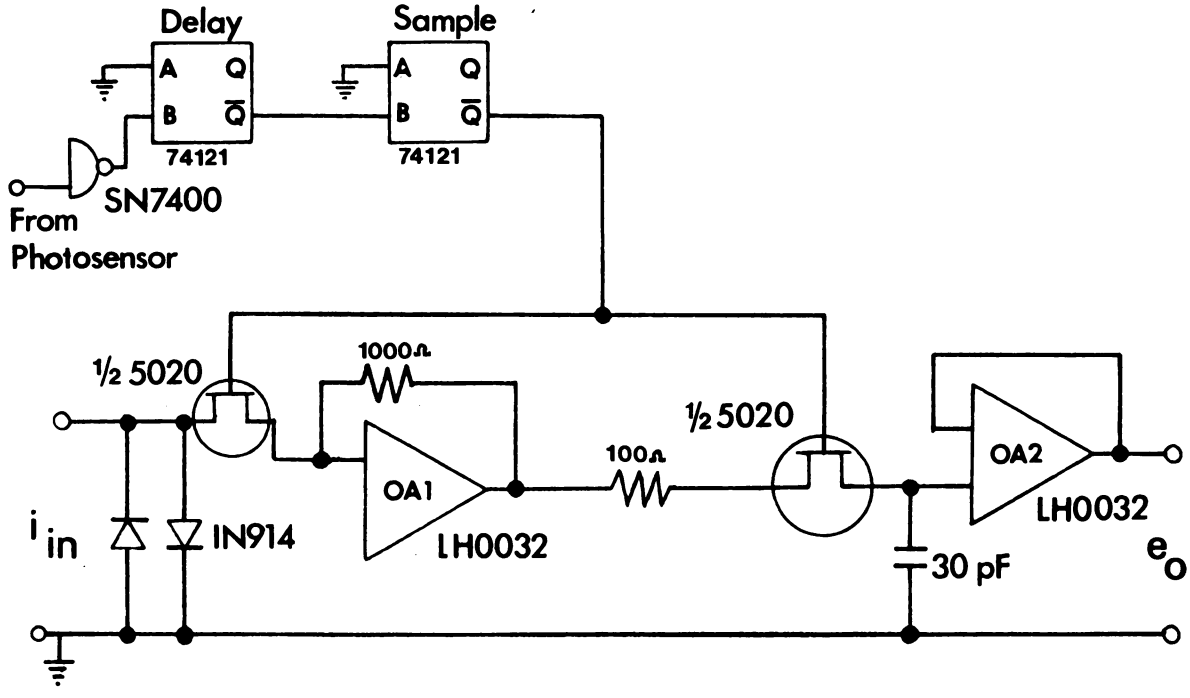

Figure 5. Sample-and-Hold Circuit for Signal Acquisition.

to increase the signal with a Darlington-type (b,c) or other amplifier (d), as shown for use with helium carrier gas. With selected fast transistors, e.g., TIL 25 (Texas Instruments) with betas of 70 or more, current gains of nearly 5000 could be obtained for the Darlington configuration, which provided adequate base current to the transistor connecting a NAND gate (SN7400) input to common. No commercial photodarlington had an adequate rise-time, and available laser detectors would have cost more than the remainder of the NSS. It was necessary to choose the sensor, the amplifier type, and the sensor position based on the carrier gas used and on the detector configuration. Due to the larger (20-50x) and longer-lived (100-200 μsec) background emission for argon carrier, high amplification caused retriggering even 150 μsec after spark initiation. When the carrier gas was changed, the spark sensor circuits were also changed. Similarly, logic control of the analog circuits was changed with the circuit type.

c. Data Acquisition Circuits

Signal acquisition was accomplished by use of a gated integrator (Figure 4), or by a fast sample-and-hold (Figure 5), each of which was controlled by the digital electronic circuitry shown. Due to the RF noise and oscillatory "ringing" pulses from the spark itself through the

circuitry, logical and electrical isolation of digital and analog circuitry was necessary. Indeed, the earlier work of Zynger (266) had used the extraneous high-frequency pulses which traversed the entire system after spark formation to monitor the instant of spark formation and to trigger the digital timing circuit. The triaxial capacitor shield design also tended to decrease RF interference.

Two distinct signal acquisition methods were developed for physical studies and for the gathering of analytical data. A gated integrator had been used initially, but proved to possess exceedingly long aperture times, and was unable to monitor the rapidly changing spark emission during the first few microseconds of the afterglow. Therefore, a fast sample-and-hold (S/H) amplifier was designed and constructed such that an overall response time of 300 nsec was realized. A gated integrator with improved characteristics was also made for general analytical applications. No assumption was initially made with regard to the superiority of a circuit type for analytical purposes, as the ultimate data storage device, either a minicomputer or a recorder would greatly effect such a choice.

Sample-and-hold circuits are dependent in response on the slew rates of the operational amplifiers used, the capacitance and resistance of all circuit components, on

the circuit design itself, and on the input bias current of the amplifiers, which determines droop rate.

Two design types for the sample-and-hold circuit are common. One circuit type contains both operational amplifiers in a single feedback loop, and is generally used for high accuracy, slower response S/H. A second circuit type, with each amplifier in its own feedback loop has significantly improved response time, but with degraded accuracy.

Only one commercially available S/H possessed the desired response speed, but at high cost (Intel SHM-1). Therefore, a low-cost, high-speed sample-and-hold was constructed (Figure 5). High-speed integrated-circuit operational amplifiers (National Semiconductor LH0032CG) and analog current switches (Siliconix AH5020) were used. Switching transients due to switch capacitance were present, but were smaller with the analog current switches than with the more complex, driver-actuated voltage switches (e.g., Signetics DG182BA) which also had been used. The amplifiers used had rather high input bias current levels, (I_B = 20pA) but this was much less important than their great speed (t_r = 30 nsec). The final sample-and-hold had approximately 100 nsec aperture and acquisition times, as determined by oscilloscope tracing. The droop rate was insignificant with respect to the time scale of the measurement.

The gated integrator, Figure 4, was of a common design, and the low bias-current operational amplifiers (National Semiconductor LH0042 or RCA 3130) gave high accuracy with slower response time than did the LH0032. The gated integrator could not be used for measurements of the light output during the first two μsec after spark formation, but was adequate for most other applications. Polycarbonate capacitors were used to reduce leakage currents, but were to be not essential in either circuit type.

3. Physical Parameters of the Nanosecond Spark Detector

Several physical parameters of the spark were measured in order to help understand the spark and to make the NSS a better chromatographic detector. Experiments were divided into two groups:

1) electrical character of the Nanosecond Spark, and
2) carrier gas properties and temperature.

a. Electrical Character of the Nanosecond Spark

The spark capacitance was measured by placing the spark and/or coaxial cable in an RC circuit consisting of a resistance-substitution box, a function generator, and an oscilloscope, with which the time constant of the discharging circuit was determined. Table 3 shows that the

Table 3. Miniature Spark Capacitance vs. Firing Rate.

Pulsed Supply	C	D	Hz
Spark Chamber #1 (LC)	180pF	0.020"	1200
Spark Chamber #2 (particle)	370	0.013	680
Spark Chamber #3 (GC)	480	0.010	790
Spark Chamber #3	300	0.020	2000
Spark Chamber #3	140	0.030	2600
DC Supply			
Spark Chamber #3 (GC)	---	0.010	120
Spark Chamber #3 (GC)	---	0.020	280
Spark Chamber #3 (GC)	---	0.030	430

Cable (2.5 ft. of RG/58) 100 pf.

Argon carrier, 130°C.

C is capacitance in picofarads.

D is the dielectric thickness in inches.

Hz is the maximum firing rate in Hz.

coaxial cable did provide 10-30% of system capacitance, and that the repetition rate was inversely related to capacitance. Detector capacitance was changed by varying the diameter of the aluminum bar electrode and the thickness of the dielectric.

All spark systems used showed one or more best, and worst, firing rates which were affected by carrier gas, temperture, and capacitance. The overall effects on firing rate, spark emission, and spark stability were more easily predictable for the dc-powered system than for the pulsed system. At higher frequencies, with the pulsed supply, the rate of spark formation did not seem to be wholly dependent on gap potential, and significant over-volting occurred. The probable causes for this have been discussed extensively by Rees (268) and Howatson (269). The improved spark reproducibility at high frequency may be due to the existence (270) of a long-lived (microsecond time scale) cavity left by each spark through which succeeding sparks may form more easily. This is further supported by the observation that the spark may be blown down stream by the carrier. The maximum firing rate decreases at higher carrier gas flow rates. The spark then also has the same appearance and irreproducibility that it has at even lower firing rates for low flow conditions when the spark cavity might be able to diffuse before the next spark could form.

System inductance was also increased by the series addition of small wire-wound inductors. Although the spark on-time was measurably increased (up to 300 nsec), there was no improvement in analytical results for gases. The lengthened time of background emission only interferes with gas analyses. It has been suggested by a co-worker (271), that the lengthened spark on-time may be beneficial for particulate analysis.

Several electrode materials were used, but only tungsten and tungsten alloys were hard enough to resist errosion. Thorium and zirconium (1% and 2%, Linde Division, Union Carbide) alloys of tungsten were analytically equivalent to pure tungsten, but Th-W electrodes were more errosion-resistant than the others. Alloys with lower work functions decomposed too quickly for adequate measurements of their properties in the spark.

Similarly, no effects on spark repetition rate, stability or emission were observed when strong light was focused on or between the spark electrodes. The light beam from a Spectra-Physics He-Ne 1 mW laser, a high-pressure mercury pen lamp (Ultraviolet Products, Inc.) or a 150 watt Xenon arc (Farrand Instruments Co.) was focused on the spark gap or electrode with a 1" diameter quartz lens. Helium and argon carriers both were used. Although the lack of effect may have been because streamer formation (avalanche initiation) was not limiting, the

light sources also may have been too weak to produce a noticeable effect. An α or β particle source was not available.

b. Carrier Gas Properties and Temperatures

Carrier gas choice was of major importance in routine use of the NSS for analysis. Neon and other rare gases were unacceptable due to their expense or physical inadequacy. Nitrogen was not compatable with the low energy, high-power, high repetition rate spark we desired and had to be effectively excluded from the spark. Nitrogen carrier would also have precluded nitrogen analysis. Therefore, it was necessary to choose between argon and helium as the carrier gas.

Commercially available ("water pump grade") argon and helium give large background signals for carbon, oxygen, nitrogen and hydrogen, and thus require the purification system described earlier. No changes in breakdown voltage (V_B) or other physical parameters are measurable when commercial or purified helium and argon are used, but "impurities" in the spark from analytes do affect the plasma. As analyte concentrations near 1% in the carrier, the spark plasma ceases to be an argon or helium plasma, but becomes a mixed carbon, hydrogen, and oxygen plasma, with decreased V_B. The low ionization potential species provide a much less energetic plasma which contains

polyatomic species such as C_2^+, CN, and OH. Polyatomic emission bands often are seen 1-2 μsec after spark initiation when the concentrations of organic compounds reach 1% in carrier, even though such bands do not appear prior to 15-20 μsec post-spark under usual operating conditions.

c. Excitation Temperature Measurement

Table 4 gives excitation temperatures (T_{ex}) and electron densities (N_e) for the spark in argon, 3% methane in argon, and for a continuous microwave argon plasma (277).

Excitation temperatures were calculated by procedures developed by Reif et al. (272) and Adcock and Plumtree (273), based on the dependence of the distribution of excited states on the spectroscopic (excitation) temperature. By assuming negligible self-absorption, which would repopulate excited states, uniform photometric sensitivity over the narrow wavelength range used, and a Boltzmann distribution, T_{ex} may be determined graphically. The following symbols are used in the development of the final expressions which indicate the quantities which are plotted for the graphical determination of the spectroscopic temperature of a system for a transition from a state i to a state j.

A_{ij} = transition probability for the transition from $i \rightarrow j$.

Table 4. Spectroscopic Temperature and Electron Concentration.

	Argon-Spark			CH_4 in Argon-Spark			Microwave	
time (μsec)	Stark Width (nm)	Ne(e/ml)	T_{ex}(°K)	Stark	Ne(e/ml)	T_{ex}(°K)	Stark (nm)	Ne(e/ml)
0.5-3	3.1	5.7×10^{16}	4050	1.1	9.4×10^{15}	4400	-----	--------
3-5	1.6	2.2×10^{16}	4600	0.9	7.8×10^{15}	4150	-----	--------
5-10	0.8	7.0×10^{15}	4500	0.3	2.4×10^{15}	4250	-----	--------
10-15	0.47	3.2×10^{15}	4450	0.3	2.4×10^{15}	3900	-----	--------
15-25	0.25	1.3×10^{15}	3900	6.3	2.4×10^{15}	3950	0.25	1.7×10^{15}

Due to the high imprecision of the measurements, temperatures as stated are rounded to the nearest 50°K.

I = emission intensity at wavelength λ for the transition $i \rightarrow j$

N_i = population of the ith species

g_i = statistical weight of the ith species

λ = wavelength corresponding to the transition $i \rightarrow j$

E_i = energy of the ith species

Z = the partition function

C = arbitrary constant

For two independent states, 1 and 2, the number of atoms in state 2 is given by

$$N_2 = \frac{N g_2 e^{-E_2/kT}}{2} \tag{13}$$

The intensity of emission for the transition from state 2 to state 1 is

$$I = \frac{C\, A_{21}\, N_2}{\lambda} \tag{14}$$

therefore, on substitution for N_2 from Equation (13) into Equation (14) yields

$$I = CN \frac{g_2 A_{21}\, e^{-E_2/kT}}{2\lambda} \tag{15}$$

which gives on rearranging Equation (15) and expressing the resulting equation in log form

$$\text{Log } \left(\frac{I}{g_2 A_{21}}\right) = \log \left(\frac{CN}{Z}\right) - \left(\frac{E_2}{2.303\ kT}\right) \qquad (16)$$

A plot of the left side of Equation (16) vs. E_2 results in a line whose slope is approximately proportional to the spectroscopic temperature. The observed neutral argon lines (4150-4300 Å) are from one spectral series, 5P - 4S, whose transition probabilities are well known (274). Four spectra were obtained for each time interval, and the intensities averaged for each plasma. The changes in spectroscopic temperature with time after spark initiation are shown in Table 4.

d. Electron Density Measurement

Calculations (275) based on an improved theory of Stark broadening were used to calculate electron density (N_e). The dominant line-broadening mechanism in dense plasmas ($N_e \geq 10^{12}$ e/cc) is Stark broadening caused by the electric fields of free electrons and ions surrounding the radiating atoms. Hydrogen is subject to a linear Stark effect. Therefore the broadening of the hydrogen Balmer lines, which are emitted strongly by the miniature spark, is nearly completely dependent on electron density (276).

Four determinations of the H_β half-width at half-height were made for each plasma type. N_e was calculated from the half-width, to the 2/3 power, times a proportionality coefficient (275). As the coefficient was slightly

temperature-dependent, and the electron temperature (T_e) was not well known, T_e was assumed to be 10,000 K - 30,000 K and the resultant coefficients averaged.

The data in Table 4 indicate a decreased N_e and T_{ex} in time and with increased carbon content in the carrier for the NSS. T_{ex} and N_e both decrease sharply over the first 50 μsec, indicating a change of the plasma from "spark-like" to "arc-like". This is in accord with the appearance of polyatomic species in the plasma. T_e and N_e also varied along with spark axis. Further work showed similar decreases in N_e, and T_{ex} and increased molecular [(C_2^+)] emission with smaller concentrations of the halogens than of methane. Neither phenomenon is surprising on consideration of the known effects on other plasmas of electron donating and electron capturing species (14). Wentworth's (14) work, intended to explain the operation of the electron-capture detector, applies equally well to halogen overloading in the nanosecond spark. It is only at high (>0.2%) halogen concentration in gaseous analyte that the effect appears in the NSS. Halogens in salt particles cause no observable effect, and the analytical usefulness of the NSS is not compromised for gases if the proper spark geometry is used. Carbon analysis is not limited by self-absorption at the 2478 Å C(I) line, but is limited by the altered plasma at high (>1%) carbon content in the spark gap.

e. Carrier Gas Choice

Background emission (Bremstrahlung and radiative recombination) are much smaller for helium than for argon, as is carbon background in the purified gas. Argon carrier causes greater analyte signal intensities and is much less in need of purification than is helium, but gives more atomic emission of its own. Many of the argon lines seen by Denton (171) and others for continuous plasmas are not visible with the NSS. The oxygen content of most tank helium is nearly 1,000 times that in tank argon, but the maximum firing rate in helium is nearly 3 kHz, as opposed to 1.2 kHz in argon, and the spark is more reproducible and "better behaved" in helium than in argon. Figure 6 shows photographs of the spark in helium and in argon. Both carriers are used for analytical experiments, for the choice of gas is not necessarily an argon conclusion.

An important physical property of any carrier gas is its thermodynamic (gas) temperature. Figure 7 shows the changes in breakdown voltage and repetition rate with temperature for dc supply operation. Note that increasing temperature significantly improves spark reproducibility. Where possible, measurements were made at constant flow rate to minimize effects of increasing gas viscosity with temperature. Due to the simplicity of the chromatograph used, most analytical separations were not made under

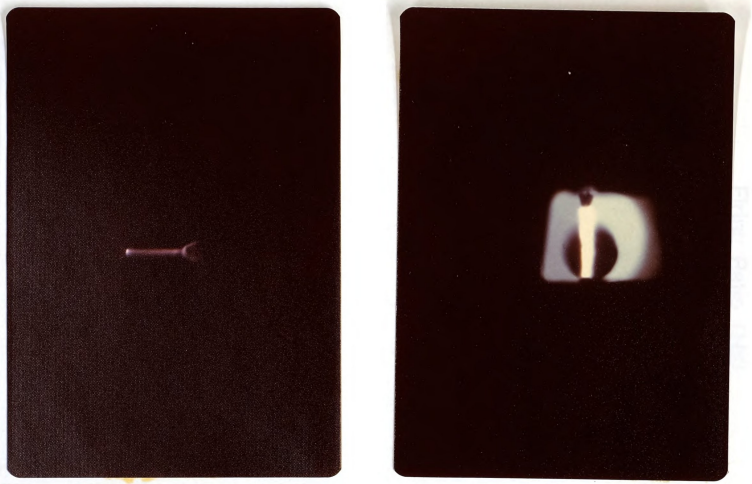

Figure 6. The Nanosecond Spark Source in Helium and in Argon.

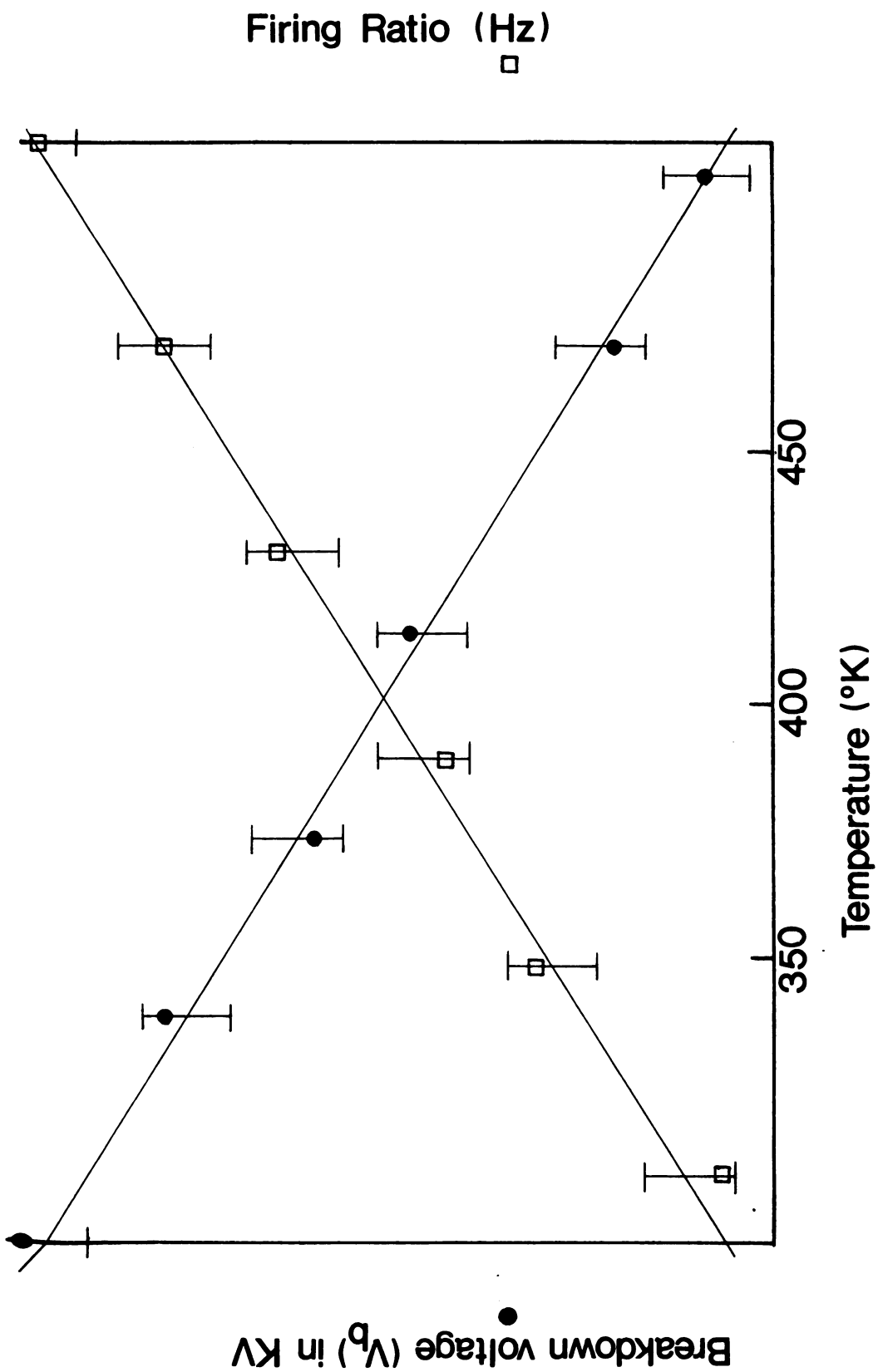

Figure 7. Breakdown Voltage and Firing Rate vs. Temperature in Argon.

constant flow conditions, although average flow rates were recorded at most operating temperatures. Even without proportional flow controllers, the background intensity of individual sparks did not increase significantly, although the integrated signal did increase due to the larger number of sparks included at higher firing rates. The NSS actually is a mass-sensitive detector, and is not degraded at higher temperatures, unlike nearly all of the commercially available detectors. Further evidence of its mass linearity is presented in succeeding sections on individual element analysis.

B. Evaluation of the Nanosecond Spark Source For Chromotographic Detection

The response of any detectors to analyte should be proportional to the number of carbon or other atoms actually present in the effluent at any instant. "Atom number" and functional-group effects present in previous universal GC detectors ought to be eliminated with any new detector, while sensitivity, precision, accuracy, and reliability are maintained or improved. The nanosecond spark system possesses these features. That is, it is a mass-sensitive detector, generally free of inter-element and structural interferences.

1. Detection Limits

Chromatographic detector sensitivities are often difficult to define and compare. Detection limits for analytical systems whose analyte concentrations are static are relatively easily described, but the dynamic nature of the chromatograph output makes mathematical descriptions troublesome, and chromatographic factors unrelated to the detector itself often compound the problem of detector comparisons.

Three methods were used to overcome the difficulty:

1. Introduction of a series of gaseous and particulate standards directly into the spark chamber,
2. placement of the nanospark on a commercial gas chromatograph, and
3. Use of the NSS detector on a chromatograph designed specifically for it.

Continuous introduction of sample into the spark without an intervening chromatograph was accomplished by two separate methods to provide both gaseous and particulate carbon standards. Controlled-temperature vaporization of n-decane (Figure 8) was used to produce several concentrations of carbon in the carrier gas. By maintaining a constant temperature of the water bath for each run, it was possible to calculate the rate of vaporization of n-decane and the concentration of n-decane in the resultant

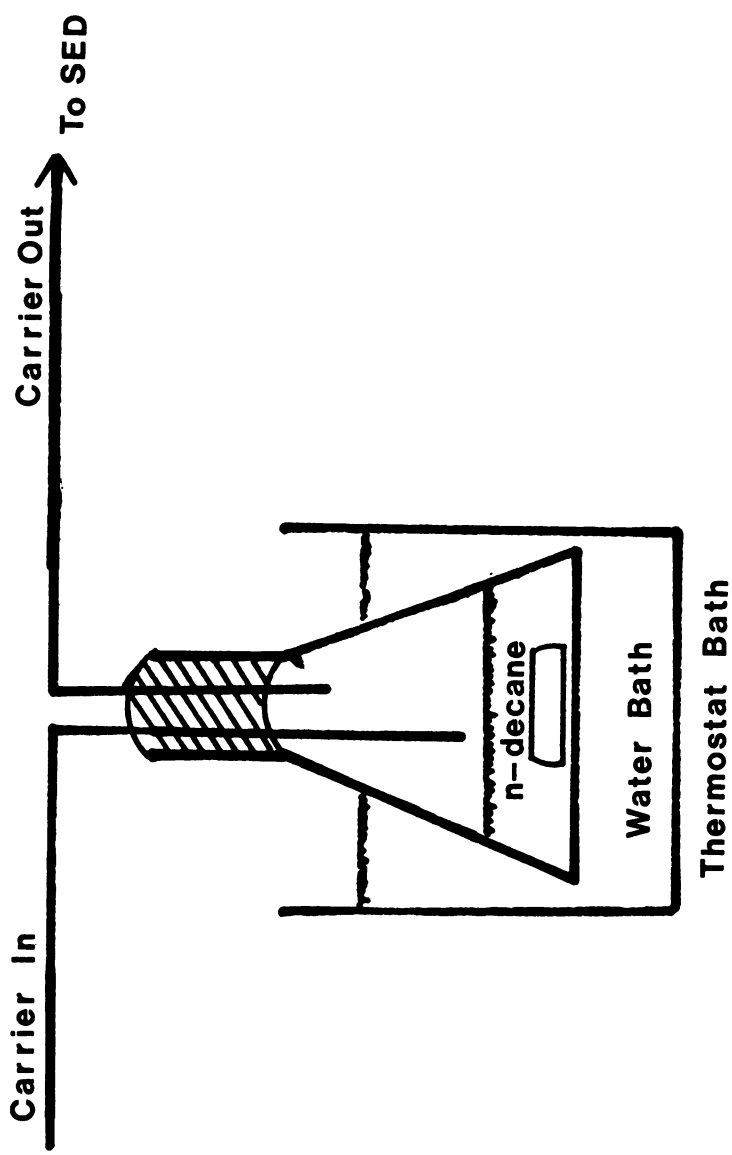

Figure 8. Controlled-Temperature Evaporation Apparatus.

gas mixture. Though the method was useful at carbon concentrations greater than 10 ppm, decane evaporated too quickly at 0°C and too slowly at easily maintained sub-zero C° temperatures for accurate production of lower concentration mixtures. All further detection limit studies with continuous sample introduction were made with particulate carbon standards from aqueous solution. These could be prepared more accurately over a larger concentration range than could gas mixtures. Carbon in gas mixtures for injection were prepared by the addition of small amounts of volatile liquid into an argon or helium purged chamber similar to that used for the controlled-temperature vaporization of n-decane. A working plot of decane mass injected vs signal intensity minus background is shown in Figure 9. Linearity is excellent from the detection limit (2×10^{-12} g) to 10^{-5} g.

Particulate analytes were much more easily used than were gaseous standards. Figure 10 shows the mass vs emission intensity plot obtained with asparagine HCl standards. Asparagine HCl was chosen because it contained nitrogen, oxygen, hydrogen, and chlorine in addition to carbon. Solutions of low concentration standards showed marked decreases in carbon control after a few hours due to adsorption of the asparagine to the glass walls. That interelement effects were not found was significant for the probable usefulness of the nanosecond spark

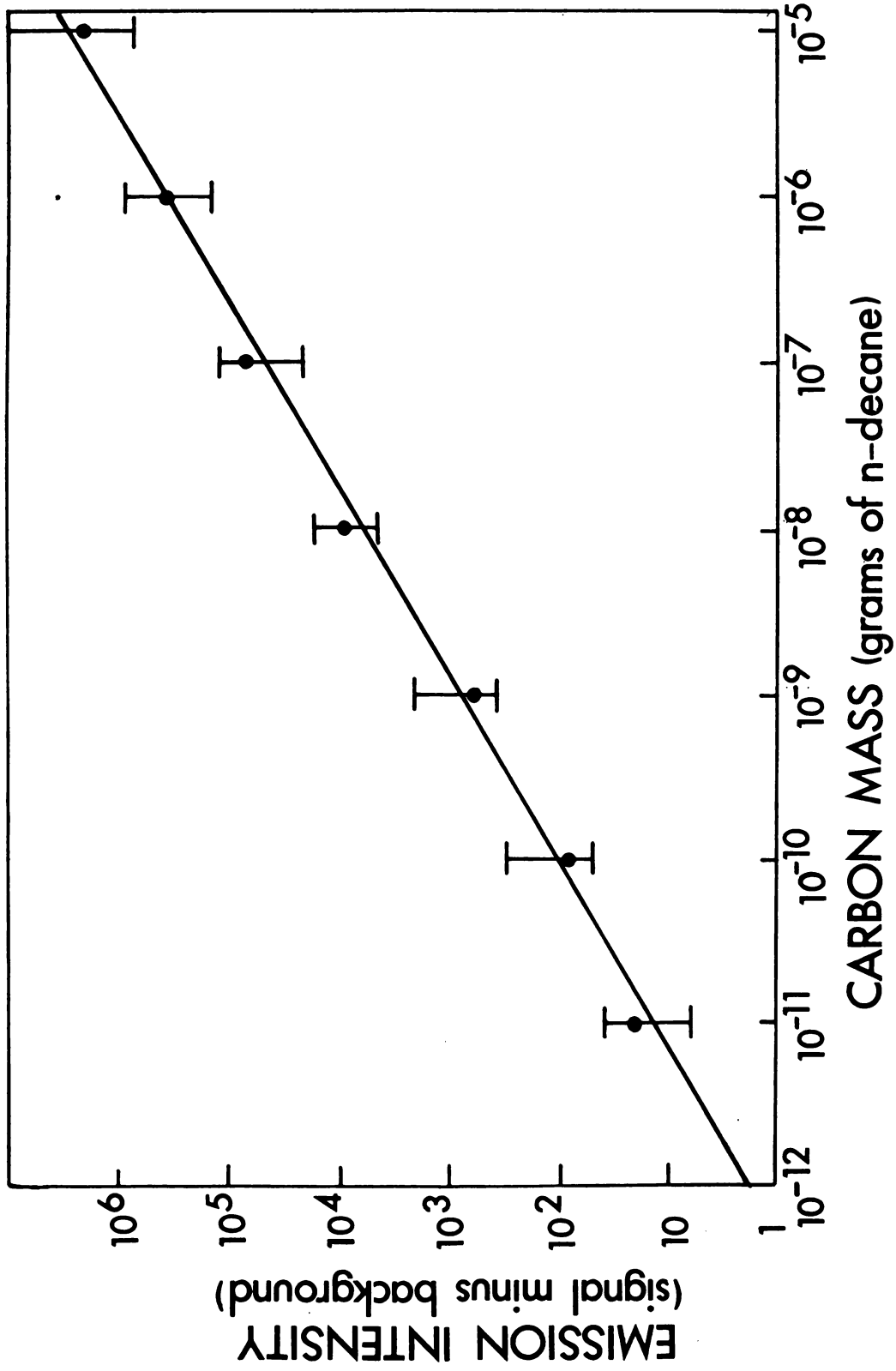

Figure 9. Carbon Emission from a Gaseous Analyte.

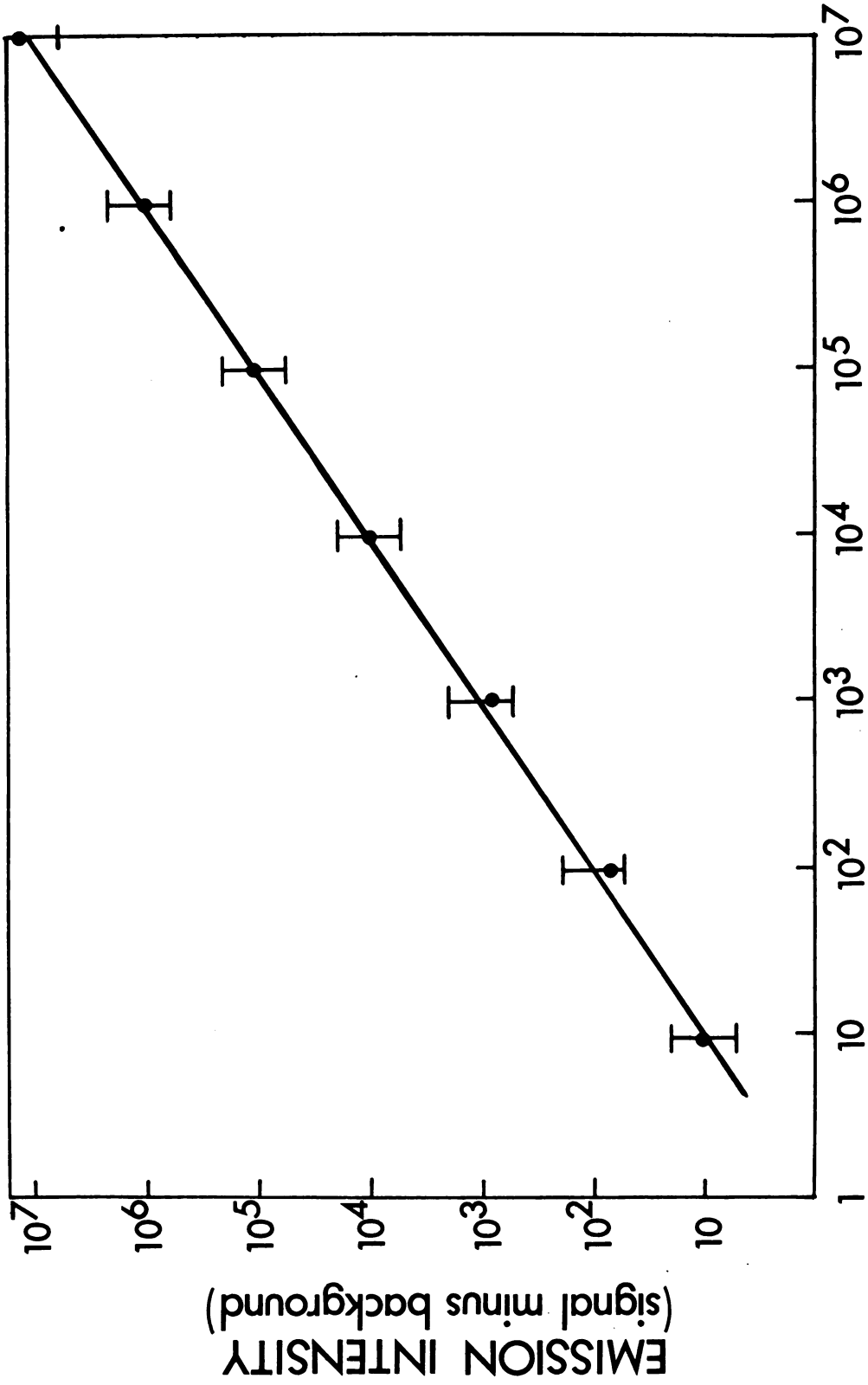

Figure 10. Carbon Emission from a Particulate Analyte.

detector.

After several hours' operation, the Veillon-Margoshes desolvation system often produced an increasing background carbon signal and noise level. Therefore, measurements were made on a freshly-cleaned system. Hydrofluoric acid (10%) immersion of the desolvation chamber, followed by its thorough rinsing was generally needed after 200 hours operation, but aspiration of 2N HCl for 5 minutes was adequate for daily cleaning.

A freshly cleaned desolvation system, a 10^4 spark computer-average of the signal, and standard tank argon, gave a detection limit ($\frac{S}{N} = 2$) of 15 ppb carbon in solution. Purification of the argon carrier gas lowered the detection limit to 3 ppb, and use of a real, inverted spark image improved it to less than 1 ppb carbon. A log-log representation would obscure most non-linearities, therefore individual linear plots of smaller segments of the intensity/concentration plot were made, and showed remarkable linearity from 1 ppb to slightly more than 1 ppt carbon in solution. The slope of the log-log plot, for 10^5 point runs, was 0.99 ± 0.04 over the range 50 ppb - 500 ppm in solution. From 1-50 ppb carbon added the slope was $0.96 \pm .06$ with a positive intercept equivalent to 25 ppb carbon in solution. It was not possible to decrease argon-carrier carbon content further by any readily available means.

The second step was the comparison of the NSS and a commercial detector by replacement of the FID burner on a Varian 1400 series gas chromatograph with an unheated brass tube connected to the NSS lamp input. Thermal conduction from the heated detector block prevented condensation in the transfer tube. Identical samples were injected into the chromatograph with the same syringe, septum, and column, operated at the same isothermal or programmed temperatures. The NSS was several orders of magnitude more sensitive than was the commercial FID. Peaks obtained with the NSS were broadened by the large dead-volume of the transfer tube, and the position of the exit port of the chromatograph made routine use of this apparatus quite inconvenient. The isothermal chromatograph built for the spark alleviated the dead-volume problem.

With that chromatograph, 2-pentanol (1 ppm in hexane), eluted well ahead of the solvent plug, but also was resolved from a contaminant, 3-pentanol (Figure 11). The amount of 3-pentanol injected was approximately 10-12 ng. The 2-pentanol had been distilled under vacuum then re-distilled on a spinning-band bolumn prior to use. The contaminant was not detectable with the Varian GC, and had been merely a minor hump on the 2-pentanol peak with the spark detector attached to the FID exit port. Therefore, the chromatograph was adequate for our needs, and nearly all of the analytical GC data were obtained with it.

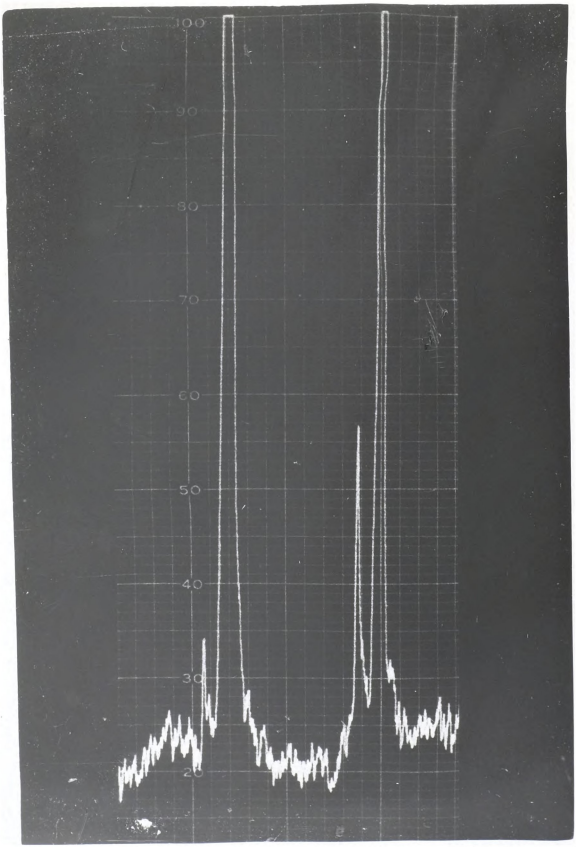

Figure 11. Chromatogram of the Separation of the Pentanol Isomers.

2. Carbon Analysis

Carbon detection, the first and most obvious of organic analytical subjects, was characterized with respect to sensitivity, linearity, and freedom from functional group effects. It is the last of these that is of particular importance to the practicing chromatographer. The flame ionization detector has excellent sensitivity and linearity, but its response is greatly affected by the presence of heteroatoms and structural ("carbon number") anomalies. Calibration plots were made for a large variety of organic compounds for the spark detector chromatograph and for the commercial (Varian 1400) chromatograph. In all cases, the stainless steel columns were simply transferred from one oven to the other, and essentially identical chromatographic conditions were used. Table 5 lists effective "carbon numbers" for the spark emission detector (SED) and the Varian 1400, for compounds containing heteroatoms or multiple bonds. Detection limits, of course, are dependent on chromatographic parameters. The response per carbon atom as compared to hexane ("carbon numbers") determined for the Varian 1400 were similar to those in published sources.

The relative standard deviation for injected samples is generally 6-10%. Syringe precision is accepted to be 3-5% RSD. Therefore, precision for the spark GC detector

Table 5. Effective Carbon Number for SED and FID.

Atom	Type	FID	Spark
C	aliphatic	1.0	1.0
C	aromatic	1.0	1.0
C	olefinic	0.95	1.0
C	acetylenic	1.30	1.0
C	carbonyl	0.00	1.0
c	nitrile	0.3	1.0
O	either	-1.0	0.0
O	1° alcohol	-0.6	0.0
O	2° alcohol	-0.75	0.0
O	3° alcohol	-0.25	0.0
X		variable	0.0
N	amines	similar to oxygen	0.0

is in agreement with that for the spark alone (3,52). Response curves determined with the nanosecond spark for all compounds in Table 5 are equivalent. Though precision improves at higher spark firing rates, dc operation gives results almost equal in detection limit and precision to thosefrom the pulsed mode. Gas temperature does not noticably affect emission intensities for individual sparks, though the firing rate does increase with temperature for dc operation.

3. Multi-Element Analysis

Were the nanosecond spark capable of no more than the carbon detection limits discussed, it would be of little importance. There are other, commercially available, detectors which have been in use for far longer, and now have equal or slightly superior overall sensitivities. However, the NSS also possesses excellent sensitivity and specificity for most metals and non-metals, and uses atomic emission to provide the necessary analytical signals. As discussed in the history of detector development, the commercially available selective detectors are generally succeptable to inter-element interference due to their dependence on polyatomic band emission or other highly non-specific processes.

The nanosecond spark requires no modification to detect non-carbon elements other than a change in the

Table 6. Carbon/Hydrogen Atom Ratios Determined by SED/GC.

Compound	C/H (Actual)	C/H (Found)
Methanol	0.250	0.241
Ethanol	0.333	0.351
2-Propanol	0.375	0.362
Ethylamine	0.286	0.293
Diethylamine	0.364	0.350
Triethylamine	0.400	0.389
Benzene	1.000	1.030
Acetic Acid	0.500	0.524
Dichloromethane	0.500	0.494
Trichloromethane	1.000	0.969

monochromator wavelength setting and the integration aperture or sample-and-hold time delay.

A. Hydrogen

As with analyses for most other elements, hydrogen determination requires non-critical optimization of the integration aperture times. In the region 2-10 μsec after spark initiation, several strong emission lines appear. Of these, the most intense are the H_β (4861 Å), and the H_α (6563 Å). Due to the rapid decay of the argon plasma, the 4876 Å and 4880 Å argon emission lines do not interfere with H_β detection, as they do in continuous plasma systems. Continuum emission is greater at 4861 Å than at 6563 Å, and H_α emission is more intense, but the H_β emission was used for analytical work because the 1P28A photomultiplier tube available during the majority of the work was far more sensitive in that spectral region.

Hydrogen could also be monitored in oxygen-containing samples or carrier by use of the hydroxyl emission band (ca. 3100 Å) and an integration aperture of 15-50 μsec after spark formation. Emission was less intense, dependent on the presence of oxygen, and prone to interference from other species.

Hydrogen analysis by atomic emission is quite sensitive, with a 450 pg detection limit, and excellent linearity (slope = 0.98 $\pm$ .04) and reproducibility. Hydrogen

sensitivity is also less than that for carbon, and its deficiencies parallel those of carbon. There is an unavoidable hydrogen background signal, even with helium carrier passed through a liquid nitrogen trap. As most solvents and liquid support phases contain both carbon and hydrogen, there is no amelioration of the solvent front or column bleed problems. Figure 12, chromatograms of three aliphatic alcohols, shows that carbon and hydrogen analysis modes give essentially equal results. Table 6 does show that C/H atomic ratios are easily acquired from successive chromatograms of the same sample, and that heteroatoms do not affect hydrogen emission. Therefore, hydrogen analysis is quite useful for empirical formula determinations, if not as the primary detection element.

b. Oxygen

Hydroxyl band emission was also employed initially for the analysis of oxygen. By use of an integration aperture of 10-50 μsec and analyte compounds containing at least a ten-fold atomic excess of hydrogen over oxygen, hydroxyl emission was linearly proportional to oxygen content over three orders of magnitude. Detection limits were 400 ppm as particles in carrier gas and 850 ng by GC. Residual solvent water made oxygen measurement following desolvation of aqueous solutions very difficult.

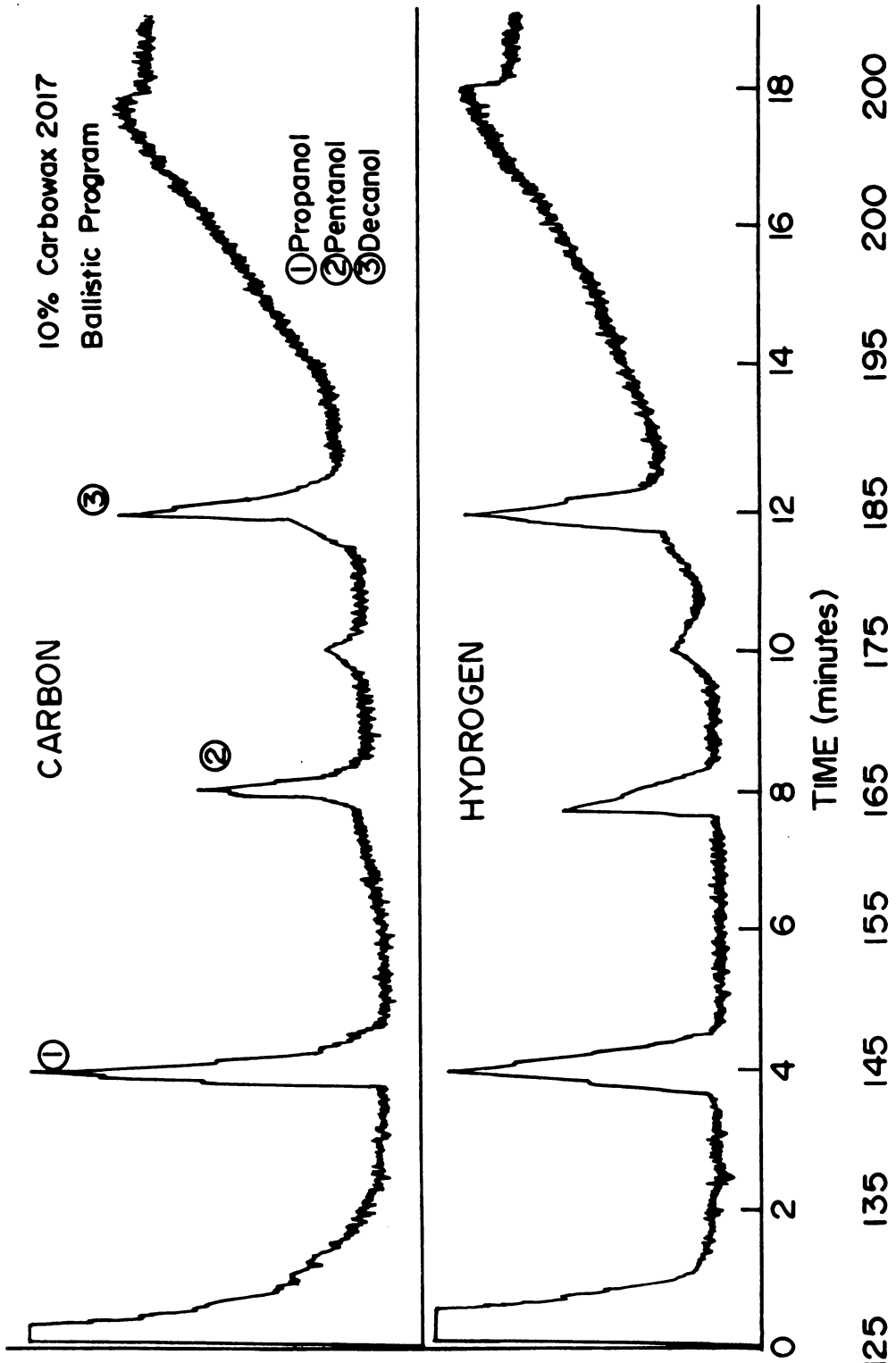

Figure 12. A Comparison of Carbon and Hydrogen Analysis Modes.

Table 7. Oxygen Analysis.

A. Relative Emission Intensity vs. n-Decanol Concentration.

ppm n-decanol	Emission
0.10	1
1.05	10.1
20.00	195.7
50.1	503.9
109.	1019.

B. Carbon/Oxygen Ratios Determined by SED/GC

Compound	C/O (Actual)	C/O (Found)
Methanol	1.0	1.06
Ethanol	2.0	2.03
Pentanol	5.0	4.98
Phenol	6.0	6.04
Acetic Acid	1.0	0.97
Formic Acid	0.5	0.53

Addition of a small fraction of hydrogen to the carrier gas gave emission intensity which was independent of analyte hydrogen and nitrogen content, but did not improve sensitivity. Further, the disadvantages common to any use of molecular emission held, making the hydroxyl-emission technique generally unsatisfactory for routine analysis.

Oxygen sensitivity improved enormously as a result of the earlier studies on the physical nature of the spark environment. The spark afterglow, as a decaying plasma for several usec after spark formation, gave a large radiation continuum at relatively short wavelengths in addition to atomic or ionic line emission. By monitoring the oxygen O (I) 7772-7774 Å lines much earlier in time with the sample-and-hold circuit (0.5-3 μsec after spark initiation), it was possible to attain a detection limit of 15 ng of oxygen as gas in carrier, without computer averaging. The sample-and-hold circuit gave approximately 10-fold improved sensitivity over the gated integrator circuit. By analogy to work with other elements, computer signal averaging should provide one to two orders of magnitude greater sensitivity. The use of a red-sensitive PMT was necessary, as the 1P28A was relatively insensitive at 7772 Å. Neither argon nor helium gives significant background continuum emission at 7772 Å. Excitation efficiencies are somewhat comparable and either

is adequate as carrier gas if sufficiently purified. Unfortunately, the oxygen content of some helium tanks is so great as to overload the BASF catalyst oxygen trap within 20 minutes' operation, making oxygen analysis effectively impossible with such helium sources.

Table 7 gives relative emission intensities vs elemental oxygen mass for successive concentrations of decanol and the relative response for oxygen in several compounds. Higher concentrations of oxygen did not exhibit self-absorption, but the expected plasma alteration was present and limited the useful range to approximately 15 ng-300 μg. Response was linear between those limits, and a plot of the data from Table 7 had a slope of 1.03 $\pm$ .08.

Figure 13 illustrates one of the important values of multiple-element capability. Though the intrinsic sensitivity is greater for carbon than for oxygen, the hydrocarbon solvent plug tail may be ignored if oxygen is detected. In neither the carbon nor the oxygen detection mode are different response factors needed as they are with the flame ionization and thermal conductivity detectors. The chromatograms in Figure 13 are the result of successive injections of 2 microliter samples of 10 ppm acetic and butanoic acids in hexane. Comparable results are obtained in the oxygen mode with sample-and-hold (S/H) or with gated integrator (G/I) data acquisition

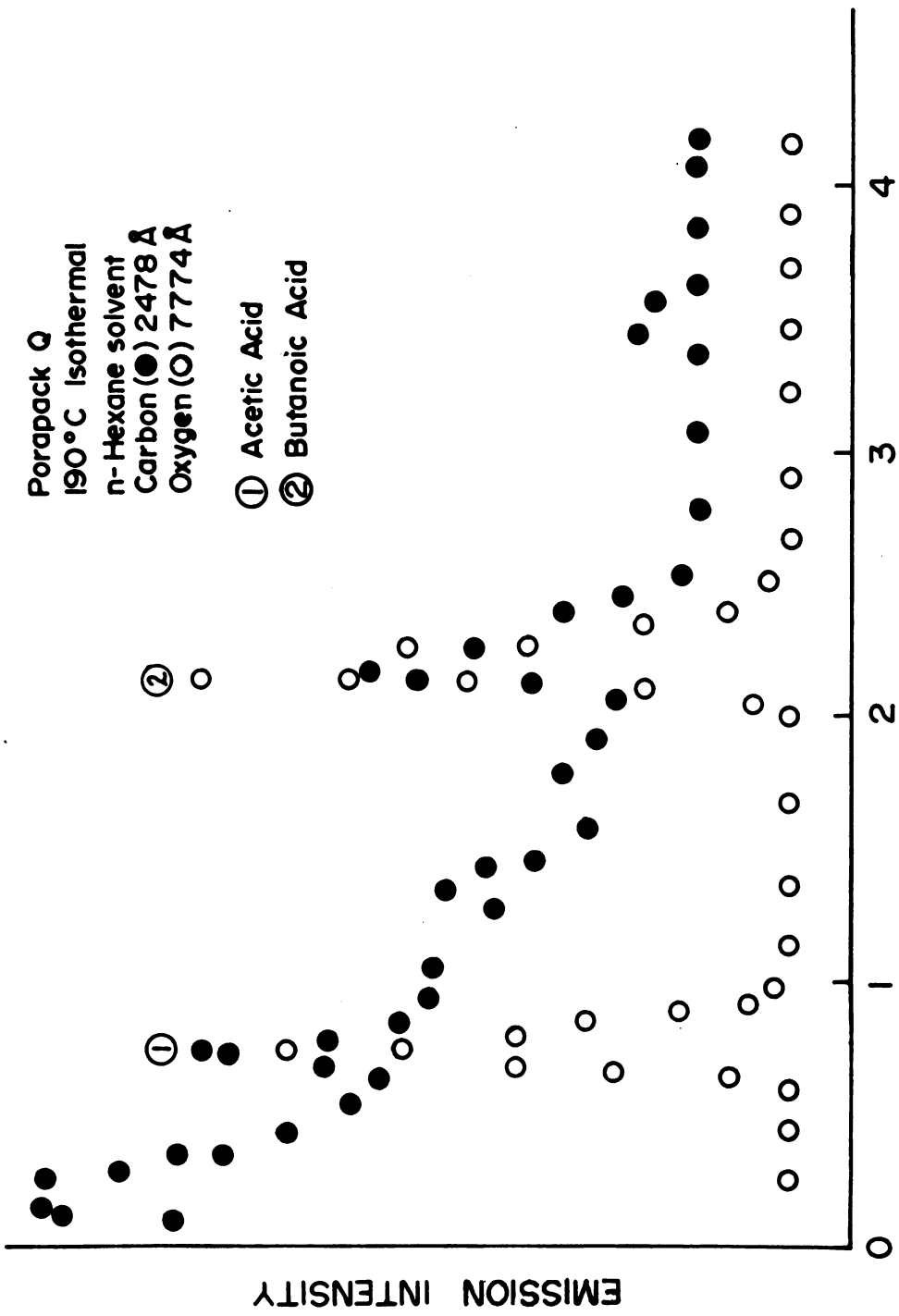

Figure 13. Carbon and Oxygen Detection Mode Analysis of Fatty Acids.

circuits, except that the sample-and-hold circuit does give 10-40 times greater sensitivity.

c. Nitrogen

Nitrogen emission was measured at 6723 Å with a 0.8 - 3.5 μsec integration window or 1.2 μsec sample-and-hold time and using a red-sensitive photomultiplier tube. The observation time used, similar to that for oxygen, was a result of the rapid decay of atomic nitrogen emission as the plasma environment cooled. Slightly superior (x5) results generally were found with the S/H data acquisition circuit. Detection limits were comparable to those for oxygen and were found to be 1.5 ng nitrogen (triethyl amine) in gas and 2 ppm N (asparagine) as particles from solution with the S/H or the G/I circuit. The response was linear with concentration (slope = 1.00 $\pm$ .06) from the detection limit to 3 ppt nitrogen (pentamethylene tetrazole (PMT) as particles from solution) or approximately 15 μg nitrogen (pentamethylene tetrazole as gas). PMT was kindly supplied by Professor A. I. Popov of this Department. Table 8 shows the relative response of the SED to nitrogen and carbon in compounds containing several heteroatoms and structures. Each C/N value is the average of four separate chromatograms for C and for N with each compound. An appropriate hydrocarbon internal standard was used to help minimize the effects

Table 8. Empirical Formulae Determined by SED-GC.

	$C/N_{theoretical}$	C/N_{found}
Barbital	4.00	4.13
Phenobarbital	6.00	5.91
Pentabarbital	5.50	5.63
Secobarbital	6.00	6.10
Aniline	6.00	6.07
Asparagine (particle)		
Nitrobenzene	6.00	5.95
Triethylamine	6.00	6.03
Pentamethylene tetrazole [$C_6H_{10}N_4$]	1.50	1.55
Guthion [$C_{10}H_{12}N_3O_3PS_2$]	3.33	3.19
Parathion [$C_{10}H_{14}NO_5PS$]	10.00	9.92
Methylamine	1.00	1.03
Phenyl propanolamine	9.00	9.10

of syringe imprecision. No internal nitrogen standard which did not contain carbon was satisfactory; therefore, none was used for these nitrogen analyses. Similar data were found for N/H ratios, including that for ammonia. Interelement effects were not found for carbon, hydrogen, and nitrogen. Although the NSS sensitivity is not equal to that ascribed to the AFID, and approximates that for various electrochemical detectors, its element specificity is certainly superior. The NSS is also not severely flow-sensitive, as is the AFID.

Three anti-convulsants and two other sedatives (Supelco, Bellefont, PA) were separated isothermally on 3% OV-17 on Supelcoport, and measured as carbon, hydrogen, nitrogen and oxygen on repeated chromatograms. All four elements were known to be free of interelement effects; therefore, pentabarbital was used as an internal standard. Chromatographic quality could have been improved by the use of methyl, pentyl or silyl derivatives, linear temperature programming, and an all-glass system without effect on the detector. Emperical formulae were adequate to differentiate the compounds without regard to retention time (Table 8). Compound identification would have been aided enormously in analysis of real samples, even if only C/N ratios were used. Figure 14 shows the effect of nitrogen detection when several of the same barbiturates were analyzed from a serum matrix.

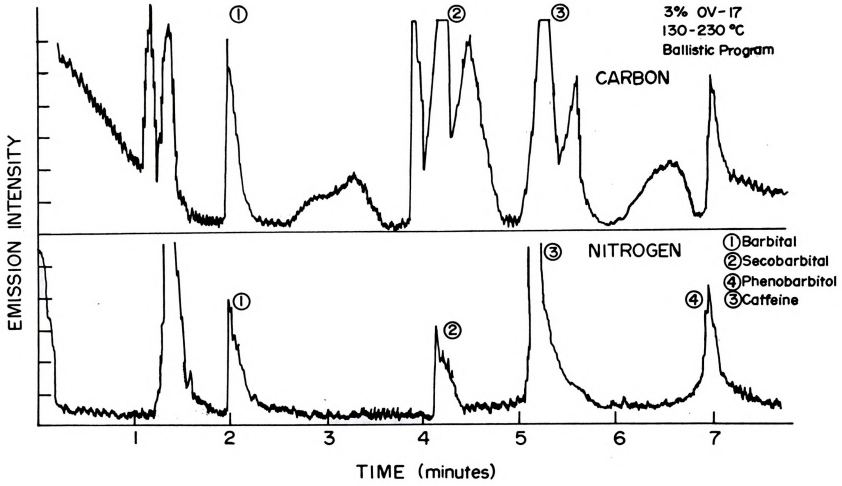

Figure 14. Analysis of Barbituates from a Serum Matrix.

Separation of ammonia, methanol, hydrogen sulfide, CO, CO_2, and SO_2 on Porapak Q (Figure 15) was not difficult, but peak assignments with the FID and TC were equivocal. Thermal conductivity detection was made with a Carle Basic GC (Carle Instruments Co.) with a similar Porapak Q column. Nitrogen analysis with the NSS identified the ammonia and nitrogen peaks. Interference from other elements was not found, nor were weight factors needed. Table 9 compares such weight factors for the SED, TC, FID and AFID.

d. Phosphorus

Phosphorus detection is of minor clinical importance, but is of great value in environmental analysis. A large fraction of modern pesticides contain phosphorus, and organophosphorus derivatives of other compounds are relatively easily prepared (17). By use of the 2535.7 Å P(I) line and 4-10 μsec integration aperture, detection limits of 380 ppb phosphorus (adenosine triphosphate, ATP) from solution and 100 pg phosphorus (triethyl phosphate) in gas were found. Sodium phosphate, pH 7.0, and ATP were used for most solution studies, while several organophosphates were used in the gas phase. There were no discernable interelement effects with other non-metals. Divalent cations in solution analyses decreased phosphorus emission after the first 12-15 μsec of the afterglow

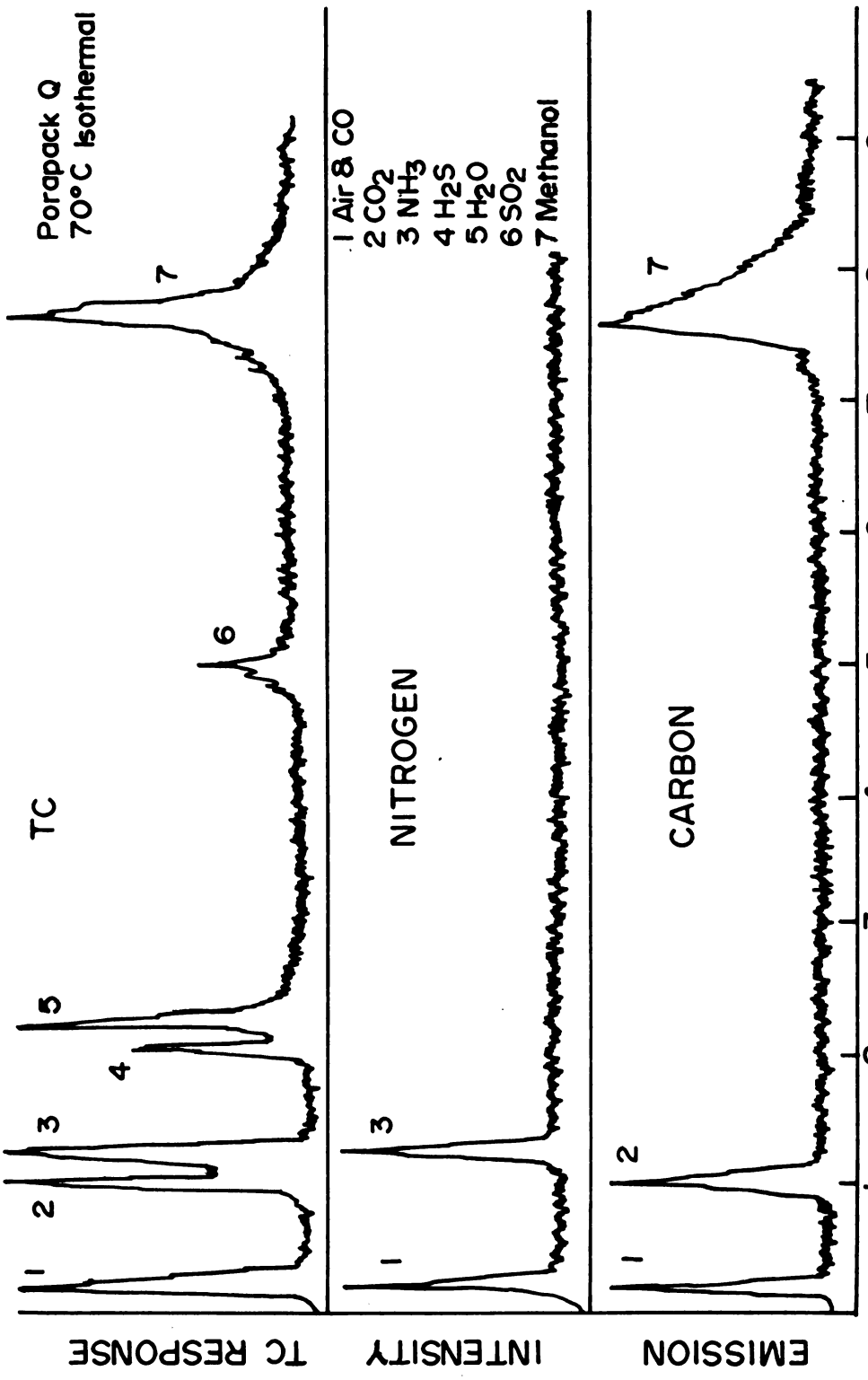

Figure 15. Separation of Simple Gases.

Table 9. Nitrogen Weight Factors for Several Detectors.

	SED	TC[≠]	FID*	AFID[@]
Nitrobenzene	1.00 ± .03			0.74
Aniline	1.01 ± .03	.82	.75	0.82
Pyridine	.98 ± .03	.79		
Ammonia	.99 ± .03	.42	nil	nil
Trimethylamine	1.00 ± .03		.46	0.91

*Relative to heptane (Reference Dietz, J. Gas. Chrom. 5, 68 (1967).

≠Relative to benzene (ibid).

@Relative to nitrobenzene (W. Aue, J. Gas Chrom. 5, 381 (1967)).

if large amounts of oxygen were present.

The sensitivity of the NSS for detection of phosphorus-containing compounds is illustrated in Figure 16 by the working curves for triethyl phosphate, guthion, and parathion pure standards in the phosphorus and sulfur modes. Figure 17 shows the separation of old-formula ISOTOX insect spray (Ortho, Inc.). Guthion as internal standard made possible the quantitation of phosphorus in each peak, though such peaks were significantly broadened, and decomposition fragments were produced due to the use of metal chromatographic columns. The peak labeled "6-unknown" may be a Tedion decomposition product, as it contains fulfur, but not phosphorus. The ISOTOX chromatograms showed many impurities, including several phosphorus-free compounds. The advantages of phosphorus-specific detection are again apparent in that sensitivity is increased, as is freedom from the noisy, rising baseline due to temperature-dependent column bleed and from interference by the many extraneous compounds found in real samples.

The phosphorus-selective detectors in common use (AFID, FPD, and electrochemical) possess generally good (200 pg - 20 ng) sensitivities, but suffer from a variety of interferences. In particular, nitrogen and halogens affect the AFID, while sulfur and the ravages of polyatomic emission distort FPD response to phosphorus.

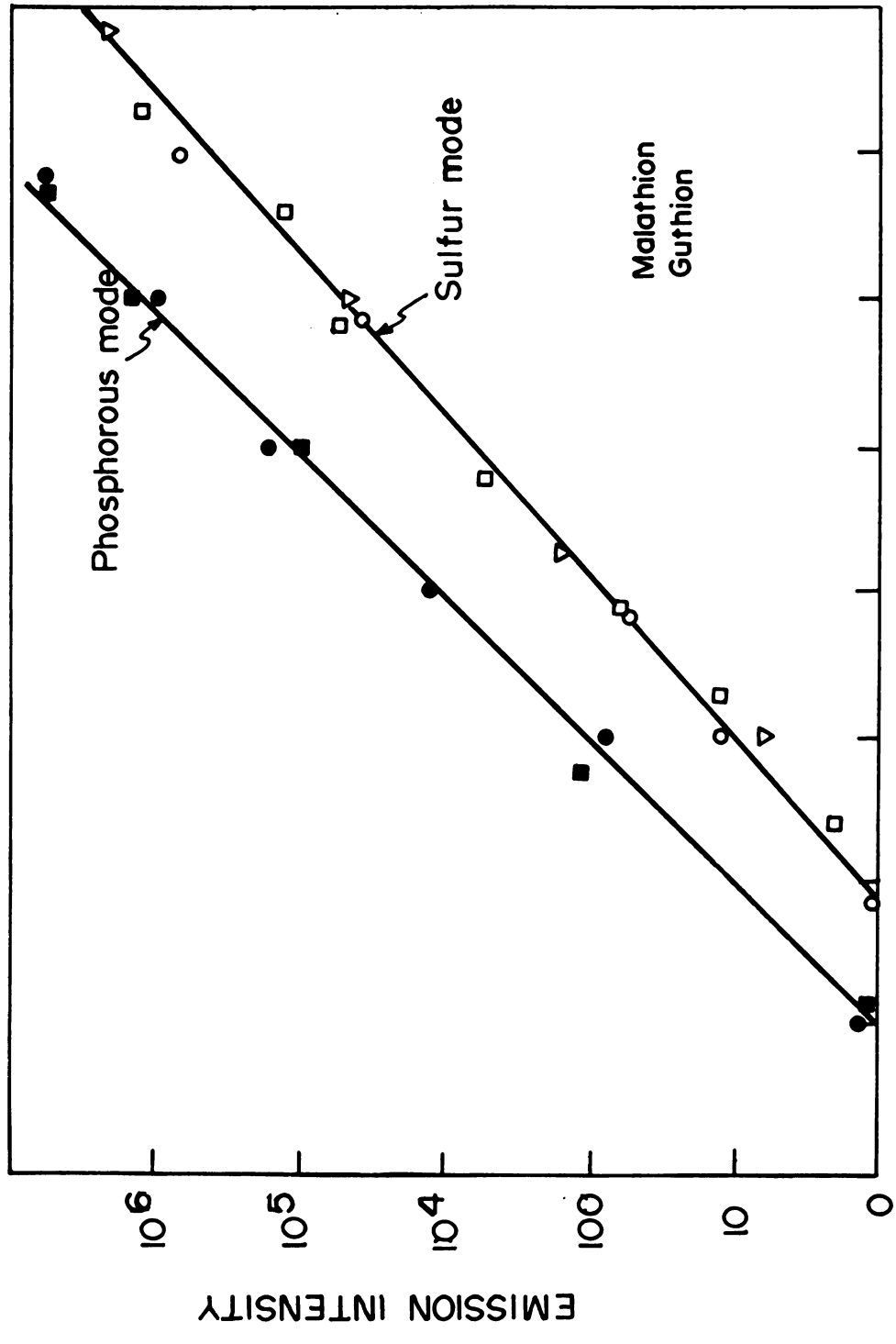

Figure 16. Quantitation of Pesticide Standards.

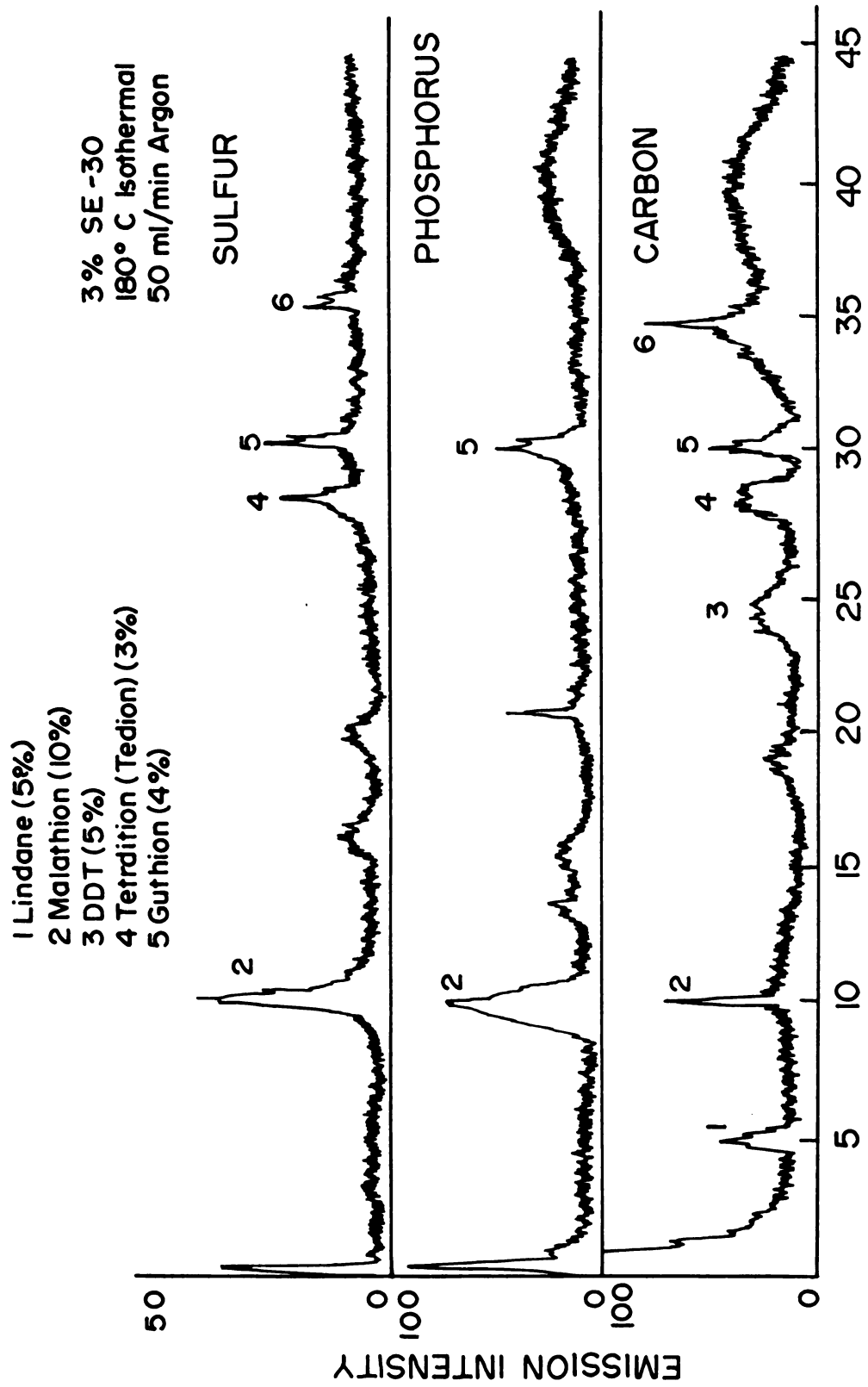

Figure 17. Separation of ISOTOX Components.

Nitrogen, sulfur, and halogens are all common elements in pesticides, so such problems are acute. Separate response factors generally are needed for each analyte compound. The NSS, an atomic emission source, is not subject to such interferences. Data listed in Table 10 again demonstrate the spark detector's total lack of any structural or substituent effects of importance to the chromatographer.

e. Silicon

Silyl derivatives of many biologically important compounds have been used extensively, and commercial sources provide convenient reagent packages. Many such silylation agents are partially functional-group selective, and combine stoichiometrically with a huge number of known analyte compounds. Silicon specific detection of silyl derivatives with the spark detector has been used to take advantage of this property.

Silicon emission from the NSS is best monitored at the 2514-2519 Å multiplet. Intensity is proportional to the silicon mass injected from 20 pg to 200 µg without computer signal-averaging, and 100 ppb to 900 ppm (Na_2SiO_4 in water) from solution with computer averaging of 500 spark emissions. Table 10 shows that silicon emission is not affected by any of the common non-metals for the optimum 3-10 µsec time window.

Table 10. Relative Response Factors for Silicon and Phosphorus.

A. Phosphorus

Compound	C/P (Actual)	C/P (Found)	RRF
Triethylphosphate	6.0	6.03	1.000
ATP			0.995
AMP			1.04
CMP			1.03
Guthion	10.0	9.89	0.97
Malthion	10.0	10.09	1.03

B. Silicon

	Relative Response
Na_2SiO_4 + 100 ppm Na_2HPO_4	1.00
+ 100 ppm NaCl	1.01
+ 100 ppm Hexane	1.03

Several amino acids were silylated according to the method of Gehrke and Leimer (18), and chromatographed on 3% SE-30 with a manual temperature program from 180-234°C. over 24 minutes. Figure 18 shows the elution of excess silylation reagent (BSTFA, Pierce Chemical Co.) and by-product (trifluoroacetic acid) prior to the silylated amino acids. The same mixture was also separated on 10% Apiezon L, which has similar McReynolds constants, but does not contain silicon. The two liquid phases cause quite different baselines for each set of carbon and silicon analyses. The methyl silicone rubber, SE-30, gives rise to the expected noisy, increasing carbon baseline, as did the hydrocarbon, Apiezon L. Both columns cause a small but detectable silicon background signal which is temperature-independent, but only the SE-30 column bleed has a temperature-dependent component.

The problem of silicon liquid phase bleed does illustrate the usefulness of some of the older non-silicone phases and of the newer organic polymeric supports/phases (e.g., Porapak) for use with silylated compounds, moderate temperature, and silicon detection by the nanosecond spark source.

Chromatograms produced by the NSS in the silicon detection mode from silylated analytes have a large, decreasing initial baseline unless the silylation agent is judiciously chosen or excess reagent is removed prior

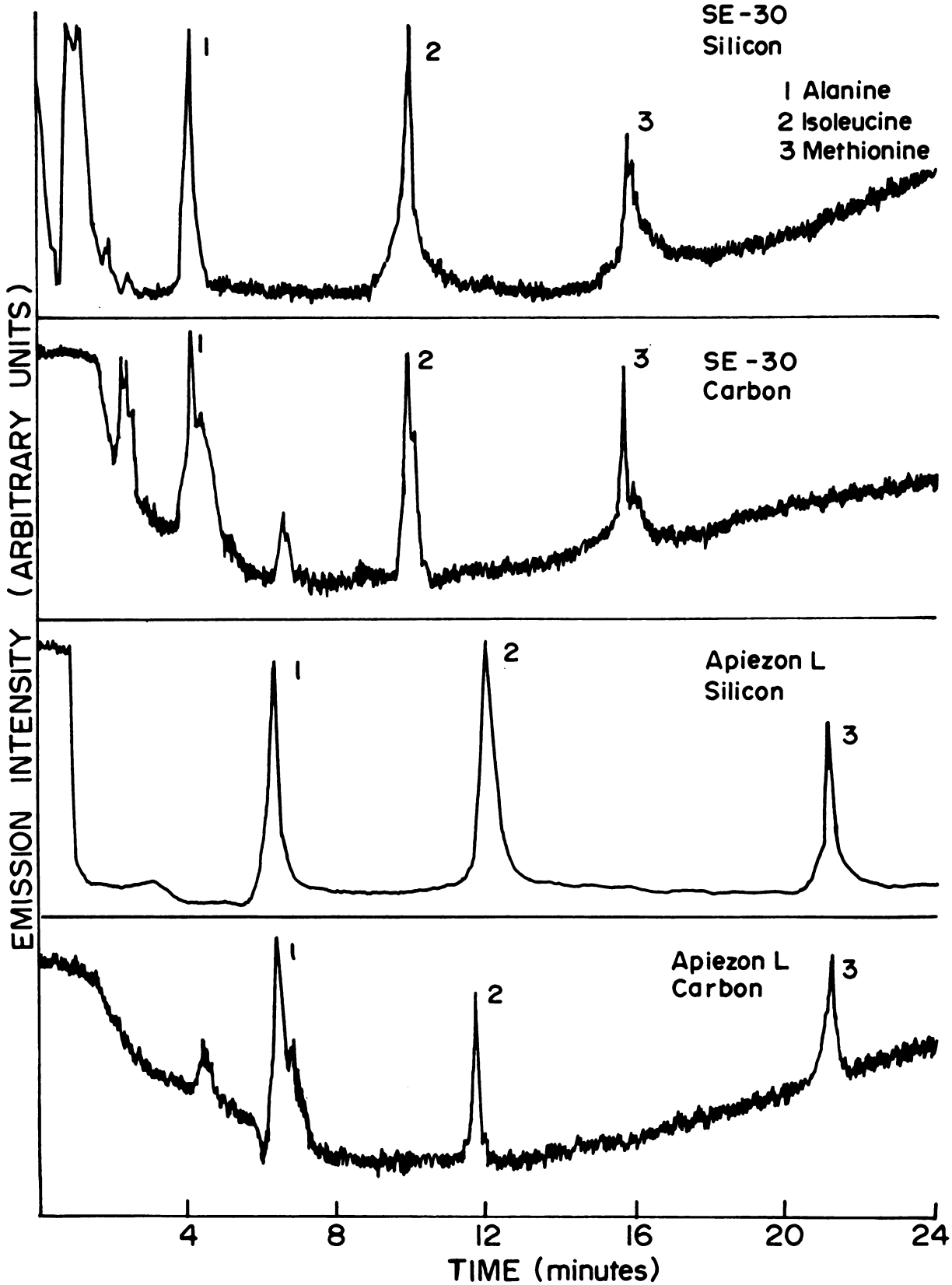

Figure 18. Separation of Silylated Amino Acids.

to sample injection. The effect is not generally seen with the flame ionization detector because the organic solvent is present at a far higher concentration than is the silylation agent and its by-products and because silicon sensitivity is minimal with the FID. Bis-trifluoroacetamide (BSTFA) is particularly suitable for derivative formation as both the reaction products and the reagent itself are volatile and can be removed with a stream of dry nitrogen after derivatization. If no analytes have short retention times, even that simple procedure is not necessary, although the trifluoroacetic acid by-product is said to damage column packings and excess BSTFA may coat the NSS quartz window.

Carbohydrates are also commonly silylated for gas chromatographic analysis. Derivatization of several sugars and sugar alcohols by use of Tri-Sil/Z (Pierce Chemical Co.) followed by separation on OV-17 (3% on Supelcoport) at 100-170°C gave the chromatogram shown in Figure 19. As with the amino acid study, excess reagent interfered, and a rising silicon baseline appeared as the oven temperature rose. Obviously, the optimum liquid phase choice for the separation (phenyl-methyl silicone) was not necessarily the best choice for detection.

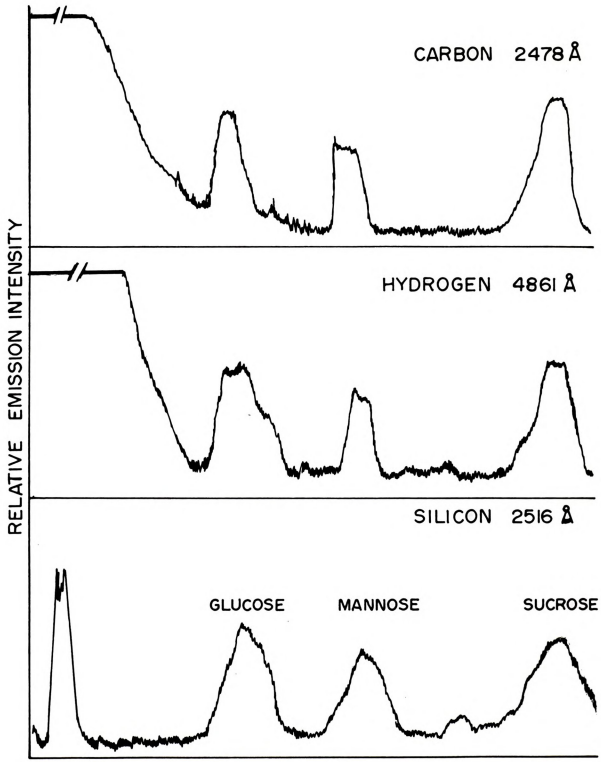

Figure 19. Separation of Silylated Sugars and Sugar Alcohols.

f. Boron

Boron analysis by gas and liquid chromatography has been neglected due to the complete lack of a boron-specific detector. Boranes and borates are quite important as synthetic agents and as by-products of commercial syntheses, and their analysis in pharmaceuticals and in chemical wastes has been mandated by agencies of many national governments. The excellent sensitivity of the nanosecond spark has made boron detection in chromatographic effluents practical.

Boron emission is monitored at 2496.78 Å/2497.73 Å B(I) with a 4-12 μsec integration window. Detection limits are 800 ppb boron from solution and 30 pg boron by gas chromatography. No detectable boron was present in carrier gases, supports or liquid phases; however, boron free glassware (except syringes) was used whenever possible in the following experiments.

Boron-specific GC detection is well illustrated by the chromatograms in Figure 20. Triply-sublimbed decaborane dissolved in hexane, was found to contain diborane, B_2H_5, as a minor impurity (approximately $1:10^4$). In this case, neither borane was detected in the carbon detection mode (2478 Å), and the solvent tail hid the diborane during hydrogen analysis. Diborane did appear, at a predictably short retention time, in the boron detection mode. Use of carbon tetrachloride as solvent,

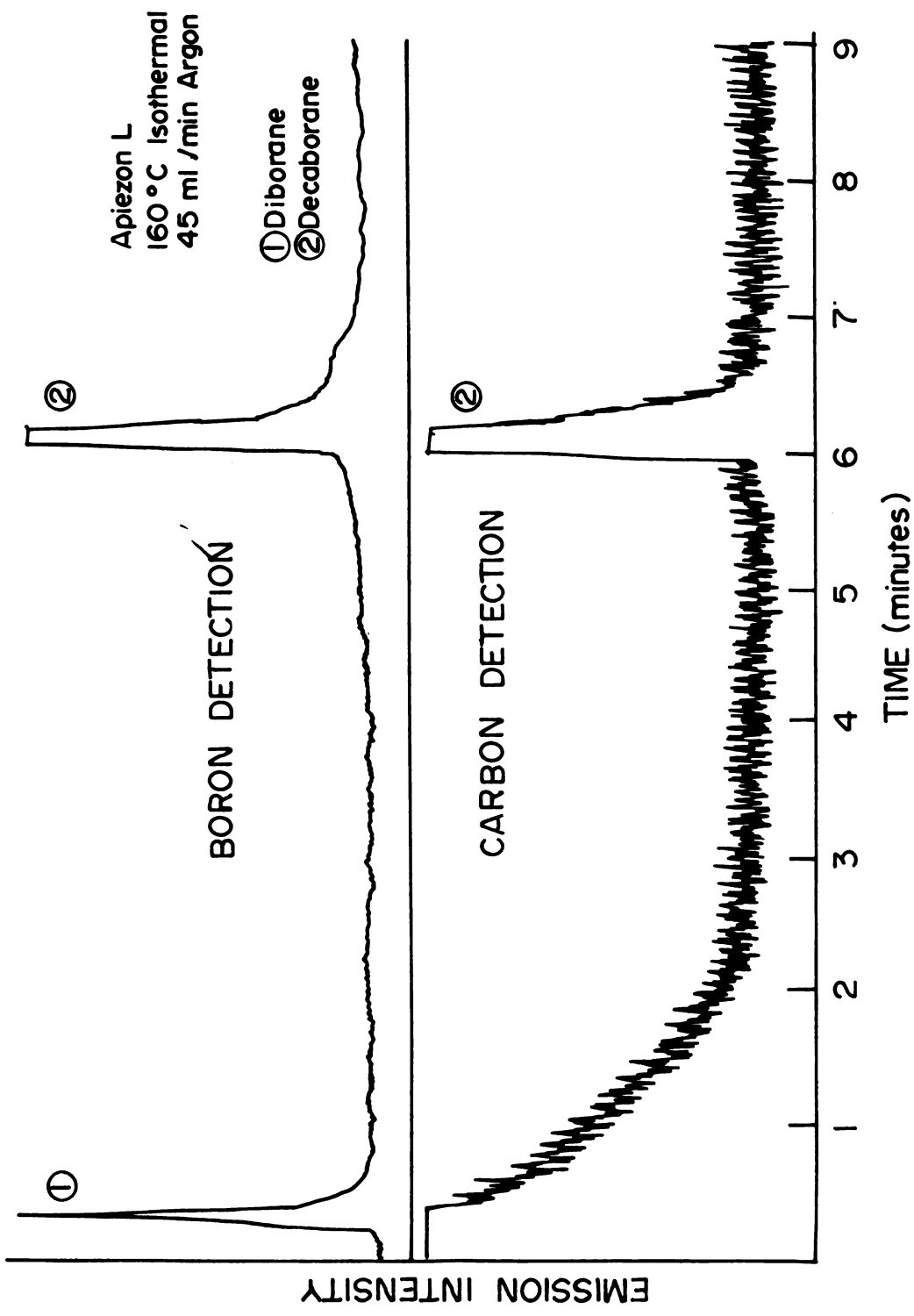

Figure 20. Separation of Boranes.

not illustrated, also allowed B/H ratio measurements for both boranes from successive chromatograms, but the large mass of chlorine atoms in the solvent plug interfered with the NSS operation.

Since no clinically important compounds, except environmental or pharmaceutical contaminants, contain boron the boron analysis capability of the NSS might easily be unused and its inherent advantages lost to the clinical chemist. Further, the instability of many organoboron derivatives and the lack of any apparent need for them for gas chromatography has limited their development. Recently, however, bifunctional boron-derivatizing agents have become quite popular for analysis of diols and aminols (281).

Cyclic n-butyl boronate esters (282) of gem-diols and polyols have been synthesized, and possess generally smaller retention times than do the analogous silyl derivatives under the same chromatographic conditions. Successive chromatograms in carbon and boron detection modes of cyclic n-butyl boronate esters of several sugar alcohols, are presented in Figure 21. The derivatives are easily prepared by the addition of 1.0 ml of 0.05% n-butyl boronic acid (Pierce Chemical Co.) in pyridine, followed by 30 minutes' reaction at 55°C. Methanol may be added to form the ester with any remaining reagent, but this is not necessary. Excess n-butyl boronic acid dehydrates to tri-n-butyl boroxine when injected into

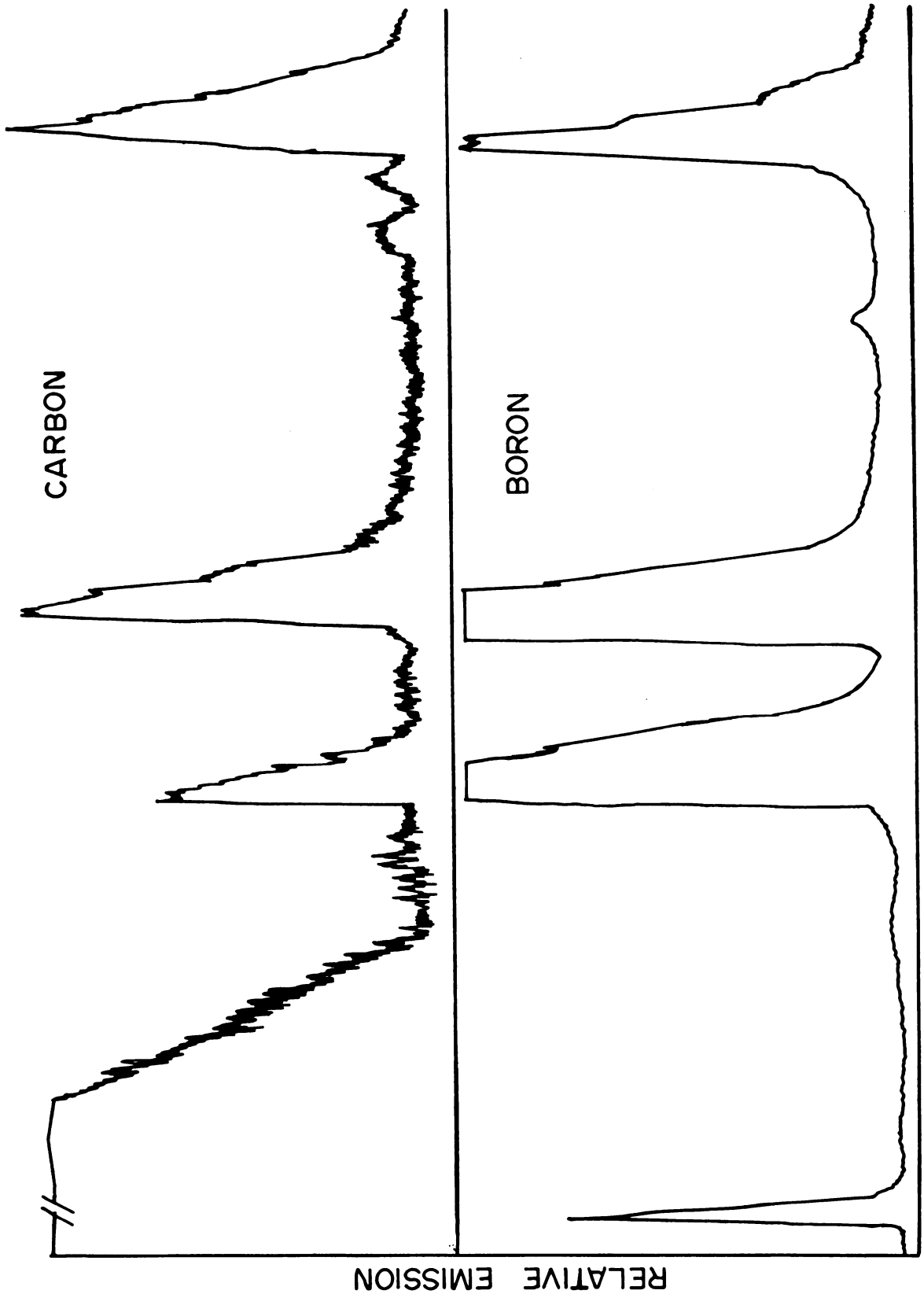

Figure 21. Boron Derivatives of Sugar Alcohols.

the chromatograph. The resulting chromatograms exhibit single peaks for each sugar alcohol or other 1, 2 or 1,3 diol analyzed and for the boroxine. That the saccharide units react stoichiometrically is further supported by the C/B ratios listed in Table 11.

Neither the solvent plug nor the column-bleed induced baseline rise appears, and the background noise level for boron is no greater than for the continuum emission. Table 11 also indicates that effective analytical sensitivity increases when boron is detected, even for compounds with large, but finite, C/B ratios. Therefore, the ability of the NSS to detect boron is a major virtue which should be exploited.

g. Sulfur

Sulfur analysis is important clinically for the detection of sulfur-containing amino acids and pharmaceuticals, but is even more valuable as an adjunct to phosphorus detection of pesticide residues. The flame photometric (FPD) and microcoulometric (MCD) detectors are the major sulfur-selective detectors available for GC. For the NSS to be of value to the working analyst, it should overcome the inherent non-linearity and non-proportionality problems of the FPD and MCD detectors discussed previously. There is no commercial sulfur-selective or specific detector for HPLC other than those modified from

Table 11. Carbon/Boron Atom Ratios for Several Sugar Alcohol Boronates.

	Theoretical	Found
Ramnitol	2.00	1.94
Fucitol	2.00	1.89
Glucitol	1.71	(erratic results)
1,2-Propanediol	3.00	3.02

Atom Ratios calculated with respect to tri-n-butyl-boroxine, $C_{12}H_{27}O_3B_3$.

GC use.

Emission from atomic sulfur is measured at 5209 Å, S(I), and at 3291 Å, S(I), with a 2-7 μsec integration window. Both are resonance lines, thus decreasing the upper limit to the linear dynamic range as compared to most other elements observed. The 3291 Å line commonly gave 40-60% greater emission than did the 5209 Å line and was used to obtain sulfur detection limits, which were 670 ppb S as particles (methionine) from solution and 2.5 ng sulfur (diethyl sulfide) in gas. Upper limits were 300 ppm and 40 μg sulfur, respectively.

Linearity and proportionality of response to sulfur is indicated by data in Table 12. The lack of functional group effects is indicated by the equal atom emission intensities for thiophene, diethyl sulfide, guthion, parathion, malathion, and dimethyl sulfoxide in gas and methionine, calcium sulfate, cysteine, copper (II) sulfate, and copper (I) sulfate as particles. Further, the slopes of emission intensity vs sulfur mass plots for guthion, malathion, and thiophene are all approximately 1.00 ($\pm$.04). Data were obtained individually with minimal chromatographic separation for guthion and malathion by the use of a short (1 foot) 1/8" o.d. pyrex tube packed with 3% SE-30 on Supelcoport. Use of metal columns caused decomposition of certain samples, but an all-glass system was not available and would have been

Table 12. Sulfur Analysis with the Spark Detector.

a. Linearity

	Conc. (ppm)	Relative Emission Intensity
Methiamine (solution)	1.0	1.0
	15.0	14.7
	30.3	28.4
	100.4	103.2

	Mass (ng)	Relative Emission Intensity
Diethyl Sulfide	10	1.0
	80	8.5
	405	42.6
	900	89.3

b. Relative Response - Interelement Interference

Compound	Relative Emission Intensity
Methimine	1.00
Calcium Sulfate	0.99
Cysteine	0.96
Cupric Sulfate	1.08
Cuprous Sulfate	1.01

	C/S (Theory)	C/S (Found)	Relative Intensity(S)
Diethyl Sulfide	4.00	4.00	1.00
Guthion	5.00	4.87	0.98
Parathion	10.00	9.82	0.97
Dimethyl Sulfoxide	2.00	2.06	1.03
Malathion	5.00	5.06	1.02

quite inconvenient with the chromatograph built and used by the author.

Isotox (Ortho Chemical Co.) spray (old formula) was also analyzed in the sulfur mode. Although decomposition products were present, sulfur-containing components were segregated as easily as were phosphorus-containing compounds in the same mixture (Figure 17). Empirical formulae were again determinable, without regard for the solvent tail, by use of one or more appropriate internal standards (triethyl phosphate and diethyl sulfide). Present stocks of ISOTOX have a quite different formulation from that used here. The peak tentatively identified as a Tedion decomposition product had a partial atom ratio different from that of any of the known components of the ISOTOX mixture. The large broad, peak was probably due to the presence of one or more surfactants in the ISOTOX.

Sulfur specificity was not utilized by means of N-thiocarbonyl or phenylthiohydantoin derivative formation with amino acids. Instead, as shown in Figure 22, the naturally-occurring sulfur amino acids were selectively identified in the mass of silyl amino acids and extraneous matter in urine. Derivatives of pure standards of alanine, phenylalanine, methionine, cysteine, and cystine were prepared by reaction with bis (trimethylsilyl) acetamide in pyridine (Tri Sil/BSA-P, Pierce Chemical Co.). Retention time for each amino acid derivative was determined.

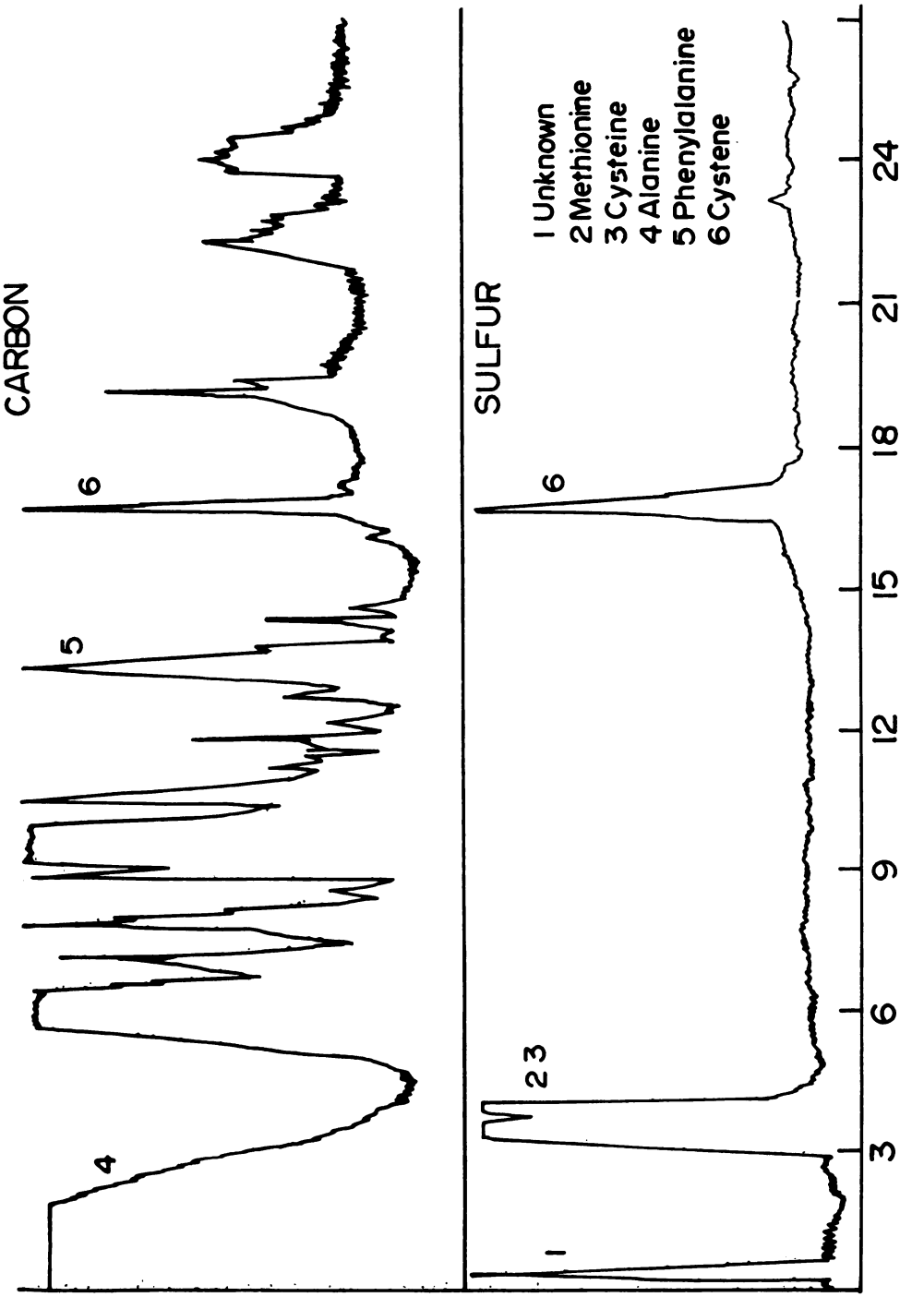

Figure 22. Sulfur Detection Mode Analysis of Silylated Amino Acids from a Urine Matrix.

Then a normal urine was prepared for analysis by the adsorption of pigments and proteins on activated charcoal followed by the evaporation of the supernatant to complete dryness under dry nitrogen prior to derivatization. Sample dryness is extremely important when amino acids are derivatized. Silylated urine extract was separated on 3% SP-2250 (equivalent to OV-17) on Supelcoport. The oven temperature was 190°C initially and was increased to 255°C over a 20 minute span. Methionine and cysteine were not separable under these conditions. Because of the large carbon background signal, the sample injected for the carbon mode analysis was diluted with pyridine and the signal was further attenuated on the graph presented in Figure 22. Sulfur detection was element-specific and selectivity coefficients were effectively infinite.

h. Halogens

Of all the non-metallic elements, the halogens were the most difficult to detect with the miniature spark source. By use of an early, narrow integration window (1.0 - 2.0 μsec) or, preferably, and early sample-and-hold point (1.2 μsec), it was possible to analyze for bromine and chlorine. Iodine emission probably occurred in the far-ultraviolet, and detectable emission was found for fluorine at 7037.45 Å. The existence of excellent, halogen-selective electron capture detectors also somewhat

obviated extensive NSS studies of halogen analysis. Detection limits for bromine, chlorine and fluorine are, respectively, 10.0 ppm/1.2 μg, 20 ppm/0.7 μg, and 40 ppm/ 1.2 μg. All three elements are determined during the most irreproducible portion of the spark afterglow, and require quite accurate temporal control of data acquisition. They should benefit greatly from current improvements in digital timing circuitry and in the reproducibility of the spark itself (278).

Headspace gas from above a solution of fluorobenzene, chlorobenzene, and bromobenzene in benzene was separated on a 6 foot long Porapak Q column (80/100 mesh) at 170°C with argon carrier. Consecutive chromatograms were run in the individual halogen modes and the FID tracing was obtained by using the same sample with Varian 1400. No interelement interferences were found, although it was obvious that the standards used contained other organohalogen contaminants. Linearity was found to be good for the halogens, but the plasma was affected by organic halides above 100 μg as gas. Particulate halides did not show the same effect.

6. Column Bleed

Two signal and noise sources in chromatography are amenable to detector improvement: the solvent plug and the column bleed. The nanosecond spark detector has

been used to alleviate the former problem by the monitoring of an element contained in the analyte but not in the solvent. The noisy, rising baseline found in temperature-programmed GC has been decreased or eliminated either by analysis for an element inherent in the analyte species or by formation of an appropriate derivative.

The very fast firing rate, and concommitant short response time of the NSS also made possible the first study of the nature of column bleed and provided a further increase in practical sensitivity for the NSS. Table 13 gives the precision (% relative standard deviation) of the signal for carbon, silicon, and boron minus % RSD of the background from the NSS at 900 Hz, 150°C, with purified argon carrier for the separate effluents from several individual chromatographic columns. Signals were computer-averaged over 5,000 firings. All columns were well-conditioned and had been protected from oxygen. Particles from solution via the desolvation system were in the form of carbonate, silicate, and borate, respectively, and were adjusted in concentration to give signals equal to each other and close to those obtained from the GC.

The data show that the precision of C, B, and Si measurements approximates that of particulate C, B, and Si analyses for those columns which have a liquid phase which contains the element in question. The high average

Table 13. Column Bleed Analysis

% RSD	Apiezon-L	OV-1	Porapak	Gas	Particle-LC
Carbon	7.7	6.4	3.2	0.12	3.6
Silicon	1.9	7.6	.35	0.10	3.6
Boron				0.15	3.4

Signal intensities equal for each element 900 Hz, 150°C, Argon Carrier, % Relative Standard Deviation of the emission signals from several different analyte sources minus % RSD of background (off-line) emission.

molecular weight and low vapor pressure of the stationary phases involved would support the conjecture that such liquid phase exits the column as aggregates, rather than as single molecules in vapor. It is also valuable to observe that silicon-containing supports (Supelcoport, or Varaport, but not Porapak Q) contribute measurably to imprecision for silicon analysis. Although it is not shown in Table 13, a silicon emission equivalent to approximately 200 ppb silicon from solution was found for the diatomite supports, but not for Porapak Q.

7. Conclusion

The nanosecond spark emission detector is thus capable of sensitive, element-specific detection on a routine basis. No inter-element interferences of any consequence to the chromatographer are present and linearity and reproducibility are excellent for most elements studied.

CHAPTER V

THE NANOSECOND SPARK AS A DETECTOR FOR LIQUID CHROMATOGRAPHY

The lack of sensitive, reliable, selective detectors has been an even greater problem in liquid chromatography than in gas chromatography. Previous HPLC detectors generally have been modified GC detectors with a solvent removal step, or optical or electrochemical detectors. As described in Chapter III, such detectors have several undesirable properties for routine analytical applications.

Detector requirements for HPLC are quite similar to those for GC, except that the maintenance of very small (<10 μl) dead volume is even more important. Similarly, specific multi-element analysis should be more valuable when applied to the resolution of overlapping LC peaks. Polarographic and post-column reactors may be made fairly selective, but the range of usable functionalities is limited. Atomic spectroscopic techniques should provide the needed element-specific capability, but has been used very little for HPLC detection. However, the inherent advantages of atomic emission spectroscopic techniques should be exceedingly useful for HPLC detection. Therefore, the miniature spark source detector has been modified for use with HPLC.

A. Liquid Chromatography

Gas chromatographic and solution experiments proved the sensitivity, proportionality, and element specificity of the nanosecond spark source. Thus, the adaptation of the SED to HPLC via a Veillon-Margoshes-type desolvation system was a logical succession.

A high-pressure liquid chromatograph (Nester-Faust Co.) with 1000 psi Milton Roy Co. reciprocating pump and double-beam UV absorbance monitor (254 nm) was used. A 5000 psi Milton Roy Co. (Riviera Beach, FL) reciprocating pump was also used. Columns were 2.1 mm i.d., 316 stainless steel with low dead-volume Swagelok fittings, and contained appropriate Dowex ion-exchange resins (80-120 mesh) or micro-particulate (37 um) pellicular supports. The UV detector effluent flowed through a two foot length of 1/32" i.d. Teflon tubing to the desolvation system. Dry analyte particles then entered a spark chamber similar to that used for gas chromatography, and were atomized and excited by the spark. Emission lines monitored and integration windows were the same as for gas chromatography detection. Carbon and nitrogen analyses were made using computer signal averaging for asparagine, and other amino acids, bovine serum albumin, and human-based commercial control serum. Purified argon carrier and glass-distilled deionized water were used for all solution

analyses and liquid chromatography.

Detection limits for carbon, nitrogen, phosphorus, and sulfur from aqueous solution are shown in Table 14. All column packings gave a measurable carbon background and, depending on the column type, noticable nitrogen and sulfur background. Hydrogen and oxygen measurements were effectively impossible, due to residual water vapor entering the spark.

The first separation and quantitation with the nanosecond spark source was made on DOWEX - 50 cation exchange resin (H^+ form) (0.5 meter X 2.1 mm stainless steel column) at 720 psi and 1.7 ml/minute flow of 0.0001 M HCl. The NSS gave a chromatogram delayed approximately 20 seconds from the UV detector chromatogram. Uric acid and phenylalanine were chosen for their fairly high molar absorptivities at 254 nm and for their atomic constitution. Bands were not significantly broadened by the use of the macroresins. System dead volume was rather large (ca. 0.5 l) in a superficial sense, but the rapid transit of the analyte and resultant plug flow with small opportunity for mixing with preceeding and following components effectively limited band spreading.

Detection of uric acid and phenylalanine by atomic emission was approximately 10^4 times more sensitive than by UV absorption. This ratio was dependent on the molar absorptivity of the molecule analyzed, and was indicative

Table 14. Detection Limits with the SED/HPLC.

	Mass	Conc.	Line (Å)
Carbon	20 pg	1 ppb	2478
Boron	40 pg	0.1 ppm	2497
Silicon	120 pg	0.1 ppm	2516
Sulfur	250 pg	670 ppb	3291/5209
Phosphorus	75 pg	0.4 ppb	2535
Nitrogen	50 ng	2 ppm	6723
Halogens	ca 600 ng	30 ppm	various
	HPLC	Solution	

Detection Limits from solution and by HPLC do not correlate in all cases because HPLC column bleed varies with the element detected.

of the major difficulty with use of absorbance, fluorescence, and refractive index measurements. No substituent effects are found for the NSS, thus no "response factors" are needed for each analyte compound.

A series of underivatized amino acids (Figure 23) was separated on a 0.5 meter X 2.1 mm Aminex A-28 microparticulate anion exchanger (hydroxide form) at 900 psi and 1.0 ml/minute of 2×10^{-4} M, pH 4.3 phosphate buffer. The chromatogram shows the great usefulness of multielement analysis, even though several runs are actually required to accomplish the complete analysis. UV detection was only marginally useful due to poor absorbance at 254 nm for most amino acids. A similar mixture was separated on a macroresin (Dowex) which provided relatively poor separation and greater band spreading. The flow rate was 1.6 ml/minute @ 700 psi for the same buffer. In that case it was possible to resolve components based on sulfur content and C/N ratio. Obviously, the superior column packing should be used, but the utility of the nanosecond spark detector for more difficult separations is implicit.

Carbohydrates should be very usefully analyzed by HPLC due to the relative difficulty of preparation of volatile derivatives. Their separation on polar bonded-phase, ion-exchange, or gel permeation materials is not difficult, though their quantitation requires either post-column

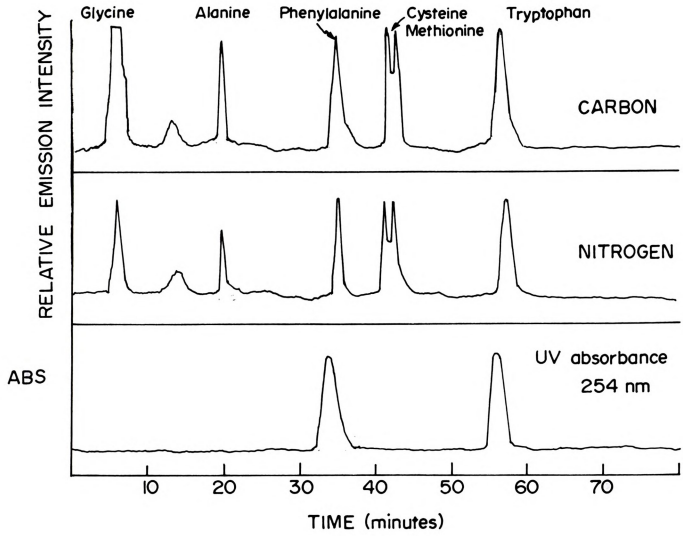

Figure 23. Separation of Amino Acids of HPLC.

reactions or a UV detector usable at 195 nm.

The Nester-Faust detector (254 nm) proved to be quite blind to all saccharides, but the NSS in the carbon detection mode was quite capable of detecting sucrose and lactose in column effluent. The separation was made on Dowex-1X8 macroresin at 840 psi and 2.0 ml/minute flow of 2×10^{-4} M borate buffer, pH 5.0. Retention times were 23 minutes for sucrose and 30.5 minutes for lactose, and apparent detection limits were 38 ng of sucrose and 65 ng lactose. Band spreading due to the choice of column material was quite visible and seriously affected detection limits. Detection limits for sucrose and lactose from solution were similar to those for other carbon sources.

The separation of 5' mononucleotides on Aminex A-28 microparticulate resin (0.5 m x 2 mm) provided an excellent opportunity to compare the absorption detector with the nanosecond spark under nearly optimum conditions. Absorptivities at 254 nm were high, although the wavelength of maximum absorbance was generally closer to 280 nm, and the separation technique was nearly state-of-the-art for an isocratic system at the time that the chromatograms were made. Both detectors would have functioned with gradient elution, albeit with a small baseline change for the absorbance monitor. Pressure was 930 psi at a flow rate of 1.0 ml/minute for 1×10^{-4} M phosphate buffer,

pH 3.1 initially. After the three mononucleotides eluted, the buffer pH was changed to 5.0 to elute ATP quickly. Figure 24 shows the chromatograms from repeated injection of three 5' - mononucleotides and adenosine triphosphate (Sigma Chemical Co.) using the UV absorbance monitor and the NSS in carbon and phosphorus modes. Sensitivity with the SED is approximately 3-4 orders of magnitude greater for the nucleotides than with the double beam absorbance monitor.

Although phosphorus and carbon sensitivities are nearly equal, analysis for both elements is preferable to single-element analysis because the C/P ratio for each peak definitely distinguishes mono from di- or tri-phosphonucleotides and from nucleosides. Residual organics leaching from the ion-exchange column packing and organics and CO_2 in the mobile phase also cause the carbon background signal and noise to be greater than that for phosphorus.

The spark source detector capabilities are effectively duplicated for GC and HPLC, except that the dead-volume is greater for the HPLC system because of the desolvation step. Particulate analytes cause decreased precision, but high concentrationsof halogens and carbon do not affect the spark nearly so adversely as when in gaseous form. Solutes may be aspirated and analyzed up to the point that particles clog the pneumatic nebulizer (2-5 ppt).

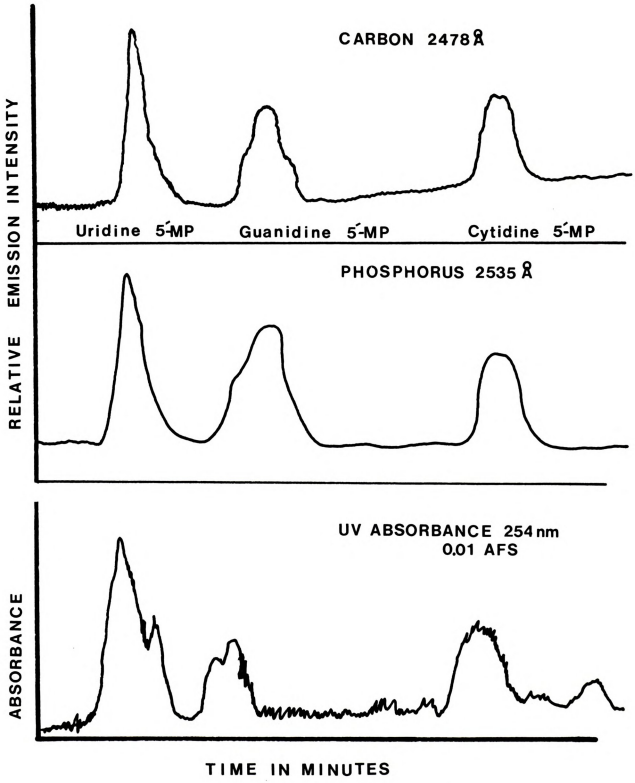

Figure 24. Analysis of 5'-mononucleotides by HPLC.

The nebulizer/desolvation system also deserves consideration because its efficiency and efficacy will help determine the usefulness of the miniature spark source as a detector for any dissolved matter.

B. Particle Size Effects

Early work on the miniature spark and nebulizer prompted interest in the particle size and size-distribution of analyte entering the spark. There was concern that variation in the anion of analyte compounds, therefore in melting point and hygroscopicity, might affect the physical character of the particles and, analyte atomic emission. It was also possible that desolvation and/or sample through-put might vary with compound structure.

Transport and aerosolformation have been characterized experimentally and theoretically with respect to both mean droplet diameter and requisite desolvation time (283, 284). Under conditions closely approximating our own, it has been found that the critical droplet radius is given by $wv^2 = 6\ s/r$, from consideration of surface energy (s), argon carrier gas density (w), and velocity of argon (v) with respect to the droplets of radius, r, themselves. Average droplet diameter may also be calculated (279), as may the size distribution about that mean.

A desolvation time of 23 msec was calculated for a

droplet size of 15 μm diameter from the following equation:

$$t_s = [\frac{\rho A_o C_p}{8}] \ln [1-C_p (T-T_b)/L]$$

where t_s is the total time for desolvation, in seconds, A_o is the initial area of the droplet, C_p is the average heat capacity of the vapor at constant pressure, T is the temperature of the chamber (230°C), T_b is the boiling point of the solvent, L is the thermal conductivity of the gas, and ρ is the density of the liquid. The equation neglects the additional transport of thermal energy to the boiling droplet by convection. This certainly would be significant in the present case and would reduce the time, t_s. The residence time of the sample mist in the desolvation chamber, neglecting the additional gaseous volume of the sample solution, is calculated to be four to five seconds. Thus, desolvation is likely to be completed in the desolvation chamber for most compounds. The analyte residence time in the desolvation chamber is consistent with the overall response time of the detector after an analyte solution change (8-12 seconds).

Desolvation has been investigated primarily in flames, where it has been shown that evaporation in a spray chamber greatly influences drop size distribution at the flame. No studies of dry particle size and size distribution have been reported, though this method of sample introduction

is becoming progressively more common in analytical chemistry. Skogerboe (280) recently has reported studies of particle character with results similar to those presented here. Such a study should be of interest to many workers using similar desolvation systems, and would be of particular value in helping to determine which of several solvent vapor removal procedures would be most promising for use with the high-pressure liquid chromatograph and nanosecond spark detector.

Preliminary studies in this laboratory had shown that particle size may have large effects on atomization efficiency and precision. Therefore, three experiments were proposed to elucidate the apparent particle size effect in our system. The first would establish particle size distributions as functions of concentration and relative hygroscopicity for several salts and organic compounds. Several salts of differing hygroscopicity and component ions as well as one amino acid (glycine) and bovine serum albumin (BSA) would be sampled and their size data compared with analytical results. As size and distribution changed it was expected that analytical precision and sensitivity would also be affected.

a. Concentration and Hygroscopic Effects on Particle Size Distribution

Particles were trapped either by impact and adhesion

to glass or nucleopore (polycarbonate) filters. After appropriate sputter-overlaying with gold, scanning electron microscopy (SEM) was used to provide hard-copy photographs for off-line analysis. The rather small (10 μm average diameter) particles adhered to a variety of surfaces, but polyester backed-Nucleopore (General Electric Co., Nucleopore Division) filters provided a much better background appearance than did either double-sided Scotch tape (3M Company) or Milipore (Milipore Corp.) cellulose acetate filters. A typical particle is shown in Figure 25.

The particle cluster photographed is hollow and the mantle is made of much smaller, spherical particles. Cupric sulfate, shown in Figure 25, does form several hydrates, but is not noticably delequescent. Figure 26 shows the result of incomplete desolvation of spray droplets, probably due to the greater hydrophyllicity of the bovine serum albumin (BSA) used. The aggregates are spread in a circle due to evaporation of the solvent water after capture of a large droplet on the Nucleopore filter. Similar photographs resulted with the hydroscopic salts, e.g., sodium perchlorate, but not from easily dried compounds.

Cupric nitrate and cupric perchlorate detection limits were determined with the nanospark. Although precision was worse for the perchlorate salt at high concentrations, the detection limits were equal. This is consistent with

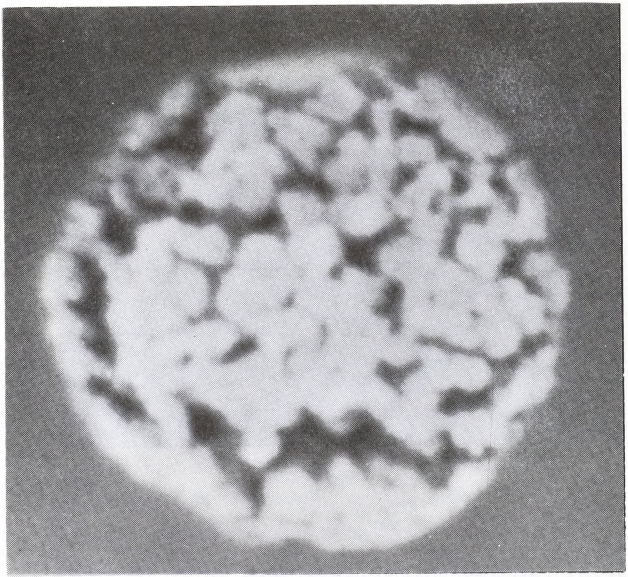

Figure 25. Cupric Sulfate Particle (X40,000).

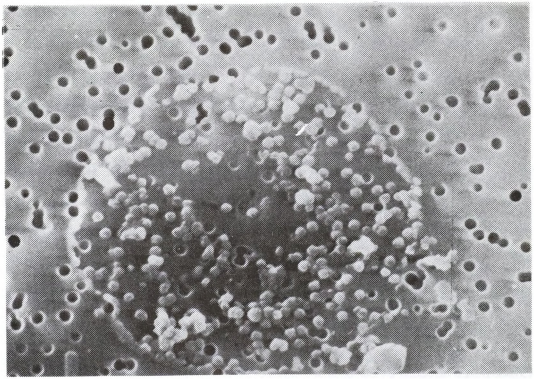

Figure 26. Bovine Serum Albumin Particle (X2000).

the possibility that desolvation efficiencies and particle sizes may be equal at low concentration yet quite different at high concentrations. It is not possible to obtain statistically valid SEM measurements for low concentration solutions, but the photographs of high concentration perchlorate solutions give effects similar to those for BSA in Figure 26. The breadth of particle sizes was greater for the perchlorate (9.3 $\pm$8 μm) than for the nitrate salt (8.5 $\pm$ 3.1 μm), but no difference in the mean diameter is certain. One interesting difference between the hydrophyllic and the easily dried salts was the total absence of the hollow-sphere conglomerates for the hydrophyllic compounds.

Particle compositions from mixed cation solutions were studied briefly with an electron-microprobe. A solution 10^{-3} N in both calcium chloride and aluminum chloride gave two particle populations: the larger (10 μm) particle gave predominately calcium emission, while the smaller (∿1-2 μm) particles gave essentially aluminum emission. The analytical effects of this may be important, as particle size discrimination by the desolvation system does occur in this diameter range. Electron microprobe tracings of a typical particle from a solution 10^{-4} M in each of cadmium, copper (II), and magnesium chloride, exhibit segregation within a single 8 μm particle, rather than between particles.

b. Condenser Effects on Particle Size Distribution

Two major sources of particle size discrimination exists in these experiments: the particle collection technique itself and the condenser and associated tubing between the heated chamber and the spark gap.

Desolvated particles were collected at points A, B, and C, marked in Figure 27. Table 17 shows that the range of particle sizes for several compounds decreases as more of the system convolutions are transversed by the salt particles. In particular, the largest grains (>25 μm) are selectively removed. That discrimination is not complete and is noticeable less for the more hydrophyllic salts may indicate a reagglomeration of particles, especially "wet" ones, after passage through the Friedrichs condenser. Small (<2 μm) and medium diameter (2-25 μm) particles do not seem to be affected by the condenser system other than that particle density on the collecting surface seems to be less a C than at A or B. This is not confirmed analytically, but is merely a subjective impression. Analyte emission could not be used to follow analyte throughput, as the argon carrier was much too humid at A for good operation of the spark.

c. Aspiration Rate Effects on Particle Size Distribution

The critical droplet radius, as discussed earlier, is inversely proportional to the square of the aspiration-gas

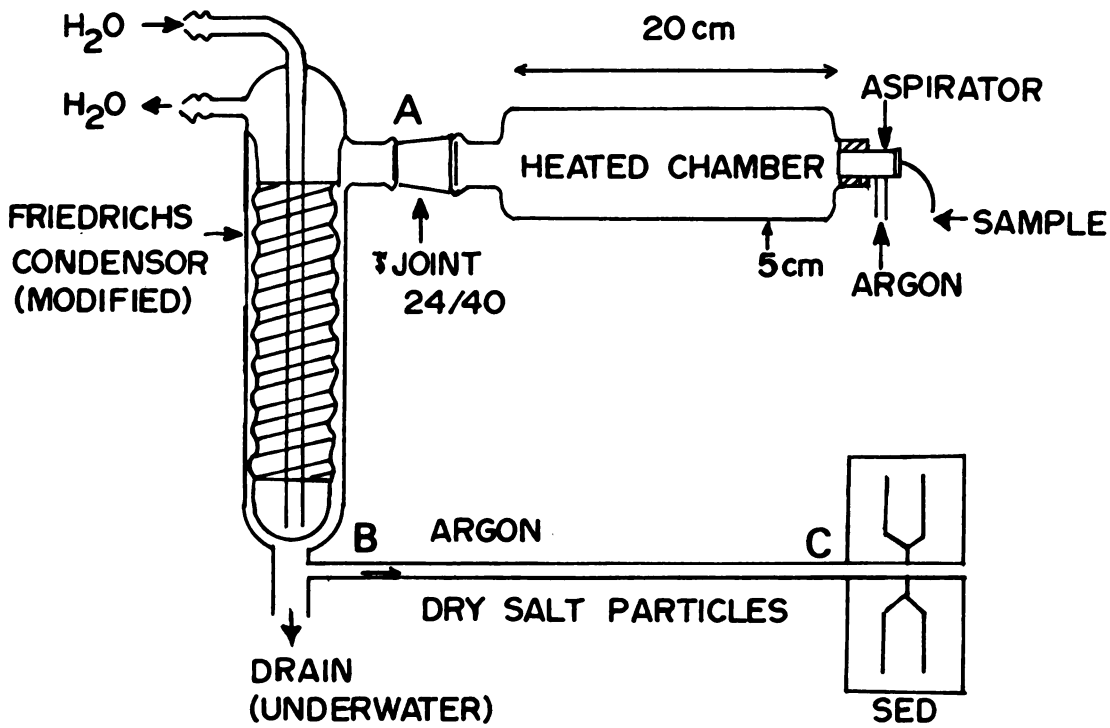

Figure 27. Desolvation System for HPLC/SED.

Table 15. Effects of the Desolvation System on the Particle Size Distribution.

	A	B	C
$CuSO_4$*	18.1 ± 23.5	12 ± 6.1	11.8 ± 8.5
$CuCl_2$	15.0 ± 19.7	12.8 ± 7.2	11.0 ± 5.2
CuCl	14.7 ± 16.9	13.2 ± 6.9	9.3 ± 4.7
$CuClO_4$	11.1 ± 17.4	9.4 ± 3.1	13.2 ± 8.1
BSA≠	-----	9.6 ± 3.3	12.1 ± 7.0
Asparagine	8.2 ± 3.6	7.9 ± 2.8	7.7 ± 2.9

Mean particle diameters ± 1 SD, stated in μm.

*Many large clusters of smaller (<3 μm) particles seen (Figure 25).

≠Many large circular masses of particles seen (Figure 26).

velocity. Therefore, particle size distributions were measured for particles produced at varying gas flow rates. It was not possible to ascertain the instantaneous gas flow velocity with respect to the droplets, so changes in the gas bulk flow rate were assumed to be proportional to flow velocity with respect to the droplets.

Performance of this experiment showed that, as the bulk flow velocity increased, the mean particle diameter decreased at point C. The frequency of large whole particles, but not obvious agglomerates, declined sharply. There were also apparently fewer clone-like phenomena akin to that in Figure 26. This should lead to improved analytical precision if particle size is actually important in the spark system.

The nanosecond spark, as configured, is itself affected by the carrier gas velocity. At high flow rates the spark appears to be blown "down wind" by the carrier, and the observation position then had to be reoptimized. Because of this, it was not possible to determine if any real improvement in detection limits or overall precision were possible by an increase in carrier flow velocity. Attempts to compare the effects of increased gas flow on particulate and gaseous analytes were not successful. Had particulate analysis deteriorated less than gas analysis with increased flow, then a particle size distribution effect could have been invoked.

CHAPTER VI

SUMMARY

1. Conclusions

The nanosecond spark emission source is a sensitive, element-specific detector for both gas and liquid chromatography. No interelement effects of concern to the chromatographer have been found, although many possible circumstances have been examined. Linearity is excellent for all elements examined. Detector response is not temperature sensitive, except that, with present power supplies, the maximum firing rate increases with temperature. Future power supplies should operate at much higher frequencies and be independent of gap breakdown voltage. Sensitivity for carbon, nitrogen, boron, oxygen, and most other non-metals and metalloids is superior to that for other chromatographic detectors, but halogen sensitivity is comparatively poor.

The NSS detector is relatively easy to operate, quite reliable, and is not significantly sensitive to carrier-flow. Its cost, excluding monochromator or filters, is approximately $200. It is quite easy to build from readily available materials, and may be made as an "add-on" to present gas or liquid chromatographs. Simultaneous multi-element analysis is possible with multichannel data acquisition devices. The author successfully coupled

an SSR polychromator (Vidicon) system to the spark. The nanosecond spark source is not without faults, but it is a good start toward the "poor man's mass spectrometer".

2. Prospectives

The nanosecond spark source needs several refinements to allow full use of its inherent capabilities. The spark should be made to operate more reproducibly, at higher repetition rate, and with greater positional stability. An SED whose firing rate would be independent of the analytical gap breakdown voltage should have improved positional and analytical precision. This could be effected by the use of an auxiliary spark gap. Entrainment of the spark in a quartz tube along the spark axis and/or supplying analyte and carrier coaxial to the spark also may improve positional stability.

Data acquisition should be improved by the simultaneous computer analysis of emission intensities and at several wavelengths for multi-element determination and background correction for individual spark emissions. It would then be possible to use the empirical formula production capability inherent in the system to resolve overlapping chromatographic peaks. Computer data acquisition at high firing rate would also show the fast sample-and-hold circuit type to be superior to the gated integrator.

The gated integrator circuit was generally more

useful in the present work because the digital control of the analog circuits was much too imprecise for close control of the S/H. The gated integrator also helped smooth the noisy signal from the spark. Timing circuits based on a 100 MHz oscillator would reduce acquisition time jitter by nearly two orders of magnitude. Increased spark stability would reduce the need for analog signal averaging, as would improved computer data acquisition.

Many analyses which were not attempted by the author should be developed. Prime examples are the boronate derivatives of aminoglycoside antibiotics (e.g. Gentamycin, Tobramycin, Amykacin, and Kanamycin) and the catecholamine-metanephrine group. Similarly, phosphoryl and thiocarbamate derivatives should be used to enhance sensitivity and selectivity where applicable.

A final need is for a better desolvation system which would remove the last traces of water or which could be used for removal of organic solvents.

Carthage must be destroyed

- Cato

REFERENCES

REFERENCES

1. H. A. Daynes "Gas Analysis by Measurement of Thermal Conductivity", Cambridge University Press, London, 1933.

2. E. R. Addard, CRC Critical Reviews in Analytical Chemistry 6, 1-11 (1975).

3. Gow-Mac Instrument Co., Shannon, Ireland.

4. B. Chowdhury and F. W. Karasek, J. Chrom. Sci. 8, 199 (1970).

5. H. M. McNair and E. J. Bonelli, "Basic Gas Chromatography", Varian Aerograph, Inc., Walnut Creek, CA, (1969).

8. A. J. P. Martin and A. T. James; Biochemical J. 63, 138 (1956).

6. A. M. Keulemans, "Gas Chromatography", 2nd Ed. Reinhold, NY, 1959, page 53.

7. S. DalNogare and R. S. Juvet, "Gas-Liquid Chromatography", Wiley-Interscience, NY, 1962, page 197.

9. A. G. Nerheim, U. S. Patent 3,050,984 to Standard Oil Co.

10. C. S. G. Phillips and P. L. Timms, J. Chrom. 5, 131 (1961).

11. A. Liberti, L. Conti, and V. Crescenz; Nature 178, 1067 (1956).

12. C. L. Guillemin and F. Auricourt, J. Gas Chrom. 2, 156 (1964).

13. Chromalytics Corp., Unionville, PA.

14. R. S. Swingle, J. Chrom. Sci. 12, 1 (1974).

15. G. Burton, A. B. Littlewood, and W. A. Wiseman, "Gas Chromatography 1966", Littlewood, A. B. Ed., Inst. of Petroleum, Boston 1967, 193.

16. Reaction Coulometers Ltd., Maidenhead, Berkshire, England.

17. L. Giuffrida, JAOAC 47, 293 (1964).

18. A. B. Littlewood and W. A. Wiseman, J. Gas Chrom. 5, 334 (1967).

19. S. C. Bevan and S. Thorburn, J. Chrom. 11, 301 (1963).

20. W. H. King, Anal. Chem. 36, 1735 (1964).

21. W. H. King, U. S. Patent 3,164,004 (1965).

22. E. P. Scheide and G. G. Guilbault, Anal. Chem. 45, 975 (1973).

23. V. G. Guglya and V. V. Dergumov, Zh. Anal. Khim. 27 (11), 2230 (1973).

24. D. W. Turner, Nature 181, 1265 (1958).

25. L. E. Lawley, Chem. Ind., 1954, 200 (1954).

26. F. W. Noble, K. Abel and P. W. Cook, Anal. Chem. 36, 1421 (1964).

27. H. W. Grice and D. J. David, J. Chrom. Sci. 7, 239 (1969).

28. D. J. David, Gas Chromatographic Detectors, Wiley Interscience, NY (1974).

29. S. A. Ryce and W. A. Bryce, Nature 179, 54 (1957).

30. J. Harley and V. Pretorius, Nature 178, 1244 (1957).

31. I. G. McWilliam and R. A. Dewar, Nature 181, 760 (1958).

32. P. Bocek and J. Janak, Chrom. Rev. 15, 111 (1971).

33. A. T. Blades, J. Chrom. Sci. 11, 251 (1973).

34. M. Dressler, J. Chromatog. 42, 408 (1969).

35. J. E. Lovelock, Anal. Chem. 33, 161 (1961).

36. I. G. McWilliam, U. S. Patent 3,039,856, June 19, 1962.

37. G. F. Carruth and R. Kobayashai, Anal. Chem. 44(6) 1047 (1972).

38. J. D. Winefordner and T. H. Glenn in Advances in Chromatography, Vol. I, J. C. Giddings and R. A. Keller, Eds. M. Dekker, NY (1968).

39. J. W. Otros and D. P. Stevenson, JACS 78, 546 (1956).

40. D. J. Pompeo and J. W. Otros, U. S. Patent 2,641,710 (1953).

41. O. F. Folmer, K. Yang, and G. Perkins, Anal. Chem. 35, 454 (1963).

42. J. E. Lovelock, G. R. Shoemake and A. Zlatkis, Anal. Chem. 36, 1410 (1964).

43. J. G. W. Price, Anal. Chem. 40, 541 (1968).

44. J. E. Lovelock, Nature, 188, 401 (1960).

45. R. R. Freeman and W. E. Wentworth, Anal. Chem. 43, 1987 (1971).

46. R. E. Poulson, Ph.D. Thesis, Michigan State University, East Lansing, Michigan (1959).

47. J. Sevik and S. Krysl, Chromatographia 6, 375 (1973).

48. N. Ostojic and Z. Sternberg, Chromatographia 7 3 (1974).

49. J. N. Driscoll and F. F. Spaziani, R/D 27 (5), 50 May (1976).

50. J. N. Drisscoll and F. F. Spaziani, 26th Pittsburgh Conf. on Analytical Chemistry and Applied Spectroscopy, March (1976).

51. HNU Systems, Inc. 383 Elliot Street, Newton Upper Falls, Mass.

52. O. W. Richardson, J. Nicol and T. Parnell, Phil. Mag. 8, 1 (1904).

53. E. Cremer, J. Gas Chrom. 5, 329 (1967).

54. C. W. Rice, Trans. Am. Instr. Electr. Engrs., June (1923).

55. W. White and J. Hickey, Electronics 21, 100 (1948).

56. E. Cremer, T. Krans and E. Bechtold, Chem. Ing.-Tech. 33, 632 (1961).

57. V. V. Brazhnikov, M. V. Gurev and K. I. Sakodynsky; Chrom. Rev. 12, 1 (1970).

58. A. Karmen and E. L. Kelly, Anal. Chem. 43, 1992 (1971).

59. A. Karmen, U.S. Patent 3,425,806 (1969).

60. L. Guiffrida, N. F. Ives and D. C. Bostwick, JAOKC 49, 8 (1966).

61. C. H. Hartmann, J. Chrom. Sci. 7, 163 (1969).

62. M. Dressler and J. Janak, J. Chrom. Sci. 7, 451 (1969).

63. K. Abel, K. Lanneau, and R. J. Stevens, JAOAC 49, 1022 (1966).

64. W. A. Aue, C. W. Gehrke, R. C. Tindle, D. L. Stalling and C. D. Ruyle, J. Gas. Chrom. 5, 381 (1967).

65. A. Karmen, J. Chrom. Sci. 7, 541 (1969).

66. A. Karmen and L. Guiffrida, Nature 201, 1204 (1964).

67. Hewlett-Packard Corp. Avondale, PA, N/P Detector Bulletin.

68. Perkin-Elmer Corp., Norwalk, Conn. Pub. #L-394, Sept. (1974).

69. M. Scolnick, Advances in Gas Chromatography, (1970) pp. 138-145.

70. G. Christian, Hewlett-Packard Corp., Avondale, PA.

71. A. V. Nowak and H. V. Malmstadt, Anal. Chem. 40, 1108 (1968).

72. Ettre, L. S. and W. H. McFadden, "Ancillary Techniques in Gas Chromatography", J. Wiley & Sons, NY (1969).

73. Sevik, J., "Gas Chromatographic Detectors", Academic Press, NY (1977).

74. Scott, R. P. W., J. Chrom. Sci. 11, 349 (1973).

75. Siuda, J. F., DeBernardis, J. F. and Cavestri, R. C., J. Chrom. 75, 298 (1973).

76. Bros, E. and J. Lasa, J. Chromatography 94, 13 (1974).

77. J. E. Lovelock, U.S. Patent 3,701,632.

78. C. H. Hartmann and K. P. Dimick, J. Gas Chrom. 4, 163 (1966).

79. P. J. Bourke, R. W. Dawson, W. H. Denton, J. Chrom. 14, 387 (1964).

80. J. E. Lovelock and S. R. Lipsky, JACS 82, 431 (1960).

81. Sternberg, J. C. in "Gas Chromatography 1963", 4th Int'l Symposium (L. Fowler, Ed.) Academic Press, NY Page 161 (1963).

82. Novak, J. "Quantitative Analysis by Gas Chromatography", M. Dekker, NY (1975).

83. J. E. Lovelock, J. Chrom. 1, 35 (1958).

84. Condon, R. D., T. R. Scholly, and W. Averill, in "Gas Chromatography 1960", 1st Int'l Symposium on Gas Chromatography, Edinburgh, Academic Press, NY (1960).

85. H. Purnell, Gas Chromatography, Wiley, NY (1962).

86. C. E. Mendoza, J. Chrom. Sci. 9 (1971).

87. R. J. Maggs, P. L. Joynes, A. J. Davies and J. E. Lovelock, Anal. Chem. 43, 1966 (1971).

88. J. E. Lovelock, Anal. Chem. 35, 460 (1963).

89. E. R. Adlard, CRC Crit. Rev. Anal. Chem. 4, 13 (1975).

90. J. E. Lovelock, Anal. Chem. 33, 162 (1961).

91. J. E. Lovelock, Anal. Chem. 35, 474 (1963).

92. W. E. Wentworth, E. Chen, and J. E. Lovelock, J. Phys. Chem. 70, 445 (1966).

93. Sullivan, J. J. and C. A. Burgett, Chromatographia 8, 176 (1975).

94. Fenimore, D. C. and C. M. Davis, J. Chrom. Sci. 8, 519 (1970).

95. Fenimore, D. C., A. Zlafkis, and W. E. Wentworth, Anal. Chem. 40, 1544 (1968).

96. Burgett, C. A., Application Note ANGC 1-76, Hewlett-Packard, Avondale, PA (1976).

97. Patterson, P. L. J. Felton, E. Freitas, and R. Howe, 26th Pittsburgh Conf., Cleveland, OH 1976, paper #137.

98. Wentworth, W. E. and E. Chen, J. Gas Chrom. 5, 170 (1967).

99. USAEC (ERDA), Division of Materials Licensing, 10 CFR 150-20, May, 1964.

100. Kahn, L. and M. C. Goldberg, J. Gas Chrom. 3, 287 (1965).

101. Fenimore, D. C., P. R. Loy and A. Zlatkis, Anal. Chem. 43, 1972 (1971).

102. Hartmann, C. H., Anal. Chem. 45, 733 (1973).

103. Lovelock, J. E., Nature 189, 729 (1961).

104. Nakagawa, K., N. L. McNiven, E. Forchielli, A. Vermulen, and R. I. Dorfman, Steroids, 7, 329 (1966).

105. Chen, E. and W. E. Wentworth, J. Chrom. 68, 302 (1972).

106. Pellizzari, E. D., J. Chromatogr. (Reviews) 98, 323 (1974).

107. Lovelock, J. E., R. J. Maggs, and E. R. Adlard, Anal. Chem. 43, 1962 (1971).

108. Coulson, D. M. and L. A. Cavanagh, Anal. Chem. 32, 1245 (1960).

109. Coulson, D. M., J. Gas Chrom. 3, 134 (1965).

110. Drushel, H. V. Abstracts of the ACS Spring Meeting, San Francisco, 1968.

111. Coulson, D. M., Am. Lab. 1, 33 (1969).

112. Littlewood, A. B. and W. A. Wiseman, J. Gas Chrom. 5, 334 (1967).

113. Martin, R. L., Anal. Chem. 38, 1209 (1966).

114. Klass, P. J., Anal. Chem. 33, 1851 (1961).

115. Fredericks, E. M. and G. A. Harlow, Anal. Chem. 36, 263 (1964).

116. Wallace, L. D., D. W. Kohlenberger, R. J. Joyce, R. T. Moore, M. E. Riddle and J. A. McNutty, Anal. Chem. 42, 387 (1970).

117. Moore, R. T. and J. A. McNulty, Enviro. Sci. and Techn. 3, 741 (1969).

118. Lovelock, J. E., U. S. Patent 3,701,632, October 21, 1972.

119. Frink, R. C. and D. J. David, Pittsburgh Conf., Cleveland, OH (1970).

120. Hall, R. C., J. Chrom. Sci. 12, 152 (1974).

121. Westlake, W. E. in Pesticide Identification at the Residue Level, Adv. Chem. #104, Ed. F. J. Biros, Am. Chem. Soc., Washington, D.C. (1971), pp. 73-81.

122. Lovelock, J. E., P. G. Simmonds, G. R. Shoemake, S. Rich, J. Chrom. Sci. 8, 452 (1970).

123. Tracor Co., Austin, TX 78721.

124. Bay, H. W., K. F. Blurton, J. M. Sedlak, and A. M. Valentine, Anal. Chem. 46, 1837 (1974).

125. Stetter, J. R., D. R. Rutt and K. F. Blurton, Anal. Chem. 48, 924 (1976).

126. Oswin, H. G. and K. F. Blurton, U. S. Patent 3,776,832 (1973).

127. Brody, S. S. and S. E. Chaney, J. Gas. Chrom. 4, 42 (1966).

128. Braman, R. S., Anal. Chem. 38, 734 (1966).

129. Van der Smissen, C. E., U. S. Patent 3,213,747 (1965) See also W. German Patent #1,133,918 (1962).

130. Grice, H. W. M. L. Yates and D. J. David, J. Chrom Sci 8, 90 (1970).

131. Zads, F. M. and R. S. Juvet, Anal. Chem. 38, 569 (1966).

132. Burgett, C. A. and W. J. Campbell, Hewlett-Packard, Avondale, PA, Appl. Note GC-7-7 (1974).

133. J. E. Lovelock, U. S. Patent 3,701,632 (1973).

134. Eckhardt, J. G., M. B. Denton, and J. L. Moyers, J. Chrom. Sci. 13, 133 (1975).

135. Greer, D. G. and Bydalek, T. J., Envir. Sci. and Tech. 7, 153 (1973).

136. Overfield, C. V. and J. D. Winefordner, J. Chrom. Sci. 8, 233 (1970).

137. Bowman, M. C. and M. Beroza, J. Chrom. Sci. 9, 44 (1971).

138. Gutsche, B., and R. Herrmann, Z. Anal. Chem. 258, 273 (1972).

139. Nowak, A. V. and H. V. Malmstadt, Anal. Chem. 40, 1108 (1968).

140. Bowman, M. C., M. Beroza, and K. R. Hill, J. Chrom. Sci. 9, 162 (1971).

141. Morrow, R. W., J. A. Dean, W. D. Shults, M. R. Guerin J. Chrom. Sci. 7, 572 (1969).

142. Kolb, B., G. Kemmer, F. H. Schlesser and E. Wiedeking, Z. Anal. Chem. 221, 166 (1966).

143. Longbottom, J. E., Anal. Chem. 44, 1111 (1972).

144. Segar, D. A., Anal. Letters, 7, 89 (1974).

145. Winefordner, J. D. and C. V. Overfield, J. Chrom. 31, 1 (1967).

146. Winefordner, J. D. and T. J. Vickers, Anal. Chem. 36, 1939 (1964).

147. Sevik, J. and N. Thao, Chromatograpia, 8, 559 (1975).

148. Sugiyama, T., Y. Suzuki and T. Takeuchi, J. Chrom. 80, 61 (1973).

149. Sugiyama, T., Y. Suzuki, and T. Takeuchi, J. Chrom. Sci. 11, 639 (1973).

150. Aavik, K. E., V. A. Ioonson and R. A. Kallasong, USSR Pat. 397,840 (1974).

151. Baamgordnev, R. E., T. A. Clark and R. K. Stevens, Anal. Chem. 47, 563 (1975).

152. Kulish, V. I. and A. N. Korol, Zh. Fiz. Chim. 48, 122 (1974).

153. Versino, B., H. Vissers, Chromatographa, 8, 5 (1975).

154. Giang, B. Diss. Abstr. 33, 1039B (1972).

155. Kojima, T., M, Ichise and V. Sao, Banseki Kagaku, 24, 7 (1975).

156. Wolf, W. R., Anal. Chem. 48, 1717 (1976).

157. Rodriguez-Vazquez, J. A., Anal. Chim. Acta 73, 1 (1974).

158. Juvet, R. S. and S. P. Cram, Anal. Chem. 42, 14R (1970).

159. Guiochon, G., and C. Pommier, "Gas Chromatography of Inorganics and Organometallics", Ann Arbor Science Pub., Ann Arbor, MI (1973).

160. Poulson, R. E., Ph.D. Thesis, Michigan State University (1959).

161. Shilman, A., Environ. Lett. 6, 149 (1974).

162. McCormack, A. J., S. C. Tong, and W. D. Cooke, Anal. Chem. 37, 1471 (1965).

163. McCormack, A. J., M.S. Thesis, Cornell University, Ithaca, NY (1964).

164. Dagnal, R. M., T. S. West and P. Whitehead, Anal. Chem. 44, 2074 (1972).

165. Bache, C. A., and D. J. Lisk, Anal. Chem. 38, 783 (1966).

166. Talmi, Y. and D. T. Bostick, Anal. Chem. 47, 2145 (1975).

167. McLean, W. R., D. L. Stanton, and G. E. Pewketh, Analyst. 98, 432 (1973).

168. Kawaguchi, H., T. Sakamoto, and A. Mizuike, Talanta 20, 321 (1973).

169. Lowings, B. J., Analusis. 1, 510 (1972).

170. West, C. D. Anal. Chem. 42, 811 (1970).

171. Denton, M. B. and D. L. Windsor, Pittsburg Conf. 1976, paper #284.

172. Applied Research Laboratories, Ltd., Luton, UK

173. Bramen, R. S. and A. Dynako, Anal. Chem. 40, 95 (1968).

174. Dagnall, R. M., D. J. Smith, and T. S. West, Anal. Lett. 3, 475 (1970).

175. Lantz, R. K. and S. R. Crouch, Pittsburgh Conf. 1976, paper #286.

178. Glass, E., J. Zynger, R. K. Lantz, and S. R. Crouch, Pittsburgh Conf. 1974, paper #293.

179. Fenselau, C., Appl. Spec. 28, 305 (1974).

180. Karasek, F. W. Anal. Chem. 46, 701A (1974).

181. Karasek, F. W., and D. W. Denny and E. H. DeDeaker Anal. Chem. 46, 970 (1974).

182. Karasek, F. W. and D. M. Kane, J. Chrom. 93, 129 (1974).

183. Revercomb, H. E. and E. A. Mason, Anal. Chem. 47, 970 (1975).

184. Cram, S. P. and S. N. Chesler, J. Chrom. Sci. 11, 391 (1973).

185. Keller, R. A. and M. M. Metro, J. Chrom. Sci. 12, 673 (1974).

186. Metro, M. M. and R. A. Keller, Sep. Sci. 9, 521 (1974).

187. Sadtler Researches, Inc., Philadelphia, PA.

188. Brady, R. F., Anal. Chem. 47, 1425 (1975).

189. Penzias, G. J. and M. F. Boyle, Am. Lab., 5, 53 (1973).

190. Greinke, R. A., and I. C. Lewis, Anal. Chem. 47, 2151 (1975).

191. Burchfield, H. P., E. E. Green, R. J. Wheeler and S. M. Billedeau, J. Chrom. 99, 697 (1974).

192. Wm. McKinny, Ph.D. Shell Development Corp., personal communication.

193. Hawk, J., Waters Assoc., personal communication.

194. Teranishi, R., P. Issenberg, I. Hornstein, and E. L. Wick, "Flavor Research: Principles and Techniques," M. Dekker, NY (1971).

195. Dravnicks, A., J. Pharm. Sci. 63, 36 (1974).

196. Acree, T. E., R. M. Butts, R. R. Nelson and C. Y. Lee, Anal. Chem. 48, 1821 (1976).

197. Widmark, G. in "Pesticide Identification at the Residue Level", Adv. Chem., #104, ACS, 1971.

198. Davis, J. E., A. Shepard, N. Stanford, and L. B. Rodgers, Anal. Chem. 46, 821 (1974).

199. Clark, H. A. and P. C. Juvs, Anal. Chem. 47, 374 (1975).

200. Greene, A. F., 26th Pittsburgh Conf., Cleveland, 1976, paper #285.

201. Taguchi, N., U. S. Patent 3,732,519 (1973).

202. Scott, R. P. W., Anal. Chem. 35, 481 (1963).

203. Martin, A. E. and J. Smart, Nature 175, 422 (1955).

204. Devauk, P. and G. Guiochon, J. Gas Chrom. 5, 341 (1967).

205. Scott, R. P. and J. G. Lawrence, J. Chrom. Sci. 8, 65 (1970).

206. Pye Unicam Ltd. UK.

207. Scott, R. P. W., C. G. Scott, M. Monroe and J. Hess, J. Chrom. 99, 395 (1974).

208. Jones, P. R. and S, K. Yang, Anal. Chem. 47, 1000 (1975).

209. Pretorius, V., and J. F. J. Van Rensburg, J. Chrom. Sci. 11, 355 (1973).

210. Stolyhwo, A., and O. S. Privett, J. Chrom. Sci. 11, 20 (1973).

211. Dubsky, H., German Patent 2,139,979 (1972).

212. Dubsky, H., Chem. Listy 67, 533 (1973).

213. Veening, H. J., J. Chem. Ed. 47, A549, A675, and A749 (1970).

214. Romano, J. R. and I. S. Palmer, Anal. Biochem. 49, 580 (1972).

215. Krejci, M. and N. Pospisilova, J. Chrom. 73, 105 (1972).

216. Nota, G. and R. Palombari, J. Chrom. 62, 153 (1971).

217. Balaukhin, A. A., B. G. Vtorov, V. I. Kalmanovskii and V. P. Chernokozhin, CA, 79-269428 (1973).

218. Willmott, F. W. and R. J. Dolphin, J. Chrom. Sci. 12, 295 (1974).

219. Jones, D. R. and S. E. Manahan, Anal. Lett. 8, 569 (1975).

220. Manahan, S. E. and D. R. Jones, Anal. Lett. 6, 745 (1973).

221. Julin, B. G., H. W. Vandenborn, and J. J. Kirkland, J. Chrom. 112, 443 (1975).

222. Freed, D. J., Anal. Chem. 47, 186 (1975).

123. Hey, H., Z. Anal. Chem. 256, 361 (1971).

224. Van Dijk, J. H., British Patent 1,292,754 (1972).

225. Schmermund, J. T. and D. C. Locke, Anal.. Lett. 8, 611 (1975).

226. Pusey, D. F. G., Chem. Brit. 5, 408 (1969).

227. Mowry, R. and R. S. Juvet, J. Chrom. Sci. 12, 687 (1974).

228. Freeman, N. K., F. T. Upham, and A. A. Windsor, Appl. Lett. 6, 943 (1973).

229. Rokushika, S., H. Tanaguchi, and H. Hatano, Anal. Lett. 8, 205 (1975).

230. Bowers, L. D., L. M. Canning, C. N. Sayers, P. W. Carr, Clin. Chem. 22, 1314 (1976).

231. Jordan, B. R., Anal. Biochem. 35, 344 (1970).

232. Verhassel, J. P. Messtechnik, 81, 53 (1973).

233. Scott, R. P. W., J. Chrom. Sci. 11, 349

234. Schyulz, W. W. and W. H. King, J. Chrom. Sci. 11, 343 (1973).

235. Lantz, R. K. and S. R. Crouch, unpublished data.

236. Waters, J. L., Am. Lab. 3, 61 (1971).

237. Baker, D. R., R. C. Williams, and J. C. Steichen, J. Chrom. Sci. 12, 499 (1974).

238. Schulten, H. R. and H. D. Beckey, J. Chrom. 83, 315 (1973).

239. Kudirka, P. and M. Evenson, 26th AACC Meeting, Houston, TX, 1976.

240. Thomas, A. H. and S. D. Tappin, J. Chrom. 97, 280 (1974).

241. Rasmussen, H. N. and J. R. Nielsen, Anal. Bioch. 50, 648 (1972).

242. Bylina, A., D. Sybilska, Z. R. Grabowski and J. Koszewski, J. Chrom. 83, 357 (1973).

243. Dessy, R. E., W. D. Reynolds, W. G. Nunn, C. A. Titus G. F. Moler, Clin. Chem. 22, 1472 (1976).

244. McDowell, A. and H. L. Pardue, Anal. Chem. 48, 1815 (1976).

245. Henry, R. A., J. A. Schmit and J. F. Dieckman, J. Chrom. Sci. 9, 513 (1972).

246. Maggs, R. J., Ger. Offen. 1,183,928, Aug. 1969.

247. Politzer, I. R., G. W. Griffin, B. J. Dowty, and J. L. Laseter, Anal. Lett. 6, 539 (1973).

248. Katz, S. and L. H. Thacker, J. Chrom. 64, 247 (1972).

249. Hirdina, Jirk. British Patent 1,249,476, October 1971.

250. Martin, F., J. Maine, C. C. Sweeley, and J. F. Holland, Clin. Chem. 22, 1434 (1976).

251. Katz, S., W. W. Pitt, Anal. Lett. 5, 177 (1972).

252. Katz, S., W. W. Pitt, J. E. Mrochek and S. Dinsmore, J. Chrom. 101, 193 (1974).

253. Watson, E. S., Am. Lab., 8, Sept. (1969).

254. Vandenheuvel, F. A. and J. C. Sipos, Anal. Chem. 33, 286 (1961).

255. Trenner, N. R., C. W. Warren, and S. L. Jones, Anal. Chem. 25, 1685 (1953).

256. Johnson, H. W., V. A. Campanile, and H. A. LeFebre, Anal. Chem. 39, 32 (1967).

257. Laboratory Data Control, Inc./Milton-Roy Co., St. Petersberg, FL.

258. Gow-Mac Instr. Co., Bull. SB-80, 1974, Madison, NJ

259. Kissinger, P. T., C. Refshauge, R. Dreiling, and R. N. Adams, Anal. Letts. 6, 465 (1973).

260. Kemula, W., Roczniki Chem. 26, 281 (1952).

261. Koen, J. G., J. F. K. Huber, H. Poppe, and G. den Boef, J. Chrom. Sci. 8, 192 (1970).

262. Kemala, W., Anal. Chem. 167, 241 (1959).

263. Bio-Analytical Systems, Lafayette, IN.

264. Kissinger, P. T., Anal. Chem. 49(4), 457A (1977).

265. Buchta, R. C. and L. J. Papa, J. Chrom. Sci. 14, 213 (1976).

266. Zynger, J., Ph.D. Thesis, Michigan State University, East Lansing, MI 1973.

267. Zynger, J. and S. R. Crouch, Appl. Spectr., 29, 244 (1975).

268. Rees, J. A., "Electrical Breakdown in Gases", J. Wiley and Sons, NY (1973).

269. Howatson, A. M., "An Introduction to Gas Discharges", Pergamon Press, London (1965).

270. Sheeline, A. and J. Walters, Federation of Analytical Chemistry and Spectroscopy Soc. Meeting, Indianapolis, IN (1975).

271. Glass, E., Michigan State University, personal communication (1975).

272. I. Reif, V. A. Fassel, and R. N. Kniseley, Spectrochim. Acta, 28B, 105 (1973).

273. Adcock, B. D. and W. E. G. Plumtree, J. Quant. Spectr. Rad. Transt. 4, 29 (1964).

274. Malone, B. S. and W. H. Corcoraa, J. Quant. Spectr. Rad. Transt. 6, 443 (1966).

275. Griem, H. R., "Plasma Spectroscopy", Chapter 4, pp. 74-92, McGraw-Hill Co., NY (1964).

276. Kolb, A. C. and H. R. Griem, Phys. Rev. 111, 514 (1958).

277. Taylor, H. E., J. H. Gibson and R. K. Skogerboe, Anal. Chem. 42, 1569 (1970).

278. S. Koeplin, G. Seng, S. R. Crouch, Michigan State University, work in progress.

279. Nulciyama, S. and Y. Tanasawa, Trans. Soc. Mech. Engr. (Japan) 5(18) 63 (1938), CA 35, 4258.

280. Skogerboe, R. K., Colorado State University, Ft. Collins, CO, personal communication (1976).

281. Eisenberg, F. "Gas Chromatography of Carbohydrates as Butanebronic Acid Esters" in Methods in Enzymology 28, Pt B, B. Ginsburg, Ed., Academic Press, NY (1973).

282. Wood, P. J. and I. R. Siddiqui, Carbohydrate Res. 19, 283 (1971).

283. Lews, B., R. N. Pease and H. S. Taylor (Eds.) "Combustion Processes", Princeton, Press, Princeton, NJ (1956).

284. Hermann, R. and C. Th. J. Alkemade, "Chemical Analysis by Flame Photometry", Wiley-Interscience, NY (1958) pp. 22-38.